12 Jun 2018

High Efficiency, High Performance Metal-Organic Framework (MOF) Membranes in Hollow Fibers and Tubular Modules

Sankar Nair

Kiwon Eum

Christopher W. Jones

Ali A. Rownaghi
Missouri University of Science and Technology, rownaghia@mst.edu

Recommended Citation

S. Nair et al., "High Efficiency, High Performance Metal-Organic Framework (MOF) Membranes in Hollow Fibers and Tubular Modules," *U.S. Patents*, Jun 2018.

US009994501B2

(12) United States Patent
Nair et al.

(10) **Patent No.: US 9,994,501 B2**
(45) **Date of Patent: *Jun. 12, 2018**

(54) **HIGH EFFICIENCY, HIGH PERFORMANCE METAL-ORGANIC FRAMEWORK (MOF) MEMBRANES IN HOLLOW FIBERS AND TUBULAR MODULES**

(71) Applicant: **Georgia Tech Research Corporation**, Atlanta, GA (US)

(72) Inventors: **Sankar Nair**, Atlanta, GA (US); **Kiwon Eum**, Atlanta, GA (US); **Christopher W. Jones**, Atlanta, GA (US); **Ali Rownaghi**, Atlanta, GA (US)

(73) Assignee: **GEORGIA TECH RESEARCH CORPORATION**, Atlanta, GA (US)

(*) Notice: Subject to any disclaimer, the term of this patent is extended or adjusted under 35 U.S.C. 154(b) by 50 days.

This patent is subject to a terminal disclaimer.

(21) Appl. No.: **15/061,964**

(22) Filed: **Mar. 4, 2016**

(65) **Prior Publication Data**

US 2016/0184798 A1 Jun. 30, 2016

Related U.S. Application Data

(63) Continuation-in-part of application No. 14/231,871, filed on Apr. 1, 2014, now Pat. No. 9,687,791.
(Continued)

(51) **Int. Cl.**
C07C 7/144 (2006.01)
B01D 63/06 (2006.01)
(Continued)

(52) **U.S. Cl.**
CPC ***C07C 7/144*** (2013.01); ***B01D 63/063*** (2013.01); ***B01D 67/0051*** (2013.01);
(Continued)

(58) **Field of Classification Search**
CPC B01D 67/0051; B01D 53/228; B01D 2053/224; B01D 63/063; Y10T 29/49345; C07C 7/144; B01J 19/2475
See application file for complete search history.

(56) **References Cited**

U.S. PATENT DOCUMENTS

5,968,366 A 10/1999 Deckman et al.
6,953,493 B2 10/2005 Nakayama et al.
(Continued)

FOREIGN PATENT DOCUMENTS

CN 1617761 A 5/2005
CN 1914219 A 2/2007
(Continued)

OTHER PUBLICATIONS

Ameloot, et al., *Interfacial synthesis of hollow metal-organic framework capsules demonstrating selective permeability*, Nature Chemistry 3 (May 2011) 382-387.
(Continued)

Primary Examiner — Lessanework Seifu
(74) *Attorney, Agent, or Firm* — Adams and Reese LLP

(57) **ABSTRACT**

A reactor cell for measuring gas and liquid permeation is disclosed. A hollow fiber is supported by and sealed into a first hole and a second hole of the reactor module. The first and second ends of the hollow fiber are sealed with a sealing solution. Methods for making and using the reactor cell are also disclosed. As made and used, the reactor cell further comprises a molecular sieving membrane that is uniform and free of defects grown on an inner bore surface of the hollow fiber.

30 Claims, 43 Drawing Sheets
(27 of 43 Drawing Sheet(s) Filed in Color)

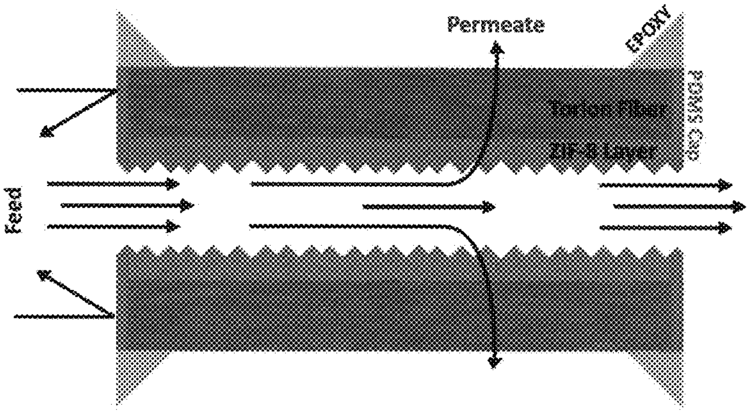

Related U.S. Application Data

(60) Provisional application No. 61/913,592, filed on Dec. 9, 2013, provisional application No. 61/820,489, filed on May 7, 2013.

(51) **Int. Cl.**

B01D 67/00	(2006.01)
B01D 69/08	(2006.01)

(52) **U.S. Cl.**

CPC ***B01D 69/08*** (2013.01); *Y02P 20/582* (2015.11); *Y10T 29/49345* (2015.01)

(56) References Cited

U.S. PATENT DOCUMENTS

7,014,680	B2	3/2006	Nakayama et al.
7,306,647	B2	12/2007	Miller et al.
7,494,610	B2	2/2009	Yeung et al.
7,553,352	B2	6/2009	Mueller et al.
7,880,026	B2	2/2011	Ni et al.
7,973,090	B2	7/2011	Suzuki et al.
8,042,695	B2	10/2011	Ishibashi
8,123,834	B2	2/2012	Masel et al.
8,132,678	B2	3/2012	Liu et al.
8,269,029	B2	9/2012	Masel et al.
8,302,782	B2	11/2012	Falconer et al.
8,518,153	B2	8/2013	Ryan et al.
8,673,057	B2	3/2014	Zhou et al.
8,725,482	B2	5/2014	Haldoupis et al.
2002/0003105	A1	1/2002	McEvoy
2002/0031303	A1	3/2002	Wang
2004/0058224	A1	3/2004	Eshraghi et al.
2004/0139908	A1	7/2004	Bowe et al.
2004/0173094	A1	9/2004	Nakayama et al.
2005/0124819	A1	6/2005	Yaghi et al.
2005/0204916	A1	9/2005	Falconer et al.
2005/0229779	A1	10/2005	Nakayama et al.
2005/0233945	A1	10/2005	Brown et al.
2006/0107830	A1	5/2006	Miller et al.
2006/0201884	A1	9/2006	Kulprathipanja et al.
2007/0022877	A1	2/2007	Marand et al.
2007/0112189	A1	5/2007	Ikeda et al.
2007/0244347	A1	10/2007	Ying et al.
2008/0047432	A1	2/2008	Nonaka et al.
2008/0177098	A1	7/2008	Bahnmuller et al.
2008/0214686	A1	9/2008	Suzuki et al.
2008/0261101	A1	10/2008	de Figueiredo Gomes et al.
2008/0287413	A1	11/2008	Aslund et al.
2009/0004084	A1	1/2009	Bell et al.
2009/0011926	A1	1/2009	Yajima et al.
2009/0060839	A1	3/2009	Boyes et al.
2009/0111959	A1	4/2009	Cao et al.
2009/0114089	A1	5/2009	Liu et al.
2009/0126570	A1	5/2009	Liu et al.
2009/0131643	A1	5/2009	Ni et al.
2009/0152755	A1	6/2009	Liu et al.
2009/0155464	A1	6/2009	Liu et al.
2009/0211440	A1	8/2009	Reyes et al.
2010/0006503	A1	1/2010	Bratton et al.
2010/0071559	A1	3/2010	Miachon et al.
2010/0072424	A1	3/2010	Petoud et al.
2010/0132549	A1	6/2010	Yaghi et al.
2010/0144512	A1	6/2010	Uchikawa et al.
2010/0226991	A1	9/2010	Horcajada-Cortes et al.
2011/0158923	A1	6/2011	Galeone et al.
2011/0160039	A1	6/2011	Himeno et al.
2011/0298115	A1	12/2011	Celaya et al.
2011/0319630	A1	12/2011	Yaghi et al.
2012/0003475	A1	1/2012	Benin et al.
2012/0058302	A1	3/2012	Eggenspieler et al.
2012/0070904	A1	3/2012	Stoddart et al.
2012/0202006	A1	8/2012	Rimer
2012/0310018	A1	12/2012	Lai et al.
2013/0064747	A1	3/2013	Zhou et al.
2013/0157837	A1	6/2013	Banerjee et al.
2013/0197235	A1	8/2013	Thompson et al.

FOREIGN PATENT DOCUMENTS

CN	103201016	B	9/2015
JP	2007045691		2/2007
WO	WO-2005099885	A1	10/2005
WO	WO-2007139766	A2	12/2007
WO	WO-2010103856		9/2010
WO	WO-2012074487	A1	6/2012
WO	WO-2012138418	A1	10/2012
WO	WO-2013020968	A2	2/2013

OTHER PUBLICATIONS

Brown, et al., *Continuous polycrystalline zeolitic imidazolate framework-90 membranes on polymeric hollow fibers*, Angew. Chem. 124 (2012) 10767-10770.

Buonomenna, *Membrane processes for a sustainable industrial growth*, RSC Adv. 3 (2013) 5694-5740.

Bux, et al., *Oriented zeolitic imidazolate framework-8 membrane with sharp* H_2/C_3H_8 *molecular sieve separation*, Chem. Mater. 23 (2011) 2262-2269.

Cao, et al., *Growth of uniformly oriented silica MFI and BEA zeolite films on substrates*, Science 334 (Dec. 16, 2001) 1533-1538.

Choi, et al., *Grain boundary defect elimination in a zeolite membrane by rapid thermal processing*, Science 325 (Jul. 31, 2009) 590-593.

Gascon, et al., *Accelerated synthesis of all-silica DD3R and its performance in the separation of propylene/propane mixtures*, Microporous & Mesoporous Materials 115 (2008) 585-593.

Gascon, et al., *Practical approach to zeolitic membranes and coatings: State of the art, opportunities, barriers, and future perspectives*, Chem. Mater. 24 (2012) 2829-2844.

Huang, et al., *Steam-stable zeolitic imidazolate framework ZIF-90 membrane with hydrogen selectivity through covalent functionalization*, J. Am. Chem. Soc. 132(44) (2010) 15562-15564.

Jang, et al., *Modified mesoporous silica gas separation membranes on polymeric hollow fibers*, Chem. Mater. 23 (2011) 3025-3028.

Kwon, et al., *Highly propylene-selective supported zeolite-imidazolate framework (ZIF-8) membranes synthesized by rapid microwave-assisted seeding and secondary growth*, Chem. Commun. 49 (2013) 3854-3856.

Li, et al., *Zeolitic imidazolate frameworks for kinetic separation of propane and propene*, J. Am. Chem. Soc. 131(30) (2009) 10368-10369.

Pan, et al., *Effective separation of propylene/propane binary mixtures by ZIF-8 membranes*, J. Membrane Science 390-391 (2012) 93-98.

Pan, et al., *Sharp separation of C2/C3 hydrocarbon mixtures by zeolitic imidazolate framework-8 (ZIF-8) membranes synthesized in aqueous solutions*, Chem. Commun. 47(37) (Oct. 7, 2011) 10275-10277.

Pan, et al., *Synthesis of ceramic hollow fiber supported zeolitic imidazolate framework-8 (ZIF-8) membranes with high hydrogen permeability*, J. Membrane Science 421-422 (2012) 292-298.

Park, et al., *Exceptional chemical and thermal stability of zeolitic imidazolate frameworks*, PNAS 103(27) (Jul. 5, 2006) 10186-10191.

Pera-Titus, et al., *Preparation of inner-side tubular zeolite NaA membranes in a semi-continuous synthesis system*, J. Membrane Science 278 (2006) 401-409.

Shah, et al., *Current status of metal-organic framework membranes for gas separations: Promises and challenges*, Ind. Eng. Chem. Res. 51 (2012) 2179-2199.

Thompson, et al., *Hybrid zeolitic imidazolate frameworks: Controlling framework porosity and functionality by mixed-linker synthesis*, Chem. Mater. 24 (2012) 1930-1936.

Tsapatsis, *Toward high-throughput zeolite membranes*, Science 334 (Nov. 11, 2011) 767-768.

Varoon, et al., *Dispersible exfoliated zeolite nanosheets and their application as a selective membrane*, Science 334 (Oct. 7, 2011) 72-75.

PCT Aug. 22, 2014 International Search Report and Written Opinion issued in International Application PCT/US14/133169.

(56) **References Cited**

OTHER PUBLICATIONS

Aug. 3, 2012 Office Action/Non-Final Rejection mailed in U.S. Appl. No. 12/971,132, filed Dec. 17, 2010.

Dec. 18, 2012 Response to Office Action dated Aug. 3, 2012 filed in U.S. Appl. No. 12/971,132, filed Dec. 17, 2010.

Jan. 28, 2013 Office Action/Final Rejection mailed in U.S. Appl. No. 12/971,132, filed Dec. 17, 2010.

Jun. 24, 2013 Response to Final Office Action dated Jan. 28, 2013 with Declaration filed in U.S. Appl. No. 12/971,132, filed Dec. 17, 2010.

Aug. 14, 2013 Office Action/Non Final Rejection mailed in U.S. Appl. No. 12/971,132, filed Dec. 17, 2010.

Feb. 11, 2014 Response to Office Action dated Aug. 14, 2013 with Declaration filed in U.S. Appl. No. 12/971,132, filed Dec. 17, 2010.

Mar. 3, 2014 Notice of Allowance/Allowability with Examiner's Amendment and Statement of Reasons for Allowance mailed in U.S. Appl. No. 12/971,132, filed Dec. 17, 2010.

Oct. 31, 2013 Office Action/Non-Final Rejection mailed in U.S. Appl. No. 13/396,411, filed Feb. 14, 2012.

Jan. 17, 2014 Response to Office Action dated Oct. 31, 2013 filed in U.S. Appl. No. 13/396,411, filed Feb. 14, 2012.

Apr. 9, 2014 Final Office Action mailed in U.S. Appl. No. 13/396,411, filed Feb. 14, 2012.

Jun. 3, 2014 Response to Final Office Action filed in U.S. Appl. No. 13/396,411, filed Feb. 14, 2012.

Jun. 11, 2014 Notice of Allowance/Allowability with Examiner's Amendment/Comment mailed in U.S. Appl. No. 13/396,411, filed Feb. 14, 2012.

Dec. 19, 2013 Notice of Allowance/Allowability with Examiner's Amendment/Comment mailed in U.S. Appl. No. 13/399,645, filed Feb. 17, 2012.

Apr. 19, 2013 Office Action Non-Final mailed in U.S. Appl. No. 13/209,957, filed Aug. 15, 2011.

Jun. 14, 2013 Response to Office Action dated Apr. 19, 2013 in U.S. Appl. No. 13/209,957, filed Aug. 15, 2011.

Jul. 11, 2013 Notice of Allowance / Allowability mailed in U.S. Appl. No. 13/209,957, filed Aug. 15, 2011.

Gordillo, et al., *Site percolation in zeolitic frameworks*, Zeolites 15 (1995) 656-659.

Moloy, et al., *High-silica zeolites: A relationship between energetics and internal surface areas*, Microporous & Mesoporous Materials 54 (2002) 1-13.

Nair, *Nanoscopic metal oxide objects via controlled creation and rearrangement of amorphous nanoparticles*, presented Dec. 11, 2007, School of Chemical & Biomolecular Engineering Georgia Institute of Technology, Atlanta, GA 30332-0100.

Skoulidas, et al., *Self-diffusion and transport diffusion of light gases in metal-organic framework materials assessed using molecular dynamics simulations*, J. Phys. Chem. B 109 (2005) 15760-15768.

Chen, et al., *Interwoven metal-organic framework on a periodic minimal surface with extra-large pores*, Science 291 (2001) 1021-1023.

Eddaoudi, et al., *Design and synthesis of metal-carboxylate frameworks with permanent microporosity*, Topics in Catalysis 9 (1999) 105-111.

Foster, et al., *A geometric solution to the largest free-sphere problem in zeolite frameworks*, Microporous & Mesoporous Materials 90(1-3) (2006) 32-38.

Hoshen, et al., *Percolation and cluster distribution. I. Cluster multiple labeling technique and critical concentration algorithm*, Physical Review B 14(8) (1976) 3438.

Keskin, et al., *Efficient methods for screening of metal organic framework membranes/or gas separations using atomically detailed models*, Langmuir 25(19) (2009) 11786-11795.

Li, et al., *Design and synthesis of an exceptionally stable and highly porous metal-organic framework*, Nature 402 (1999) 276-279.

Ockwig, et al., *Reticular chemistry: Occurrence and taxonomy nets and grammar for the design of frameworks*, Acc. Chem. Res. 38(3) (2005) 176-182.

Seki, *Dynamic channels of a porous coordination polymer responding to external stimuli*, Phys. Chem. Chem. Phys. 4(10) (2002) 1968-1971.

Yaghi, et al., *Reticular synthesis and the design of new materials*, Nature 423 (2003) 705-714.

PCT Feb. 24, 2011 International Search Report and Written Opinion mailed in International Patent Application PCT/US2010/060945.

CN Mar. 14, 2014 Notification of the First Office Action mailed in Chinese Patent Application 201080057358.8 (with English Translation).

CN Jul. 28, 2014 Response to First Office Action dated Mar. 14, 2014 filed in Chinese Patent Application 201080057358.8 (with English Translation).

CN Sep. 16, 2014 Notification of the Second Office Action mailed in Chinese Patent Application 201080057358.8 (with English Translation).

JP Nov. 26, 2013 Office Action mailed in Japanese Patent Application 2012-543346 (with English Translation).

JP Jul. 17, 2014 Examiner's Decision of Refusal mailed in Japanese Patent Application 2012-543346 (with English Translation).

KR Feb. 10, 2014 Notice of Submission of Opinion/Office Action mailed in Korean Patent Application 10-2012-7013862 (with English Translation).

Den Exter, M.J., et al., *Separation of permanent gases on the all-silica 8-ring clathrasil DD3R*, (Weitkamp, J., et al., eds. *Zeolites and Related Microporous Materials: State of the Art 1994*), Studies in Surface Science and Catalysis 84 (1994) 1159-66.

Gies, H., *Studies on clathrasils. IX crystal structure of decadodecasil 3R, the missing link between zeolites and clathrasils*, Zeitschrift für Kristallographie 175 (1986) 93-104.

Himeno, Shuji, et al., *Characterization and selectivity for methane and carbon dioxide adsorption on the all-silica DD3R zeolite*, Micropor. Mesopor. Mater. 98 (2007) 62-69.

Tomita, Toshihiro, et al., *Gas separation characteristics of DDR type zeolite membrane*, Micropor. Mesopor. Mater. 68 (2004) 71-75.

Yang, Qi-Liang, et al., *Synthesis of DDR-type zeolite in fluoride medium*, Chinese Journal of Inorganic Chemistry 25(2) (2009) 191-194.

Aguado, Sonia, et al., *Facile synthesis of an ultramicroporous MOF tubular membrane with selectivity towards CO2*, New J. Chem. 35 (2011) 41-44.

Bae, Tae-Hyun, et al., *A high-performance gas-separation membrane containing submicrometer-sized metal-organic framework crystals*, Angew. Chem. Int. Edit. 49 (2010) 9863-66.

Baker, Richard W., *Future directions of membrane gas separation technology*, Ind. Eng. Chem. Res. 41(6) (2002) 1393-411.

Baker, Richard W. and Kaaeid Lokhandwala, *Natural gas processing with membranes: An overview*, Ind. Eng. Chem. Res. 47(7) (2008) 2109-21.

Brar, Tejinder, et al., *Control of crystal size and distribution of zeolite A*, Ind. Eng. Chem. Res. 40 (2001) 1133-39.

Bux, Helge, et al., *Zeolitic imidazolate framework membrane with molecular sieving properties by microwave-assisted solvothermal synthesis*, J. Am. Chem. Soc. 131(44) (2009) 16000-01.

Caro, Jüergen and Manfred Noack, *Zeolite membranes—Recent developments and progress*, Micropor. Mesopor. Mater. 115 (2008) 215-33.

Carreon, Moises A., et al., *Alumina-supported SAPO-34 membranes for CO_2/CH_4 separation*, J. Am. Chem. Soc. 130(16) (2008) 5412-13.

Centrone, Andrea, et al., *Growth of metal-organic frameworks on polymer surfaces*, J. Am. Chem. Soc. 132(44) (2010) 15687-91.

Chen, Banglin, et al., *A microporous metal-organic framework for gas-chromatographic separation of alkanes*, Agnew. Chem. Int. Ed. 45 (2006) 1390-93.

Chiu, W. V., et al., *Post-synthesis defect abatement of inorganic membranes for gas separation*, J. Membr. Sci. 377 (2011) 182-90.

Cui, Ying, et al., *Preparation and gas separation performance of zeolite T membrane*, J. Mater. Chem. 14(5) (2004) 924-32.

Cui, Ying, et al., *Preparation and gas separation properties of zeolite T membrane*, Chem. Comm. 17 (2003) 2154-55.

(56) **References Cited**

OTHER PUBLICATIONS

Favre, Eric, *Carbon dioxide recovery from post-combustion processes: Can gas permeation membranes compete with absorption?*, J. Membr. Sci. 294 (2007) 50-59.

Forster, Paul M., et al., *A high-throughput investigation of the role of pH, temperature, concentration, and time on the synthesis of hybrid inorganic-organic materials*, Angew. Chem. Int. Ed. 44 (2005) 7608-11.

Ge, Qingqin, et al., *High-performance zeolite NaA membranes on polymer-zeolite composite hollow fiber supports*, J. Am. Chem. Soc. 131(47) (2009) 17056-57.

Hao, Ji Hua and Shichang Wang, *Influence of quench medium on the structure and gas permeation properties of cellulose acetate membranes*, J. Appl. Polym. Sci. 68(8) (1998) 1269-76.

Heng, Samuel, et al., *Low-temperature ozone treatment for organic template removal from zeolite membrane*, J. Membr. Sci. 243 (2004) 69-78.

Himeno, Shuji, et al., *Synthesis and permeation properties of a DDR-type zeolite membrane for separation of CO_2/CH_4 gaseous mixtures*, Ind. Eng. Chem. Res. 46(21) (2007) 6989-97.

Huang, Aisheng, & Jürgen Caro, *Covalent post-functionalization of zeolitic imidazolate framework ZIF-90 membrane for enhanced hydrogen selectivity*, Angew. Chem. Int. Ed. 50 (2011) 4979-82.

Huang, Aisheng, et al., *Molecular-sieve membrane with hydrogen permselectivity: ZIF-22 in LTA topology prepared with 3-aminopropyltriethoxysilane as covalent linker*, Angew. Chem. Int. Ed. 49 (2010) 4958-61.

Huang, Aisheng and Jürgen Caro, *Cationic polymer used to capture zeolite precursor particles for the facile synthesis of oriented zeolite LTA molecular sieve membrane*, Chem. Mater. 22(15) (2010) 4353-55.

Husain, Shabbir, Mixed Matrix Dual Layer Hollow Fiber Membranes for Natural Gas Separation, Dissertation, Georgia Institute of Technology, Atlanta, GA, 2006, 48-49.

Jee, Sang Eun and David S. Sholl, *Carbon dioxide and methane transport in DDR zeolite: Insights from molecular simulations into carbon dioxide separations in small pore zeolites*, J. Am. Chem. Soc. 131(22) (2009) 7896-7904.

Jie, Xingming, et al., *Gas permeation performance of cellulose hollow fiber membranes made from the cellulose/N-methylmorpholine-N-oxide/H_2O system*, J. Appl. Polym. Sci. 91(3) (2004) 1873-80.

Kanezashi, Masakoto, et al., *Gas permeation through DDR-type zeolite membranes at high temperatures*, AlChE J. 54(6) (2008) 1478-86.

Koros, William J. and Rajiv Mahajan, *Pushing the limits on possibilities for large scale gas separation: Which strategies?*, J. Membr. Sci. 175 (2000) 181-96.

Kuhn, Jelan, et al., *Detemplation of DDR type zeolites by ozonication*, Micropor. Mesopor. Mater. 120 (2009) 12-18.

Kumar, P. et al., *Ordered mesoporous membranes: Effects of support and surfactant removal conditions on membrane quality*, J. Membr. Sci. 279 (2006) 539-47.

Kusakabe, Katsuki, et al., *Formation of a Y-type zeolite membrane on a porous alpha-alumina tube for gas separation*, Ind. Eng. Chem. Res. 36(3) (1997) 649-55.

Lee, Clare, et al., *Thermodynamic and kinetic factors in the hydrothermal synthesis of hybrid frameworks: Zinc 4-cyclohexene-1,2-dicarboylates*, Chem. Comm. (2006) 2687-89.

Li, Shiguang, et al., *Scale-up of SAPO-34 membranes for CO_2/CH_4 separation*, J. Membr. Sci. 352 (2010) 7-13.

Li, Yan-Shuo, et al., *Molecular sieve membrane: Supported metal-organic framework with high hydrogen selectivity*, Angew. Chem. Int. Edit. 49 (2010) 548-51.

Li, Zong-Qun, et al., Fabrication of nanosheets of a fluorescent metal-organic framework $[Zn(BDC)(H_2O)]_n$ (BDC=1,4-benzenedicarboxylate): Ultrasonic synthesis and sensing of ethylamine, Inorganic Chemistry Communications 11(11) (2008) 1375-77.

Li, Zong-Qun, et al., *Ultrasonic synthesis of the microporous metal-organic framework $Cu_3(BTC)_2$ at ambient temperature and pressure: An efficient and environmentally friendly method*, Mater. Lett. 63 (2009) 78-80.

Lin, Zhoujia, et al., *Chiral induction in the ionothermal synthesis of a 3-D coordination polymer*, J. Am. Chem. Soc. 129(16) (2007) 4880-81.

Lindmark, Jonas and Jonas Hedlund, *Modification of MFI membranes with amine groups for enhanced CO_2 selectivity*, J. Mater. Chem. 20(11) (2010) 2219-25.

Liu, Xin-Lei, et al., *An organophilic pervaporation membrane derived from metal-organic framework nanoparticles for efficient recovery of bio-alcohols*, Angew. Chem. Int. Ed. 50(45) (2011) 10636-39.

Liu, Yunyang, et al., *Synthesis and characterization of ZIF-69 membranes and separation for CO_2/CO mixture*, J. Membr. 353 (2010) 36-40.

Liu, Yunyang, et al., *Synthesis of highly c-oriented ZIF-69 membranes by secondary growth and their gas permeation properties*, J. Membr. Sci. 379 (2011) 46-51.

Ma, Bao-Qing, et al., *Microporous pillared paddle-wheel frameworks based on mixed-ligand coordination of zinc Ions*, Inorg. Chem. 44(14) (2005) 4912-14.

Matsuda, H., et al., *Improvement of ethanol selectivity of silicalite membrane in pervaporation by silicone rubber coating*, J. Membr. Sci. 210(2) (2002) 433-37.

McCarthy, Michael C., et al., *Synthesis of zeolitic imidazolate framework films and membranes with controlled microstructures*, Langmuir 26(18) (2010) 14636-41.

Morris, William, et al., *Crystals as molecules: Postsynthesis covalent functionalization of zeolitic imidazolate frameworks*, J. Am. Chem. Soc. 130(38) (2008) 12626-27.

Nair, Sankar, et al., *Separation of close boiling hydrocarbon mixtures by MFI and FAU membranes made by secondary growth*, Micropor. Mesopor. Mater. 48 (2001) 219-28.

Pachfule, Pradip, et al., *Solvothermal synthesis, structure, and properties of metal organic framework isomers derived from a partially fluorinated link*, Cryst. Growth Des. 11 (2011) 1215-22.

Pan, Long, et al., *Microporous metal organic materials: Promising candidates as sorbents for hydrogen storage*, J. Am. Chem. Soc. 126(5) (2004) 1308-09.

Parikh, Atul N., et al., *Non-thermal calcination by ultraviolet irradiation in the synthesis of microporous materials*, Micropor. Mesopor. Mater. 76 (2004) 17-22.

Qiu, Wulin, et al., *Dehydration of ethanol-water mixtures using asymmetric hollow fiber membranes from commercial polyimides*, J. Membr. Sci. 327 (2009) 96-103.

Ranjan, Rajiv and Michael Tsapatsis, *Microporous metal organic framework membrane on porous support using the seeded growth method*, Chem. Mater. xxx(xx) (2009) 000-000.

Sommer, Stefan and Thomas Melin, *Influence of operation parameters on the separation of mixtures by pervaporation and vapor permeation with inorganic membranes. Part 1: Dehydration of solvents*, Chem. Eng. Sci. 60 (2005) 4509-23.

Son, Won-Jin, et al., *Sonochemical synthseis of MOF-5*, Chem. Commun. 47 (2008) 6336-38.

Van Den Bergh, J., et al., *Separation and permeation characteristics of a DD3R zeolite membrane*, J. Membr. Sci. 316 (2008) 35-45.

Van Den Bergh, Johan, et al., *Modeling permeation of CO_2/CH_4, N_2/Ch_4, and CO_2/air mixtures across a DD3R zeolite membrane*, J. Phys. Chem. C 114(20) (2010) 9379-89.

Venna, Surendar R. and Moises A. Carreon, *Highly permeable zeolite imidazolate framework-8 membranes for CO2/CH4 separation*, J. Am. Chem. Soc.132(1) (2010) 76-78.

Watanabe, Taku, et al., *Computational identification of a metal organic framework for high selectivity membrane-based CO_2 /CH_4 separations: $Cu(hfipbb)(H_2hfipbb)_{0.5}$*, Phys. Chem. Chem. Phys. 11 (2009) 11389-94.

Xomeritakis, George, et al., *Transport properties of alumina-supported MFI membranes made by secondary (seeded) growth*, Micropor. Mesopor. Mater. 38 (2000) 61-73.

(56) **References Cited**

OTHER PUBLICATIONS

Weh, K., et al., *Permeation of single gases and gas mixtures through faujasite-type molecular sieve membranes*, Micropor. Mesopor. Mater. 54 (2002) 27-36.

Xu, Gengsheng, et al., *Preparation of ZIF-8 membranes supported on ceramic hollow fibers from a concentrated synthesis gel*, J. Membr. Sci. 385-386 (2011) 187-93.

Yao, Jianfeng, et al., *Contra-diffusion synthesis of ZIF-8 films on a polymer substrate*, Chem. Commun. 47 (2011) 2559-61.

Yan, Yushan, et al., *Preparation of highly selective zeolite ZSM-5 membranes by a post-synthetic coking treatment*, J. Membr. Sci. 123(1) (1997) 95-103.

Yang, Lisha and Huimin Lu, *Microwave-assisted ionothermal synthesis and characterization of zeolitic imidazolate framework-8*, Chinese J. Chem. 30 (2012) 1040-44.

Yoo, Won Cheol, et al., *High-performance randomly oriented zeolite membranes using brittle seeds and rapid thermal processing*, Angew. Chem. Int. Ed. 49 (2010) 8699-703.

Zhang, Yanfeng, et al., *Blocking defects in SAPO-34 membranes with cyclodextrin*, J. Membr. Sci. 358 (2010) 7-12.

Zheng, Zhenkun, et al., *Synthesis, characterization and modification of DDR membranes grown on alpha-alumina supports*, J. Mater. Sci. 43 (2008) 2499-502.

PCT Jul. 27, 2012 International Search Report and Written Opinion issued in International Patent Application PCT/US2012/025064.

PCT May 25, 2012 International Search Report and Written Opinion issued in International Patent Application PCT/US2012/025080.

PCT Nov. 6, 2012 International Search Report and Written Opinion issued in International Patent Application PCT/US2012/054817.

PCT Feb. 23, 2012 International Search Report and Written Opinion issued in International Patent Application PCT/US2011/047769.

PCT Oct. 18, 2013 International Search Report and Written Opinion issued in International Patent Application PCT/US2013/042075.

Mar. 5, 2013 Office Action mailed for U.S. Appl. No. 13/611,988, filed Sep. 12, 2012.

Jun. 5, 2013 Response to Office Action dated Mar. 5, 2013 for U.S. Appl. No. 13/611,988, filed Sep. 12, 2012.

Jun. 10, 2013 Office Action/Noncompliant Amendment mailed for U.S. Appl. No. 13/611,988, filed Sep. 12, 2012.

Jun. 14, 2013 Response to Office Action/Noncompliant Amendment dated Jun. 10, 2013 for U.S. Appl. No. 13/611,988, filed Sep. 12, 2012.

Sep. 5, 2013 Office Action mailed for U.S. Appl. No. 13/611,988, filed Sep. 12, 2012.

Nov. 5, 2013 Response to Final Office Action dated Sep. 5, 2013 for U.S. Appl. No. 13/611,988, filed Sep. 12, 2012.

Nov. 18, 2013 Notice of Allowability mailed for U.S. Appl. No. 13/611,988, filed Apr. 4, 2011.

Nov. 20, 2013 Notice of Allowability mailed for U.S. Appl. No. 13/399,645, filed Feb. 17, 2012.

Marler, et al., *Studies on clathrasils VIII. Nonasils*-[$4^1 5^8$], *$88SiO_2*8M^8*8M^9*4M^{20}$: Synthesis, thermal properties, and crystal structure*, J. Inclusion Phenomena 4(4) (1986) 339-349.

Aksay, et al., *Biometric pathways for assembling inorganic thin films*, Science 273(5277) (1996) 892-898.

Miyata, et al., *Silica films with a single-crystalline mesoporous structure*, Nat. Mater. 3(9) (2004) 651-656.

Yang, et al., *Registered growth of mesoporous silica films on graphite*, J. Mater. Chem. 7(7) (1997) 1285-1290.

JP Jun. 17, 2014 Examiner's Decision of Refusal mailed in Japanese Patent Application 2012-543346 (with English Translation).

CN Mar. 9, 2015 Response to Office Action (with English translation of claims) filed in China Patent Application No. 201180052181.7.

JP Apr. 7, 2015 Office Action mailed in Japan Patent Application No. 2013-536619 (with English translation).

JP Apr. 24, 2015 English translation of Description and Claims for JP Patent Application Laid-Open No. 2002-338229.

JP Apr. 24, 2015 English translation of Description and Claims for JP Patent Application Laid-Open No. 2008-173576.

CN Dec. 2, 2014 Response to Office Action filed in China Patent Application No. 201080057358.8 (with English translation).

CN Mar. 16, 2015 Third Office Action mailed in China Patent Application No. 201080057358.8 (with English translation).

Sep. 1, 2015 Office Action mailed in U.S. App. No. 13/897,939, filed May 20, 2013.

Dec. 1, 2015 Amendment and Response to Office Action dated Sep. 1, 2015 in U.S. Appl. No. 13/897,939, filed May 20, 2013.

JP Dec. 15, 2015 Office Action mailed in Japan Patent Application No. 2013-536619 (with English translation).

Brown, et al., *Interfacial microfluidic processing of metal-organic framework hollow fiber membranes*, Science 345(6192) (2014) 72-75.

Calvo, et al., *Pore size distributions in macroporous membranes*, J. Colloid & Interface Sci. 176(2) (1995) 467-78.

Khare, et al., *A quantitative method for measuring nanocomposite dispersion*, Polymer 51 (2010) 719-29.

Korelskiy, et al., *Characterization of flow-through micropores in MFI membranes by permporometry*, J. Membr. Sci. 417-418 (2012) 183-92, Accepted manuscript (2015).

Zhang, et al., *Unexpected molecular sieving properties of Zeolitic Imidazolate Framework-8*, J. Phys. Chem. Lett. 3(16) (2012) 2130-34.

Feb. 2, 2016 Final Office Action mailed in U.S. Appl. No. 13/897,939, filed May 20, 2013.

Mar. 15, 2016 Amendment and Response to Final Office Action dated Feb. 2, 2016; and First Request for Continued Examination filed in U.S. Appl. No. 13/897,939, filed May 20, 2013.

Mar. 22, 2016 Notice of Allowance / Notice of Allowability mailed in U.S. Appl. No. 13/897,939, filed May 20, 2013.

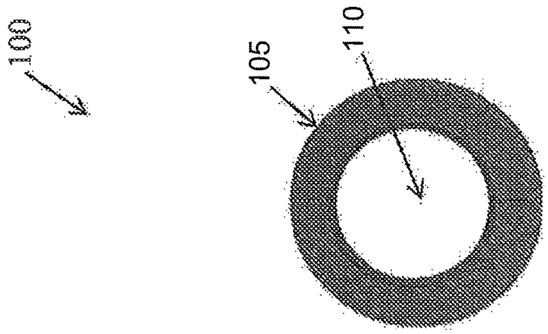

FIG. 1B

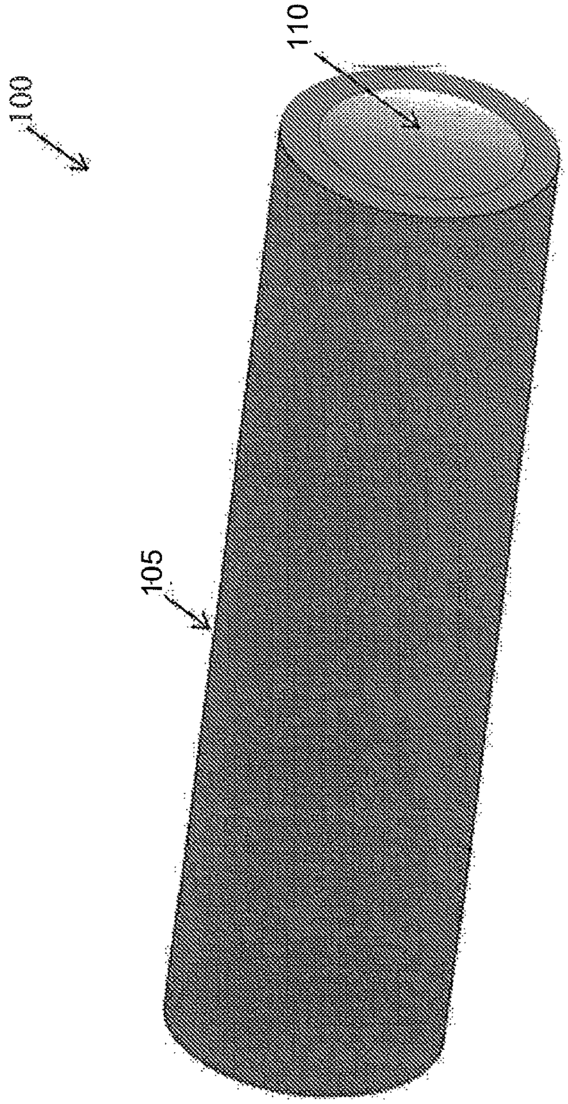

FIG. 1A

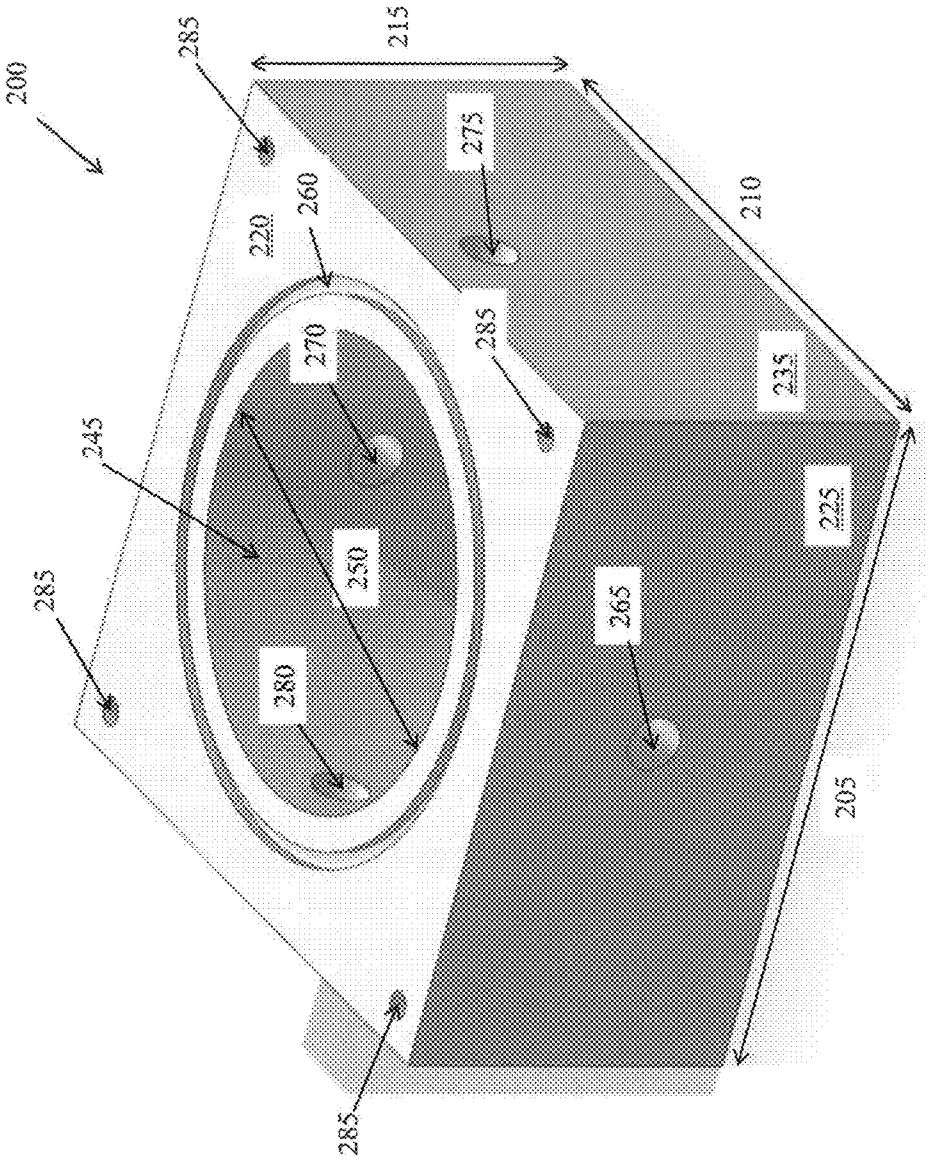
200
285
215
275
210
220
260
270
285
235
245
250
225
265
285
280
205
285

FIG. 2

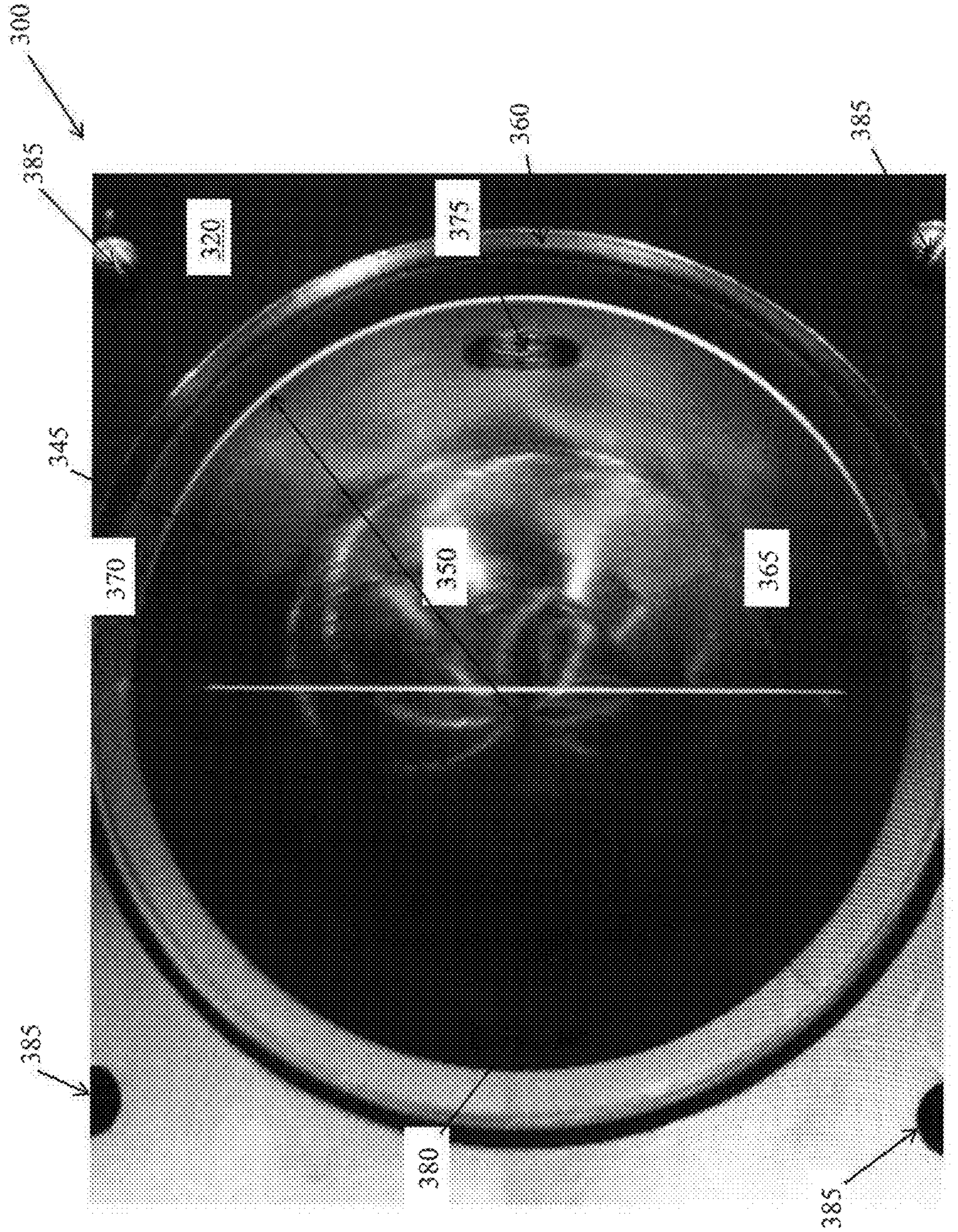

FIG. 3

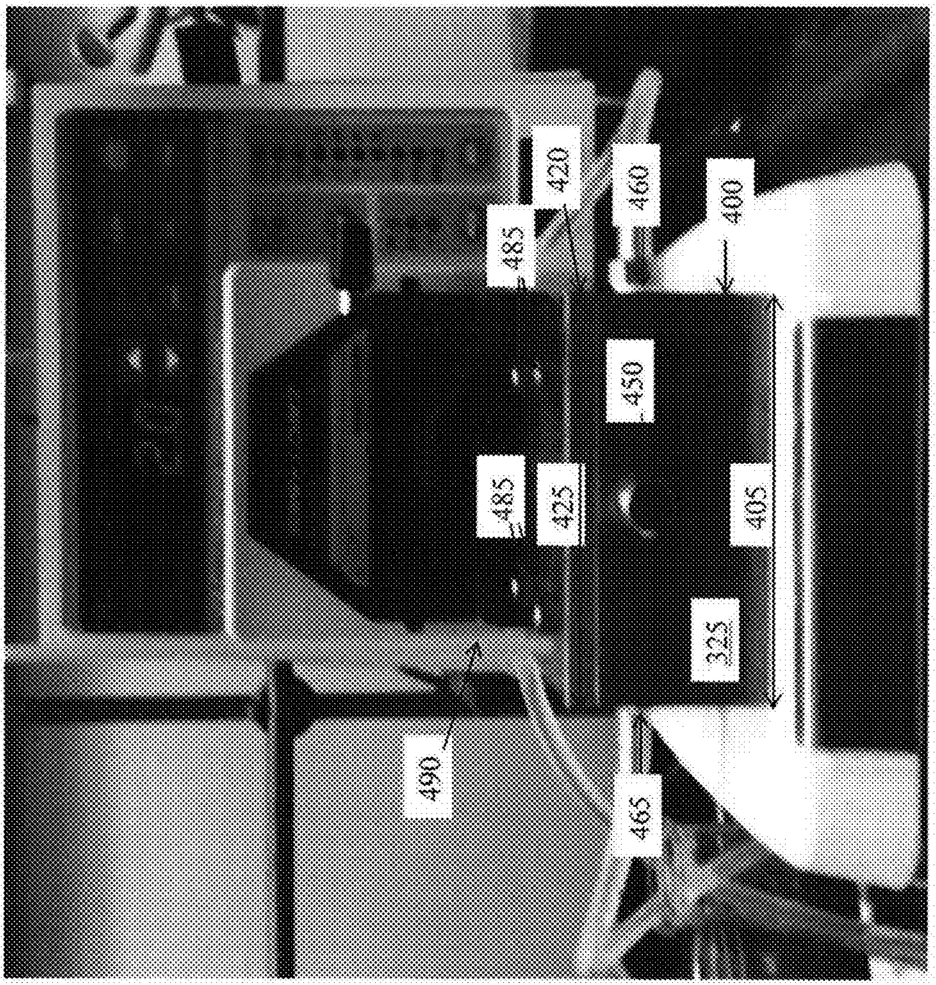

FIG. 4

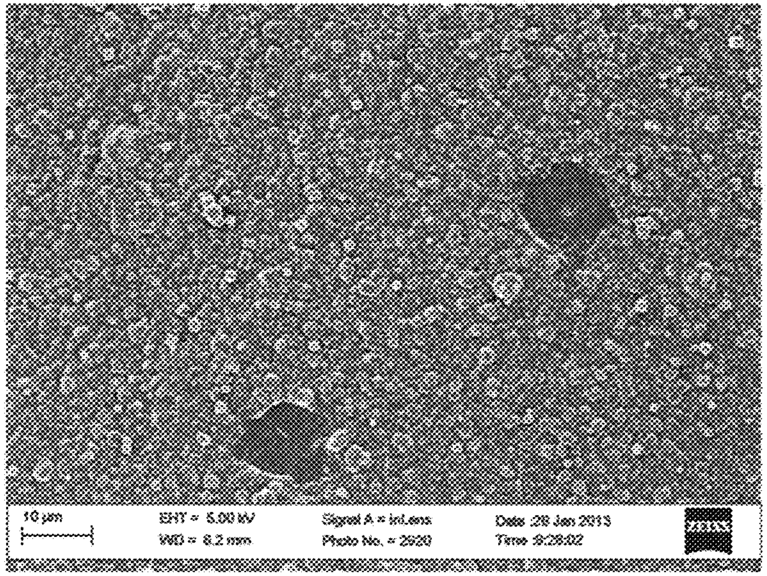
10 µm
EHT = 5.00 kV
WD = 8.2 mm
Signal A = InLens
Photo No. = 2920
Date :28 Jan 2013
Time :9:28:02

FIG. 5A

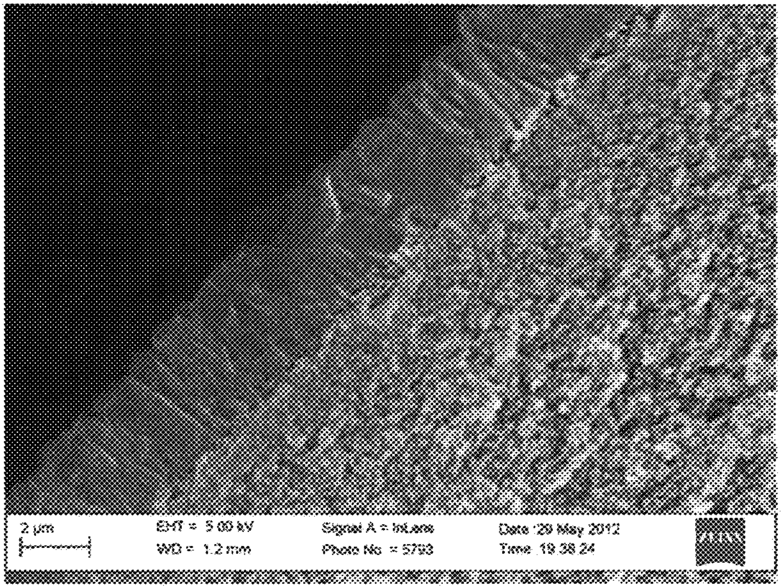
2 µm
EHT = 5.00 kV
WD = 1.2 mm
Signal A = InLens
Photo No. = 5793
Date :29 May 2012
Time :19:38:24

FIG. 5B

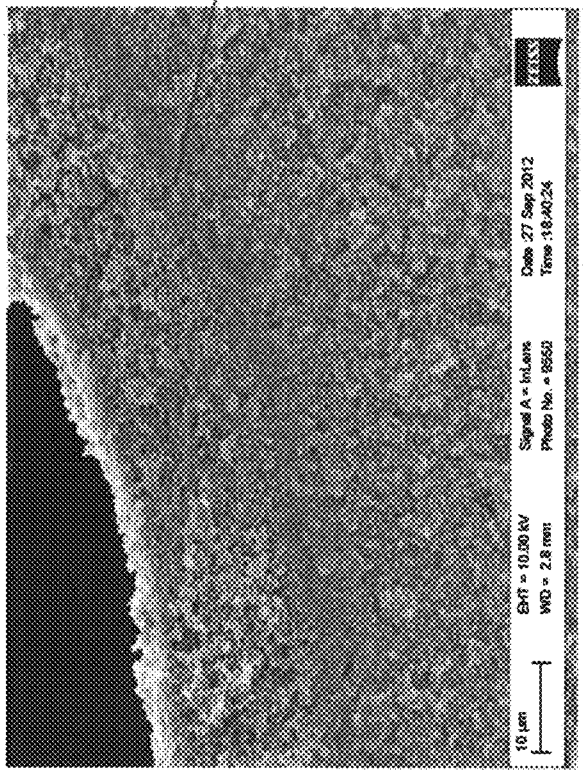
10 µm
EHT = 10.00 kV
WD = 2.8 mm
Signal A = InLens
Photo No. = 9550
Date :27 Sep 2012
Time :16:40:24

FIG. 6A

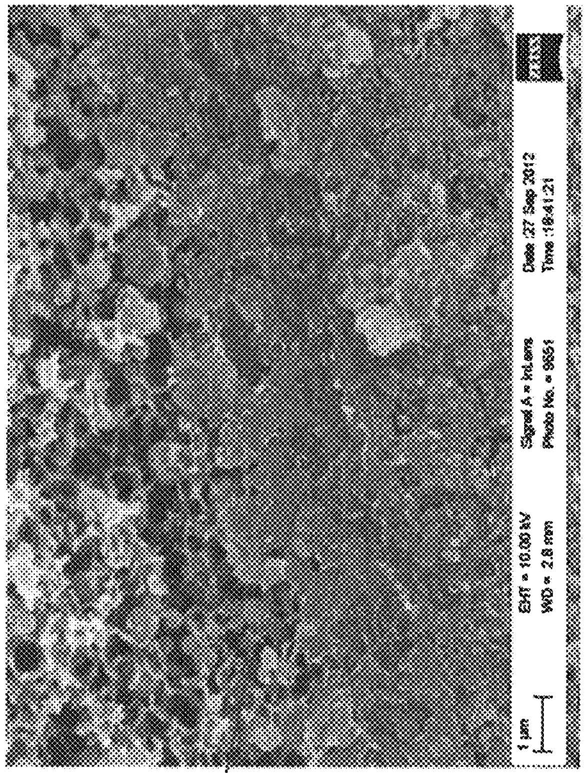
1 µm
EHT = 10.00 kV
WD = 2.8 mm
Signal A = InLens
Photo No. = 9551
Date :27 Sep 2012
Time :16:41:21

FIG. 6B

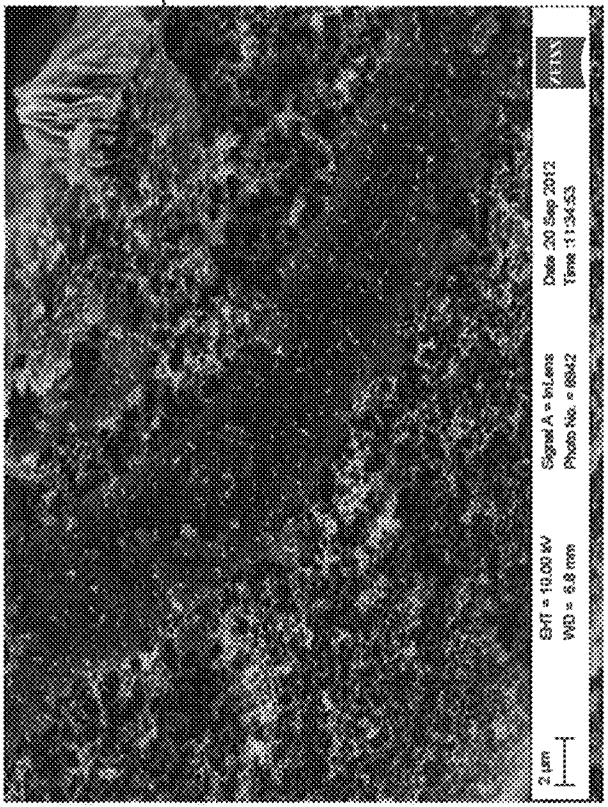
2 µm
EHT = 10.00 kV
WD = 6.8 mm
Signal A = InLens
Photo No. = 6842
Date :20 Sep 2012
Time :11:34:53

FIG. 7A

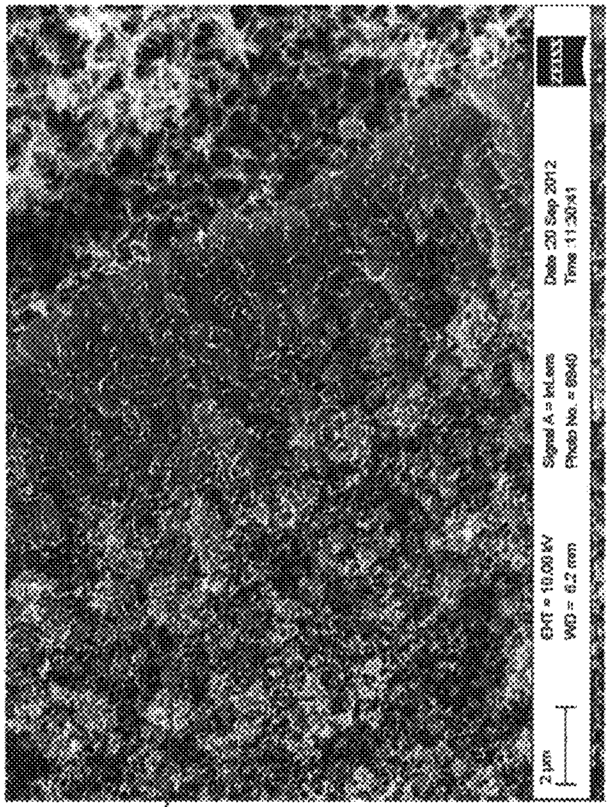
2 µm
EHT = 10.00 kV
WD = 6.2 mm
Signal A = InLens
Photo No. = 6840
Date :20 Sep 2012
Time :11:30:41

FIG. 7B

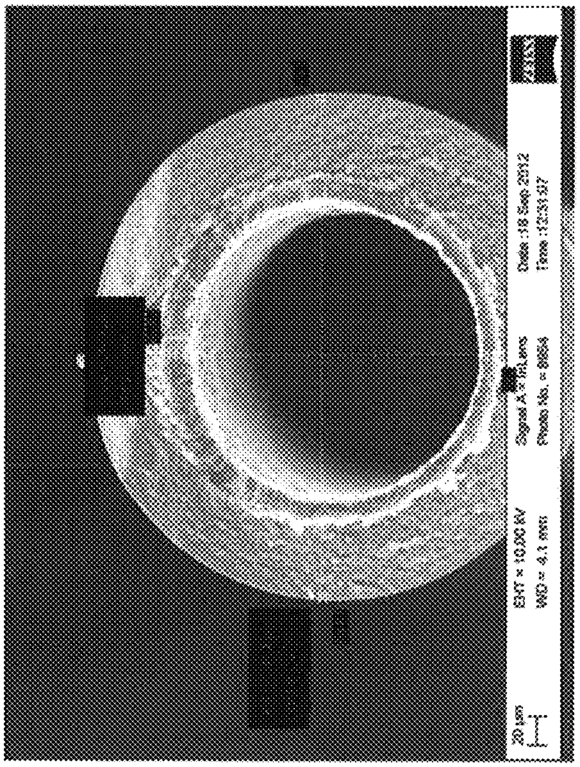
20 µm
EHT = 10.00 kV
WD = 4.1 mm
Signal A = InLens
Photo No. = 9854
Date :18 Sep 2012
Time :12:31:37

FIG. 8A

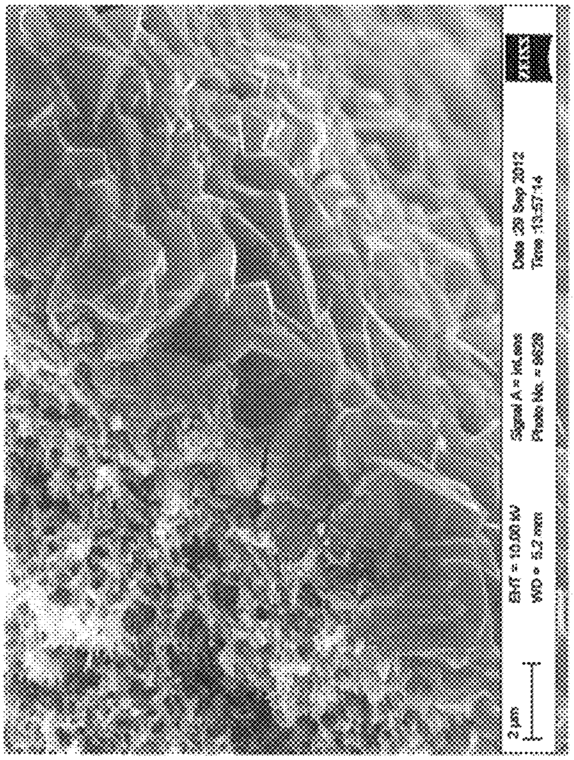
2 µm
EHT = 10.00 kV
WD = 5.2 mm
Signal A = InLens
Photo No. = 9628
Date :20 Sep 2012
Time :13:57:14

FIG. 8B

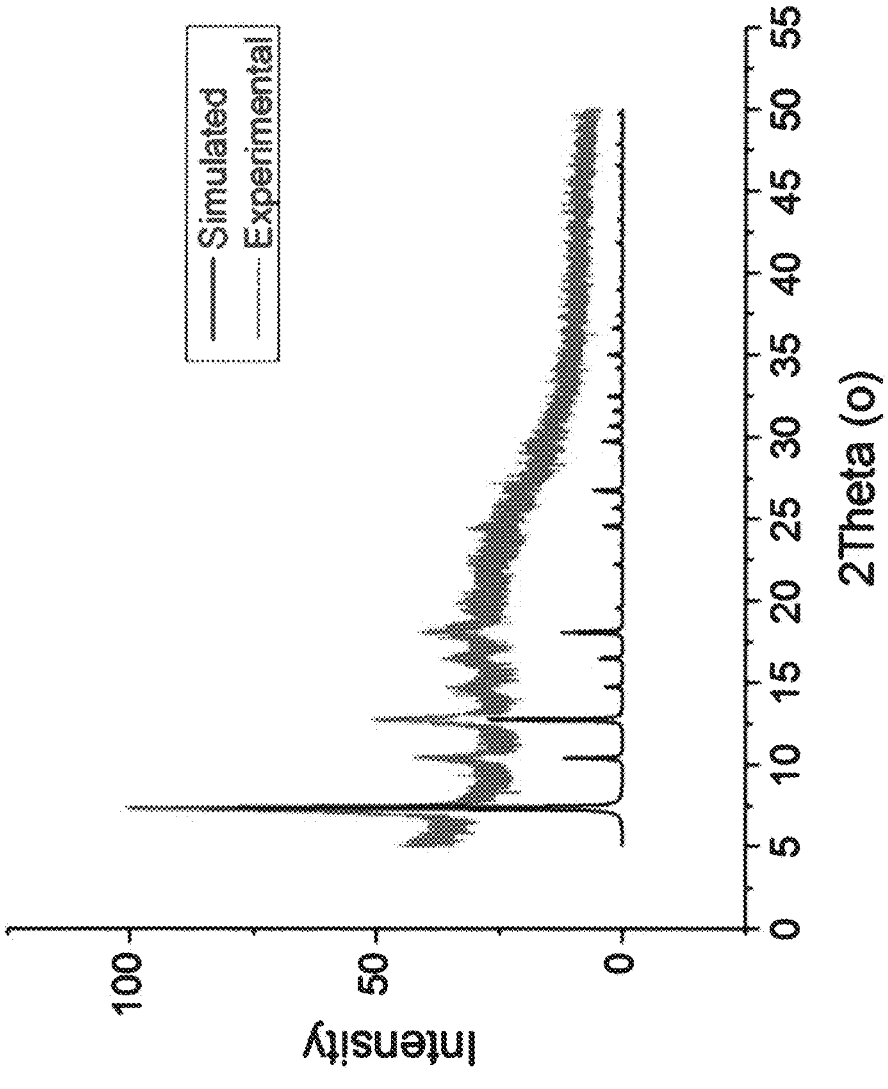
Intensity
100
50
0
0
5
10
15
20
25
30
35
40
45
50
55
2Theta (o)
Simulated
Experimental

FIG. 9

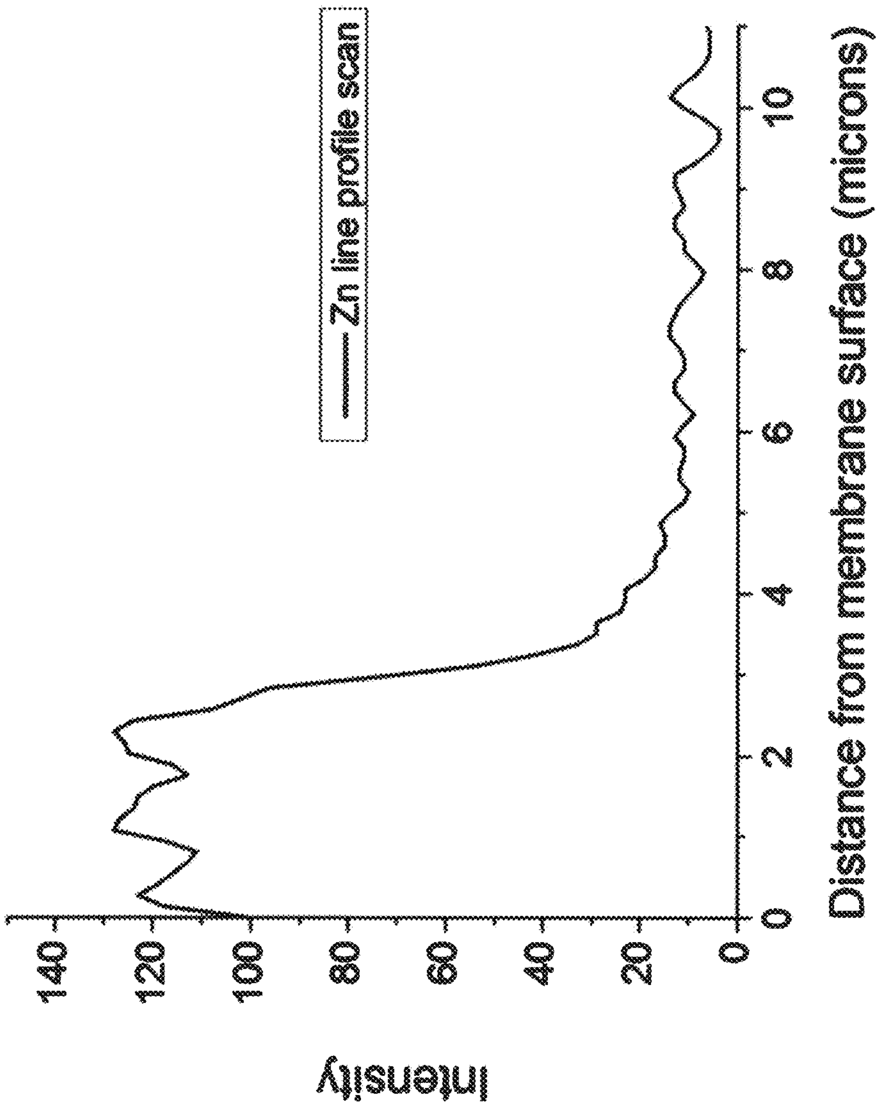
Zn line profile scan
Intensity
140
120
100
80
60
40
20
0
0
2
4
6
8
10
Distance from membrane surface (microns)

FIG. 10

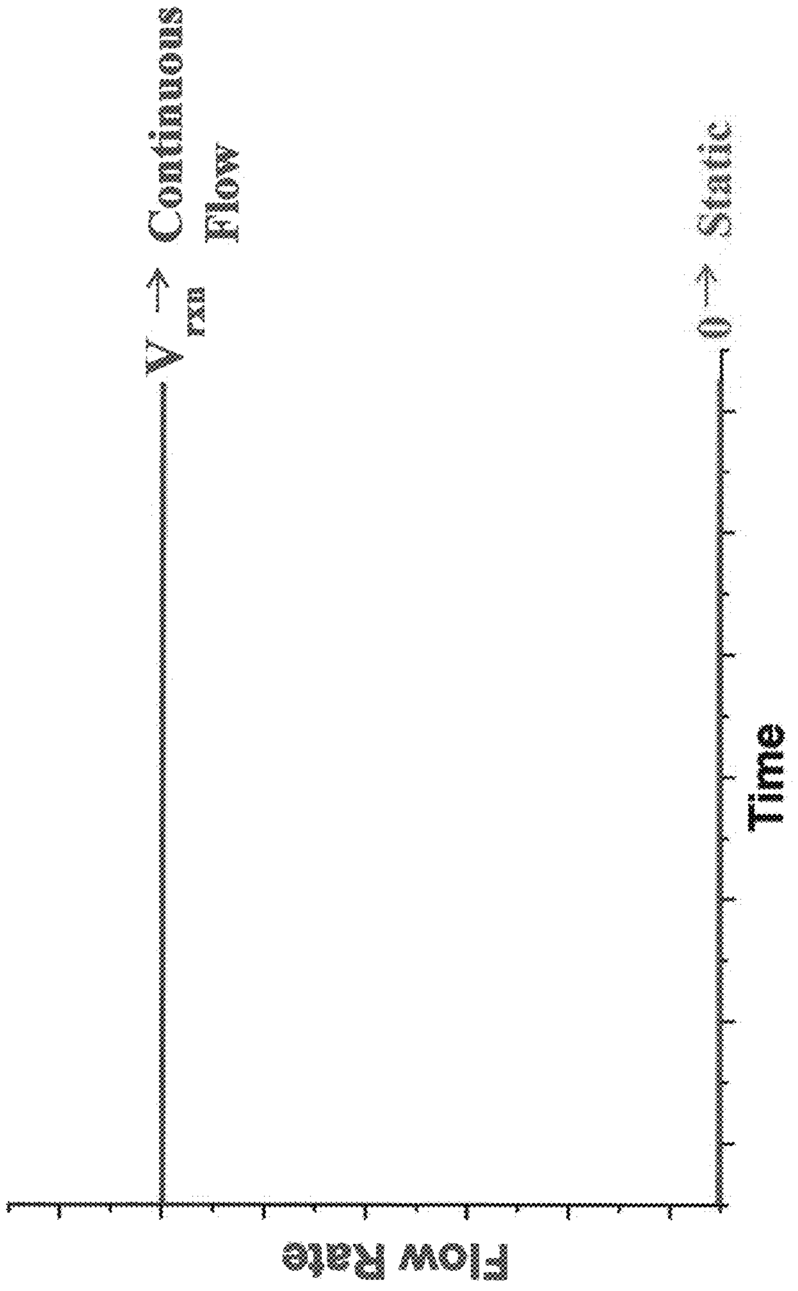

FIG. 11

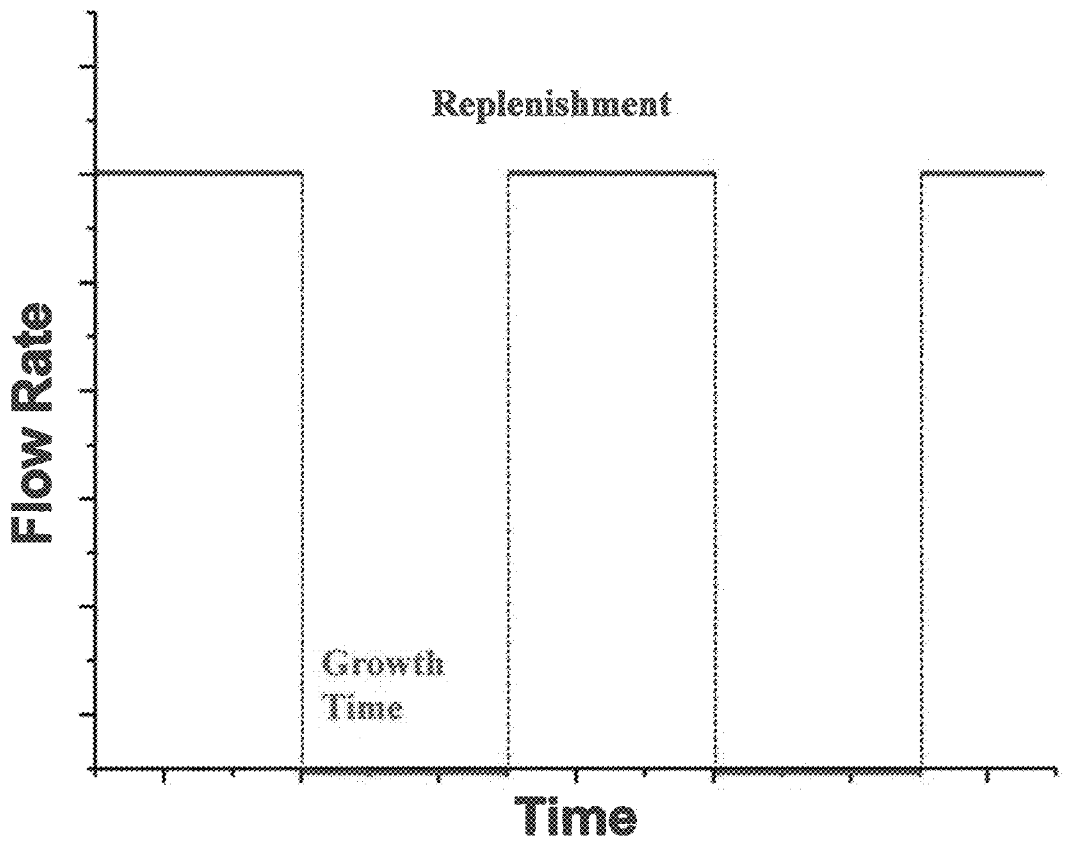

FIG. 12

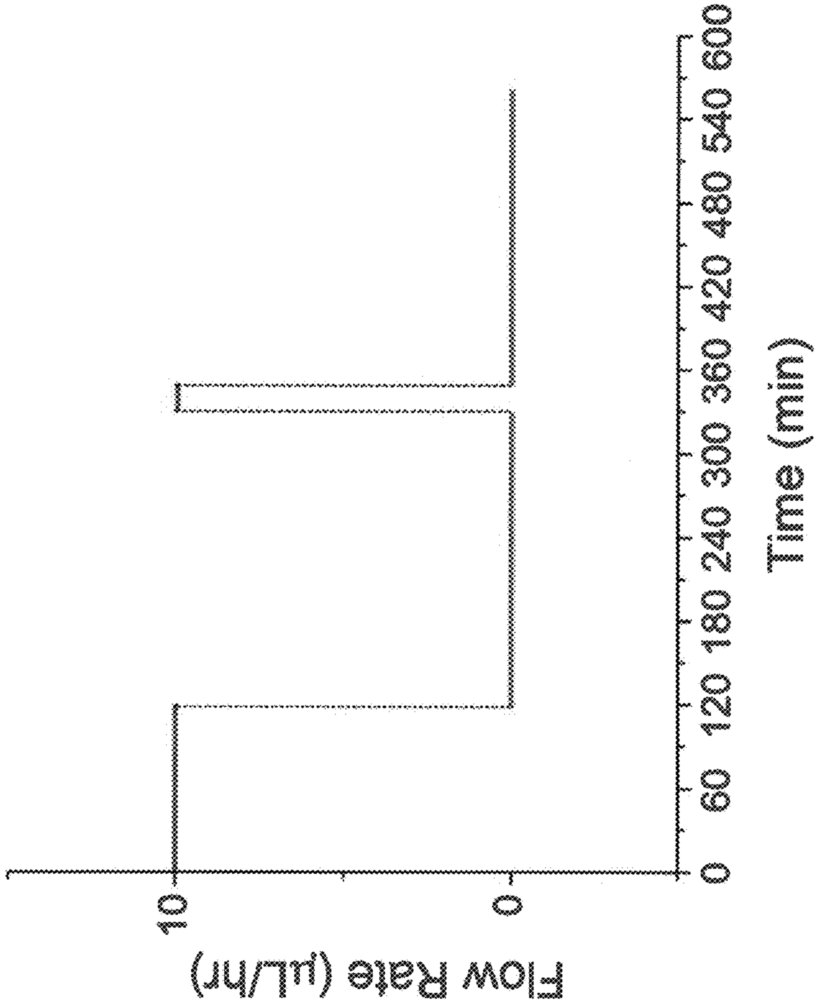
Flow Rate (µL/hr)
10
0
Time (min)
0
60
120
180
240
300
360
420
480
540
600

FIG. 13

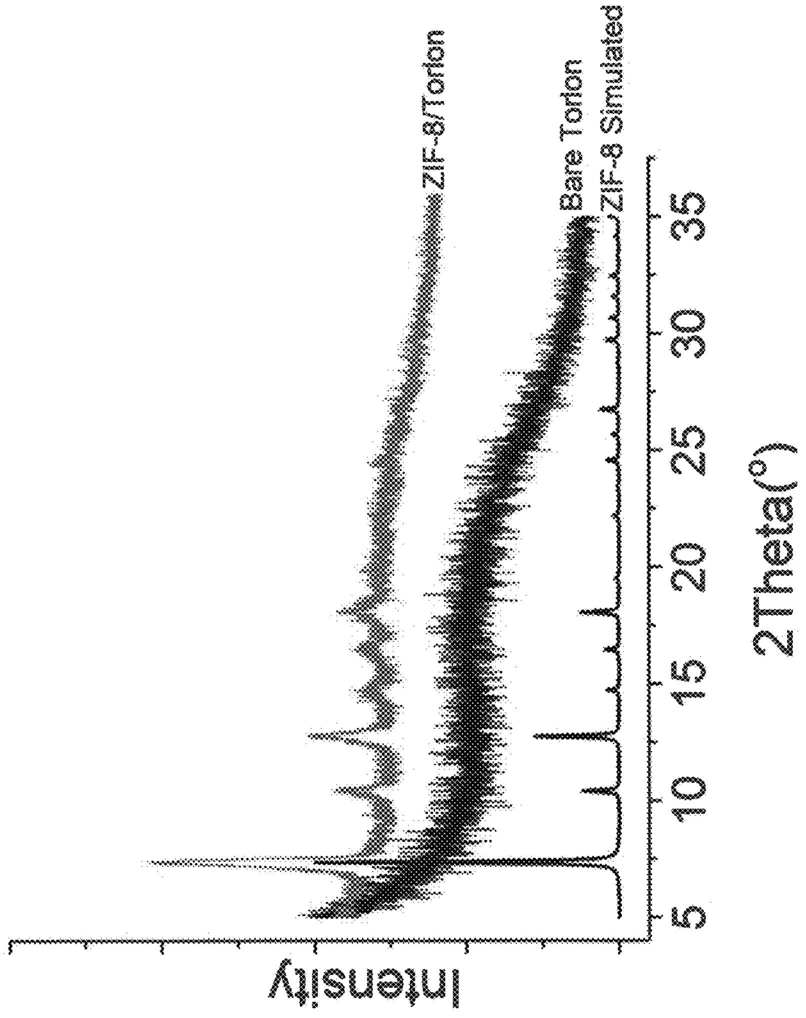
Intensity
2Theta(°)
5
10
15
20
25
30
35
ZIF-8/Torlon
Bare Torlon
ZIF-8 Simulated

FIG. 14

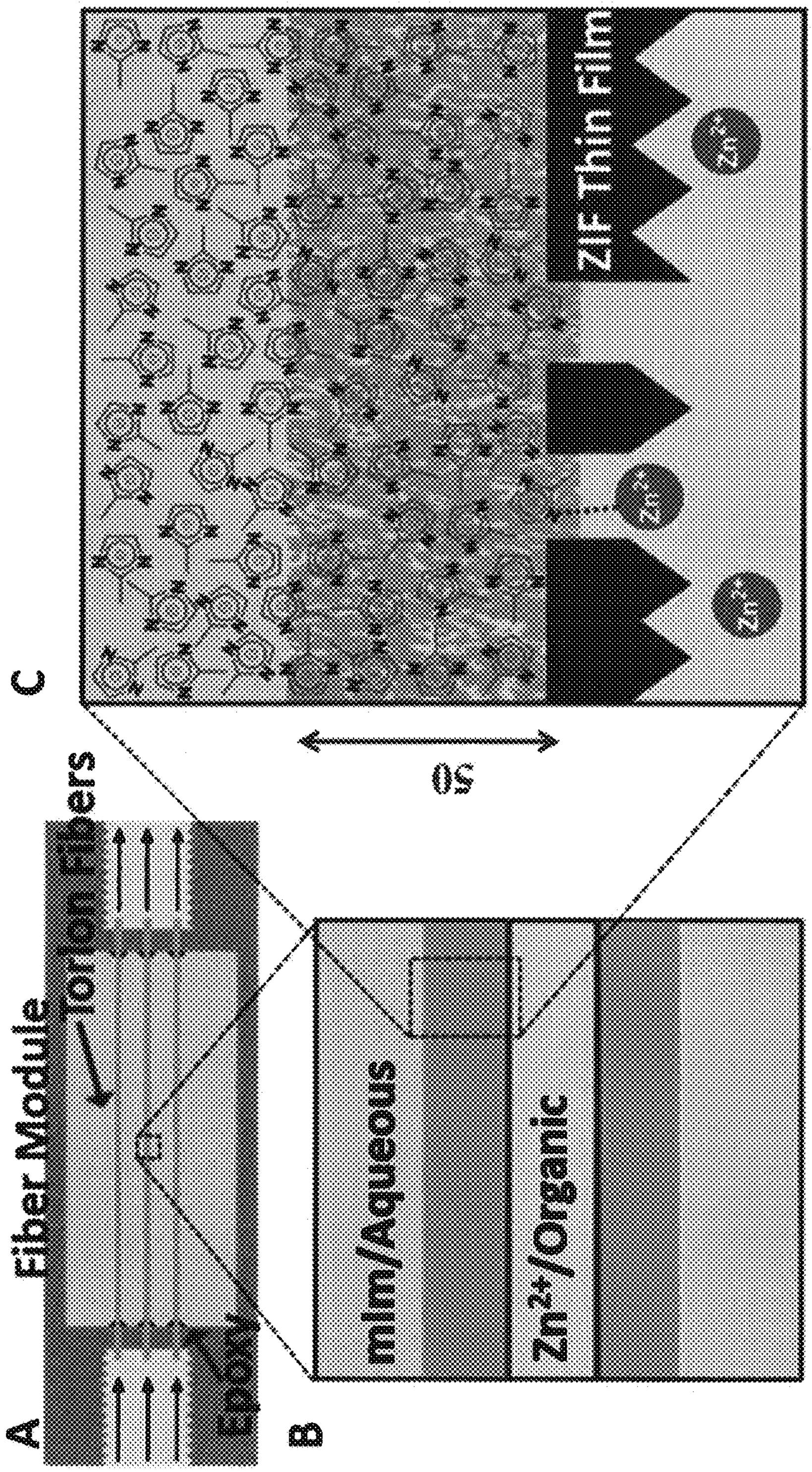
A
Fiber Module
Torlon Fibers
Epoxy
B
mIm/Aqueous
Zn^{2+}/Organic
C
ZIF Thin Film
Zn^{2+}
Zn^{2+}
Zn^{2+}
Zn^{2+}
50

FIG. 15

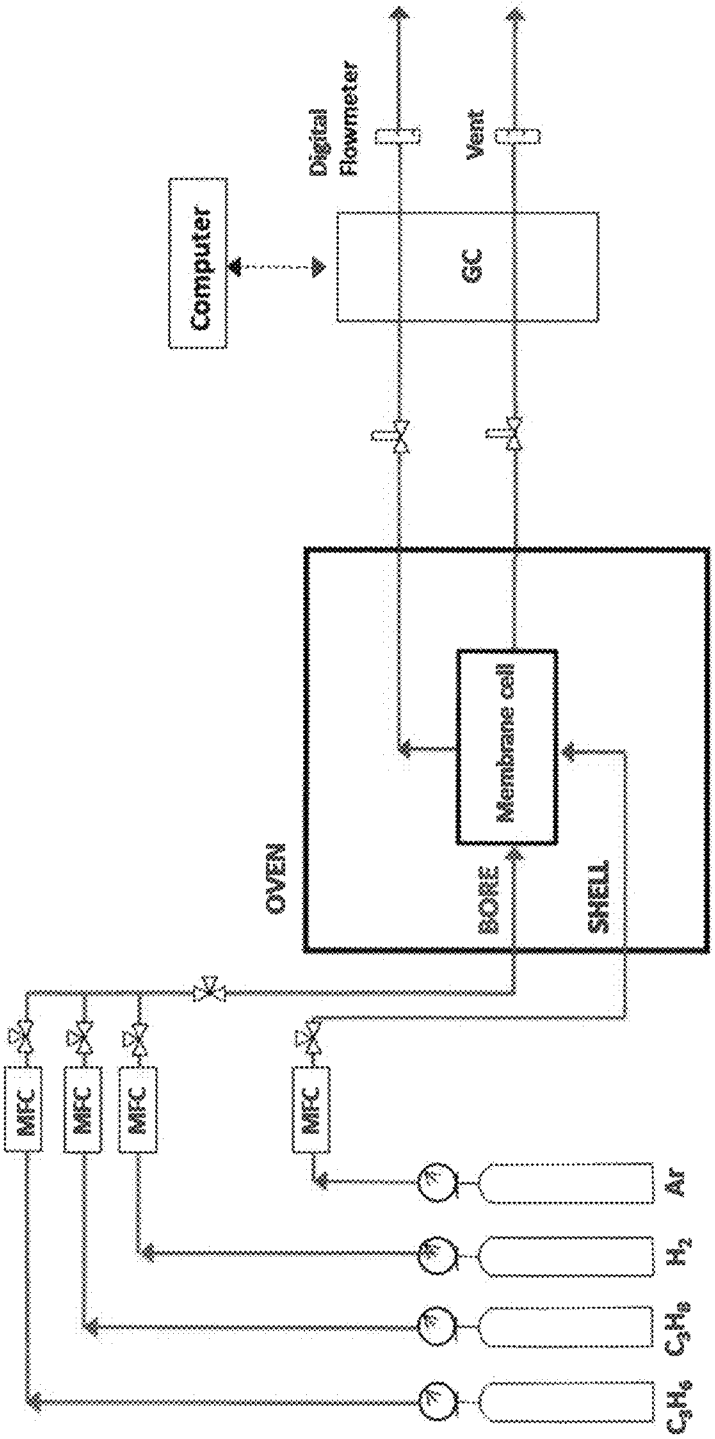
Computer
GC
Digital Flowmeter
Vent
OVEN
Membrane cell
BORE
SHELL
MFC
MFC
MFC
MFC
Ar
H_2
C_3H_8
C_3H_6

FIG. 16

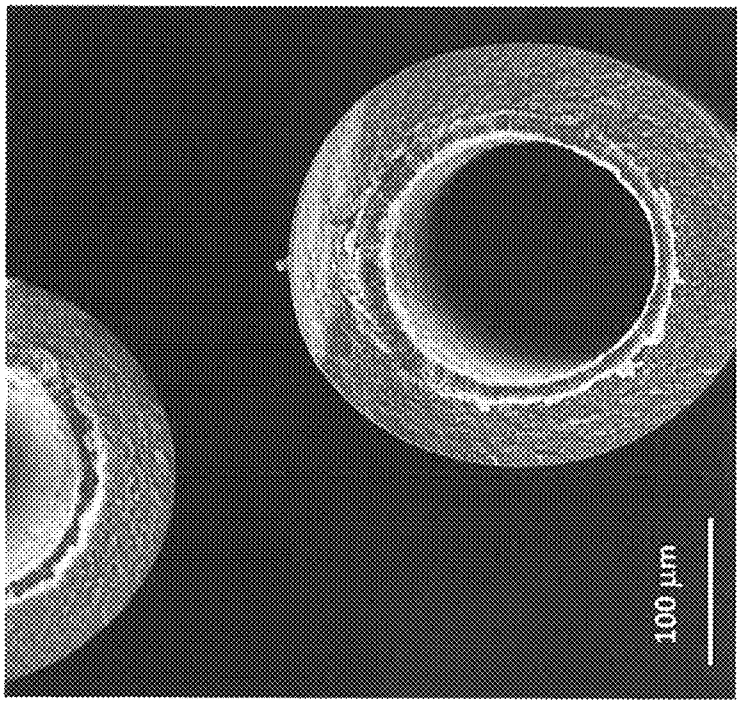

FIG. 17A

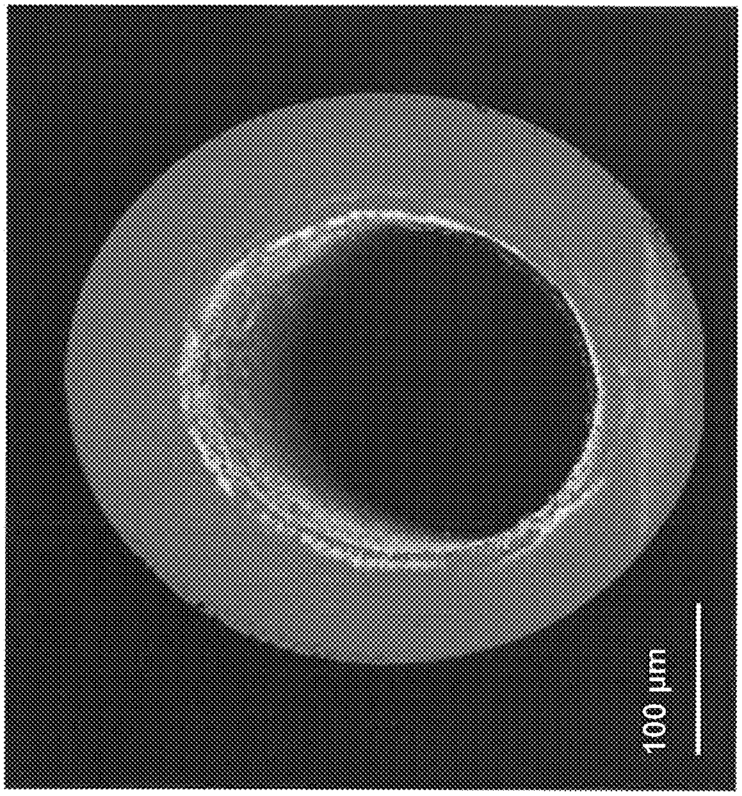

FIG. 17B

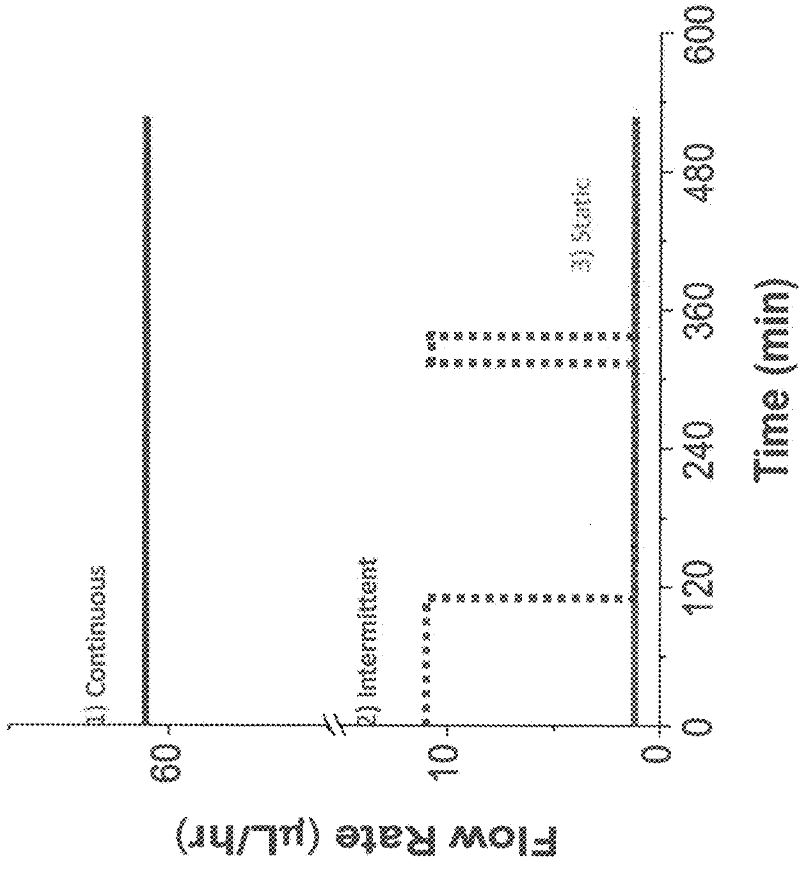
Flow Rate (µL/hr)
60
10
0
0
120
240
360
480
600
Time (min)
1) Continuous
2) Intermittent
3) Static

FIG. 18A

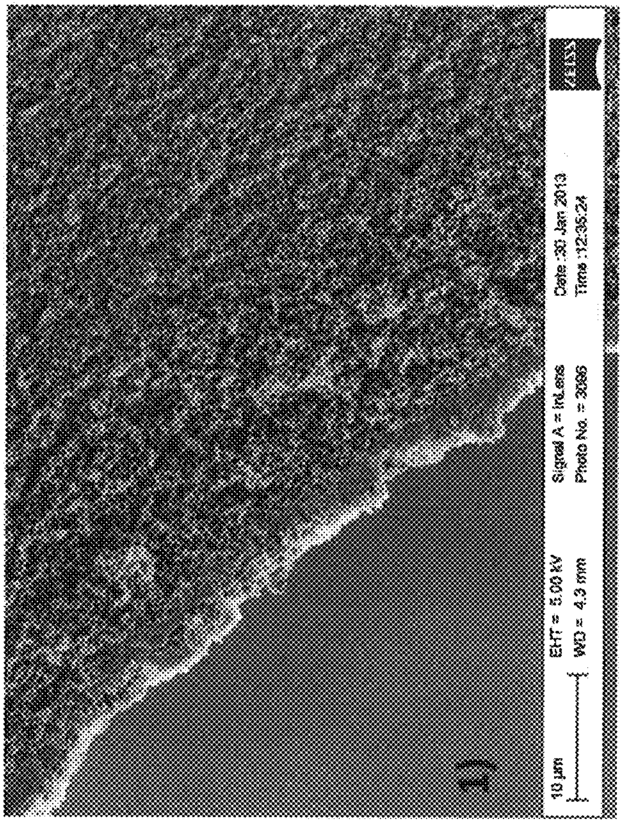

FIG. 18B

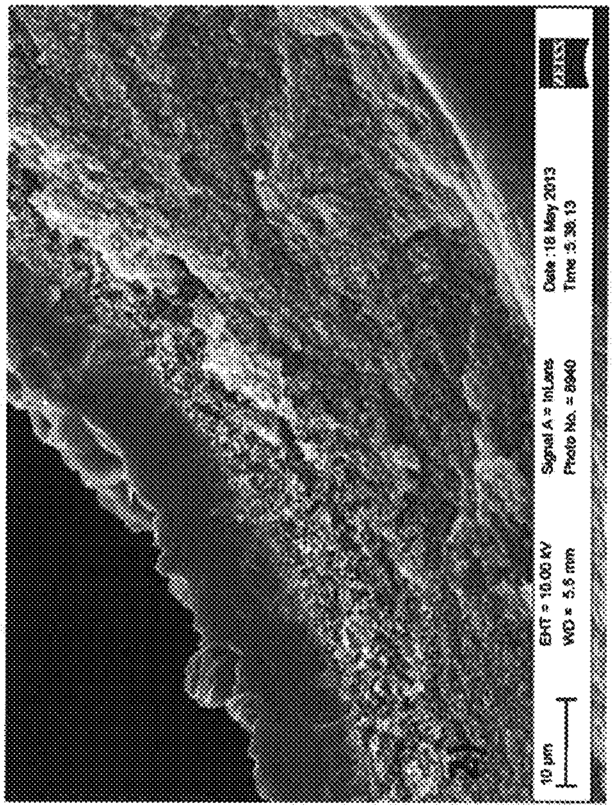

FIG. 18C

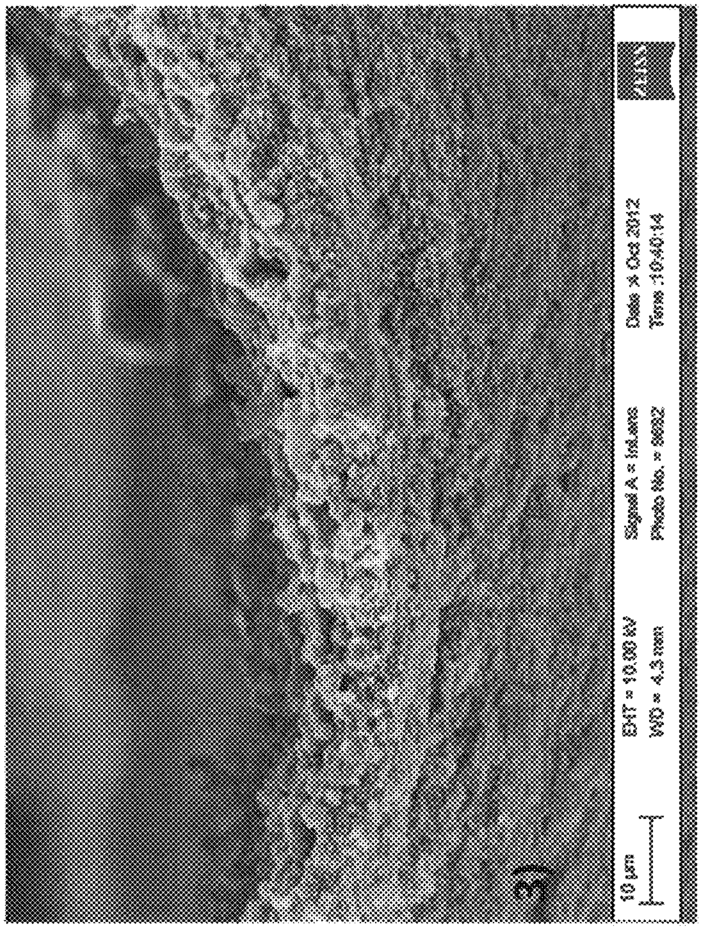
3)
10 µm
EHT = 10.00 kV
WD = 4.3 mm
Signal A = InLens
Photo No. = 8682
Date :4 Oct 2012
Time :10:40:14

FIG. 18D

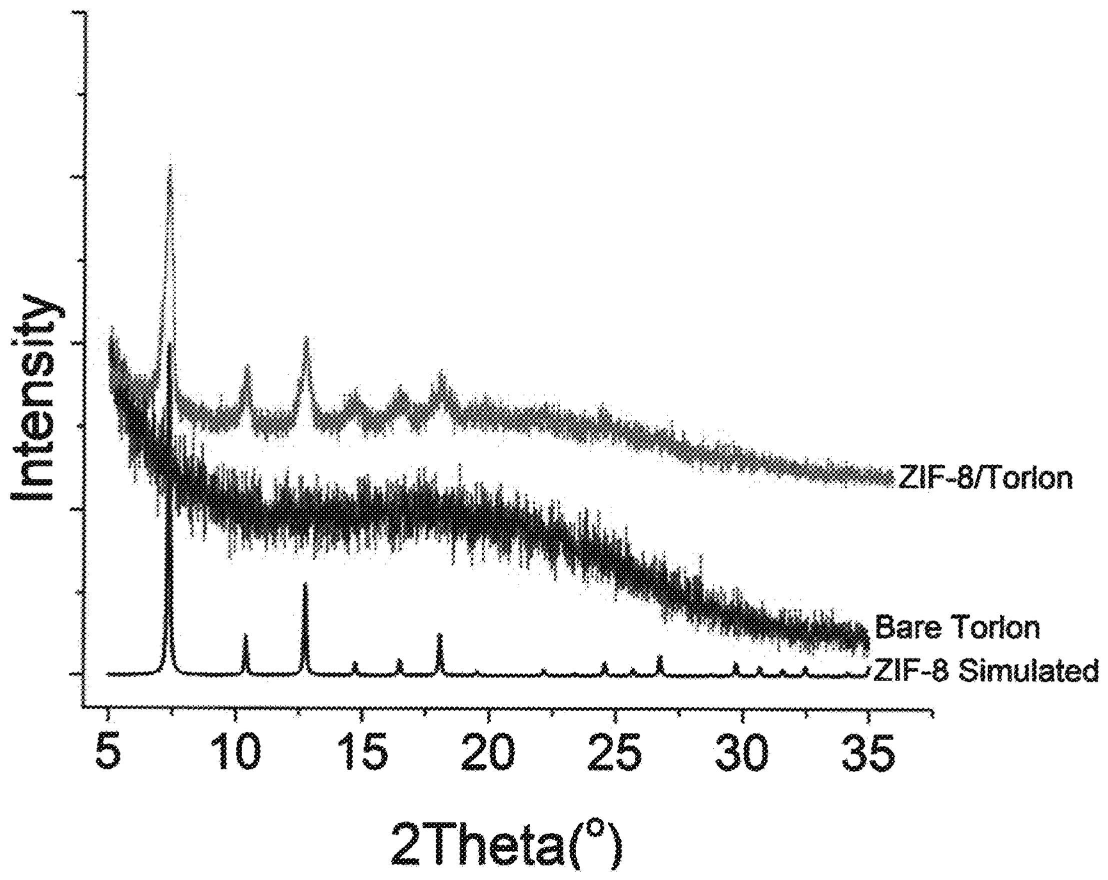
Intensity
ZIF-8/Torlon
Bare Torlon
ZIF-8 Simulated
5
10
15
20
25
30
35
2Theta(°)

FIG. 19

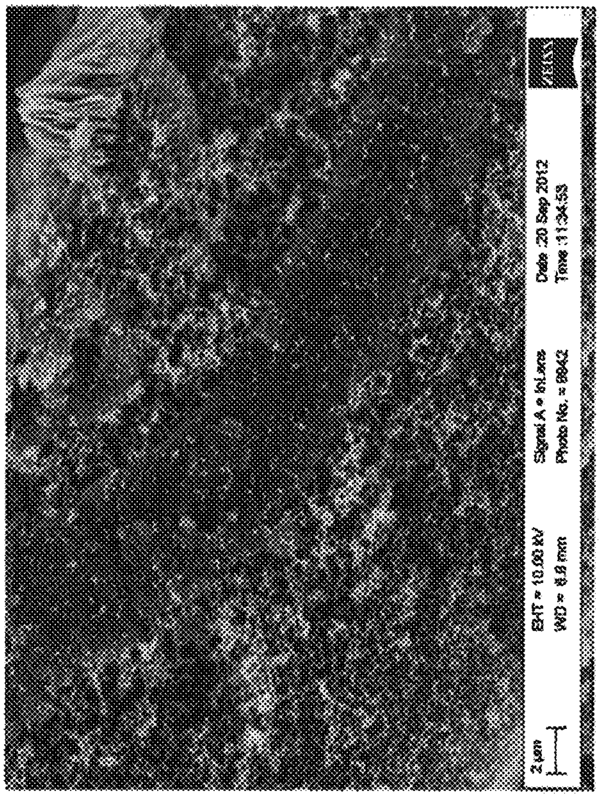

FIG. 20B

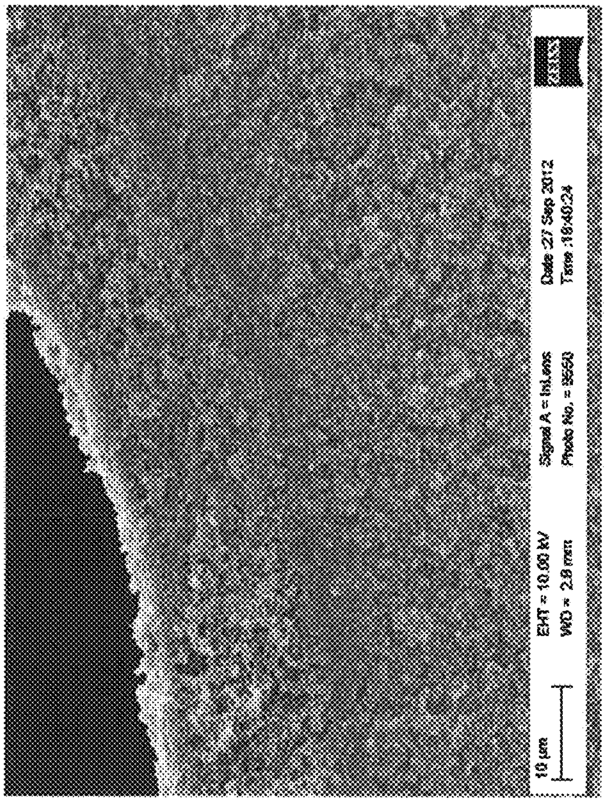

FIG. 20A

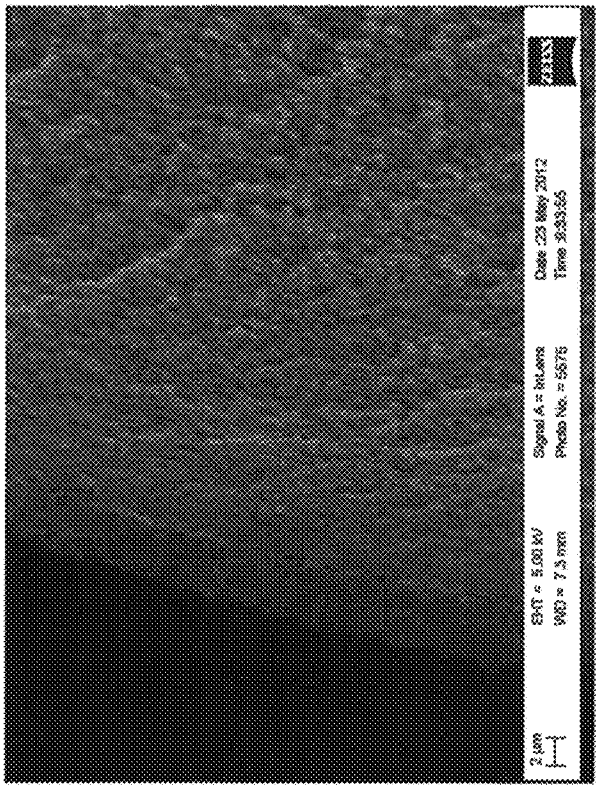

FIG. 20D

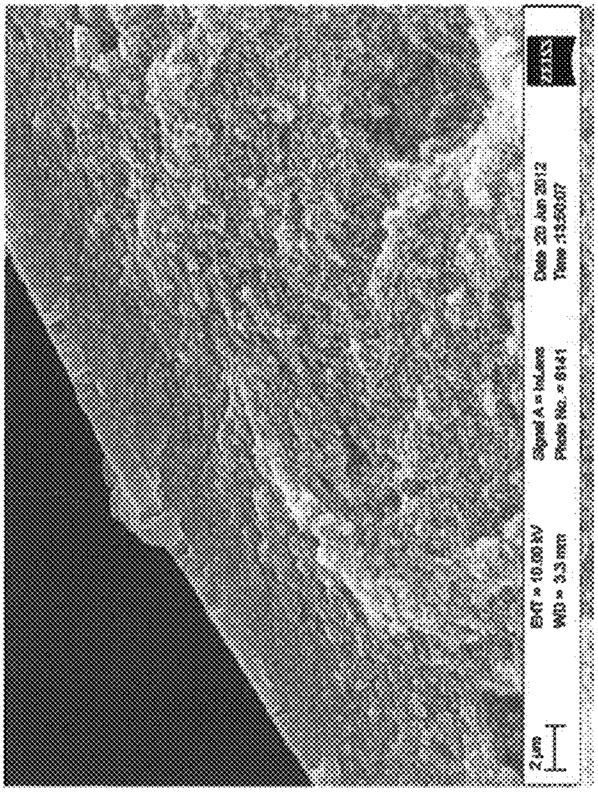

FIG. 20C

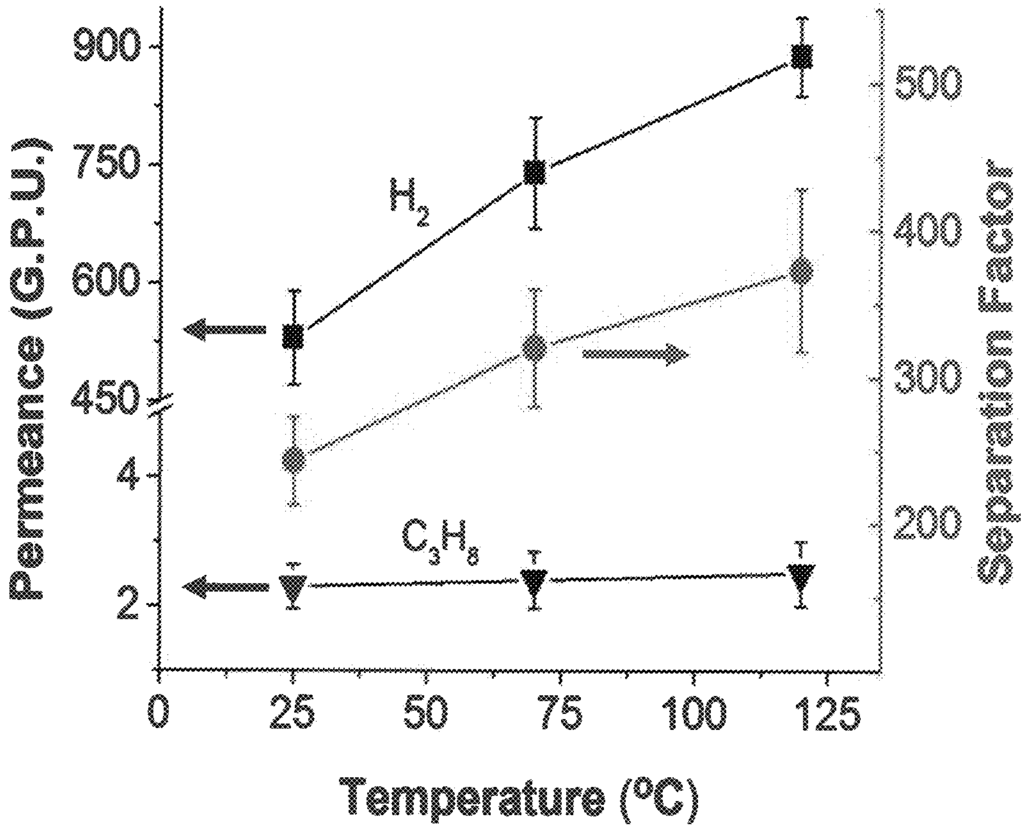
Permeance (G.P.U.)
900
750
600
450
4
2
Separation Factor
500
400
300
200
H$_2$
C$_3$H$_8$
0
25
50
75
100
125
Temperature (°C)

FIG. 21A

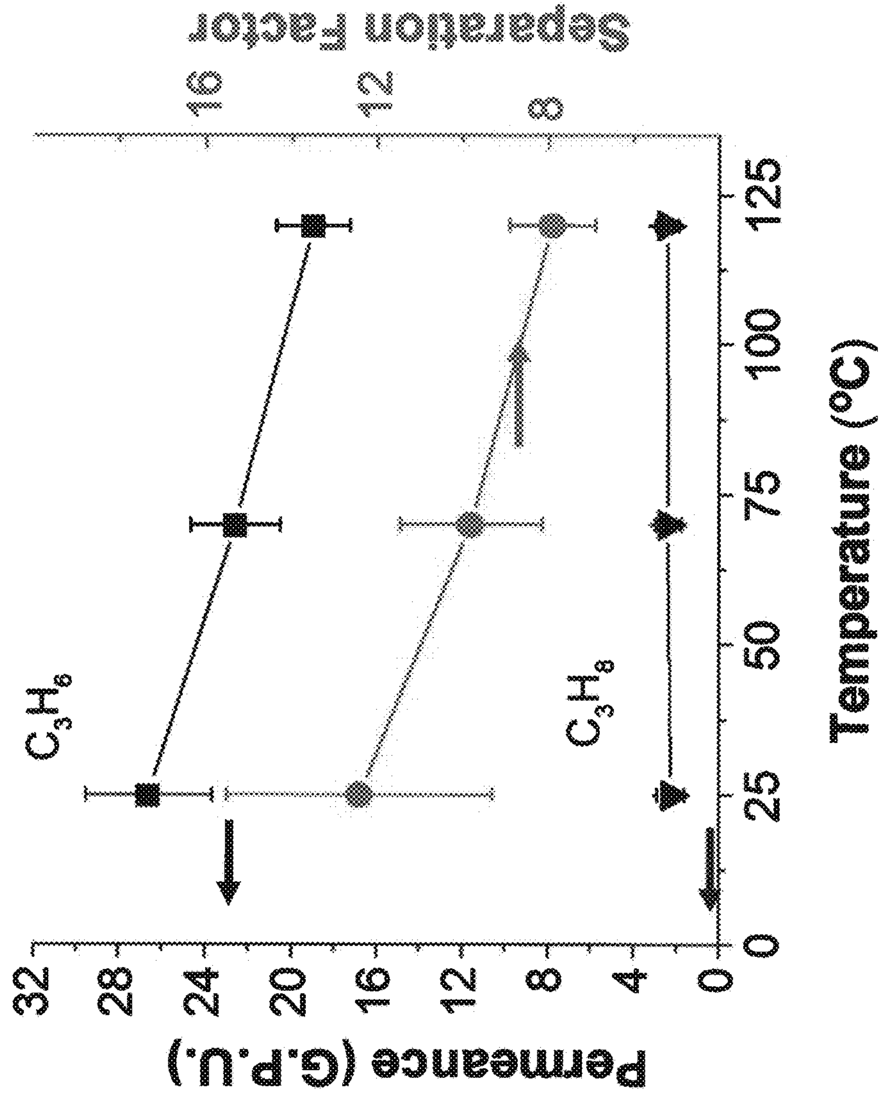
Permeance (G.P.U.)
0
4
8
12
16
20
24
28
32
Temperature (°C)
0
25
50
75
100
125
Separation Factor
8
12
16
C_3H_6
C_3H_8

FIG. 21B

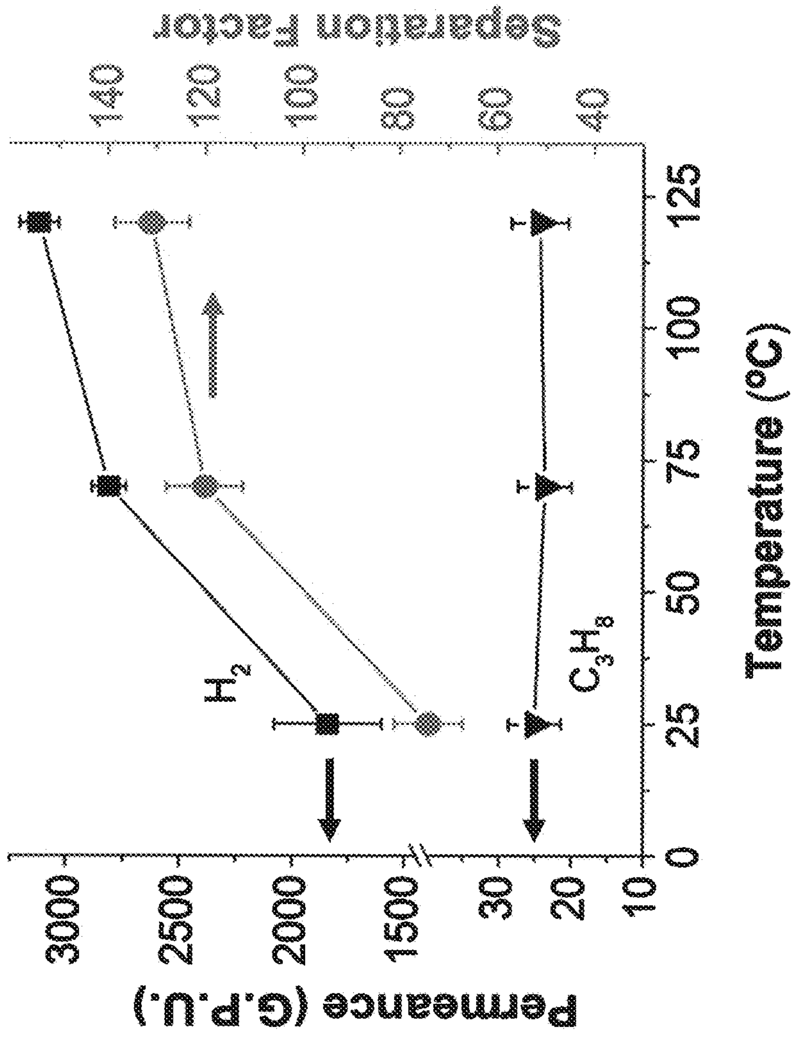
Permeance (G.P.U.)
3000
2500
2000
1500
30
20
10
0
25
50
75
100
125
Temperature (°C)
Separation Factor
140
120
100
80
60
40
H_2
C_3H_8

FIG. 22A

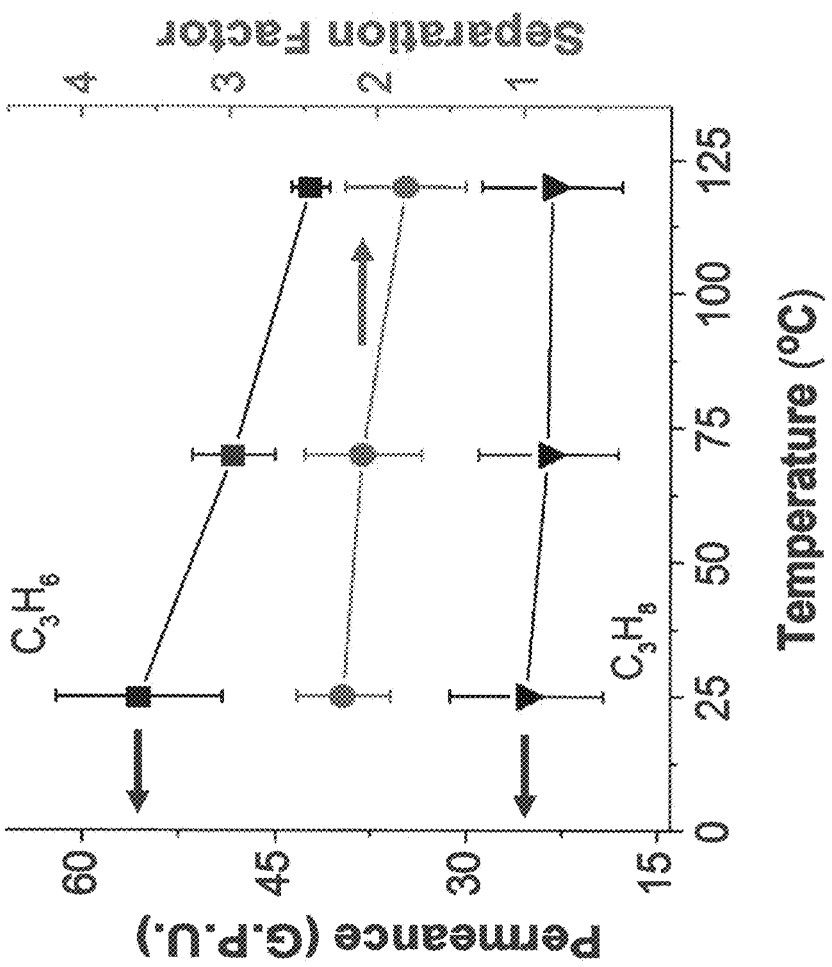
C_3H_6
C_3H_8
Permeance (G.P.U.)
15
30
45
60
Temperature (°C)
0
25
50
75
100
125
Separation Factor
1
2
3
4

FIG. 22B

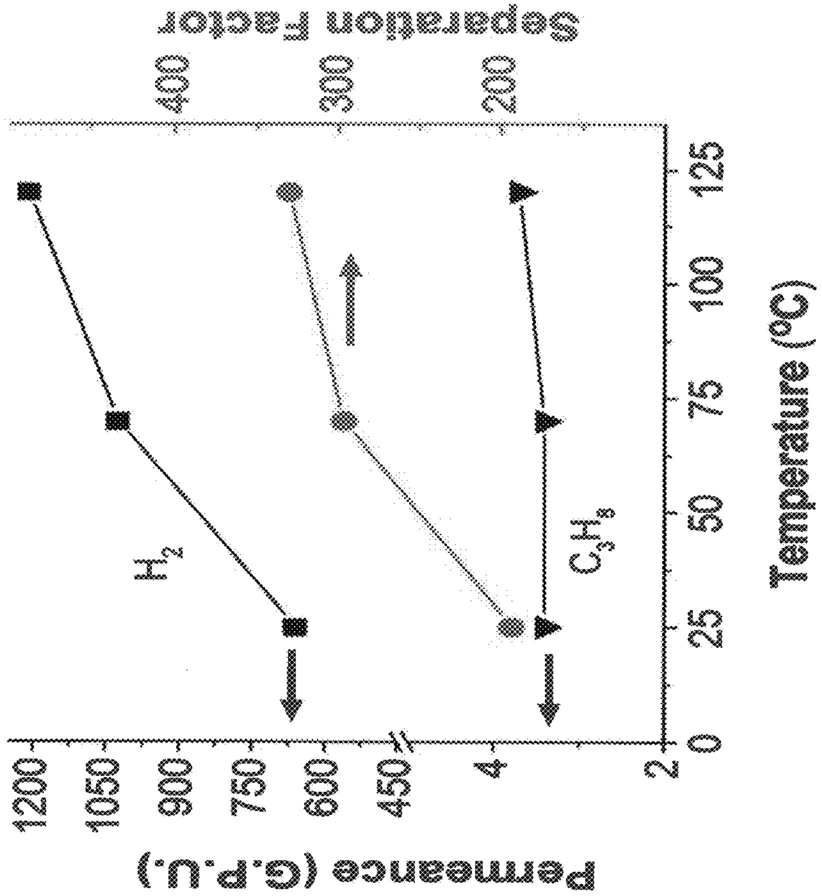
Permeance (G.P.U.)
1200
1050
900
750
600
450
4
2
Separation Factor
400
300
200
Temperature (°C)
0
25
50
75
100
125
H_2
C_3H_8

FIG. 23A

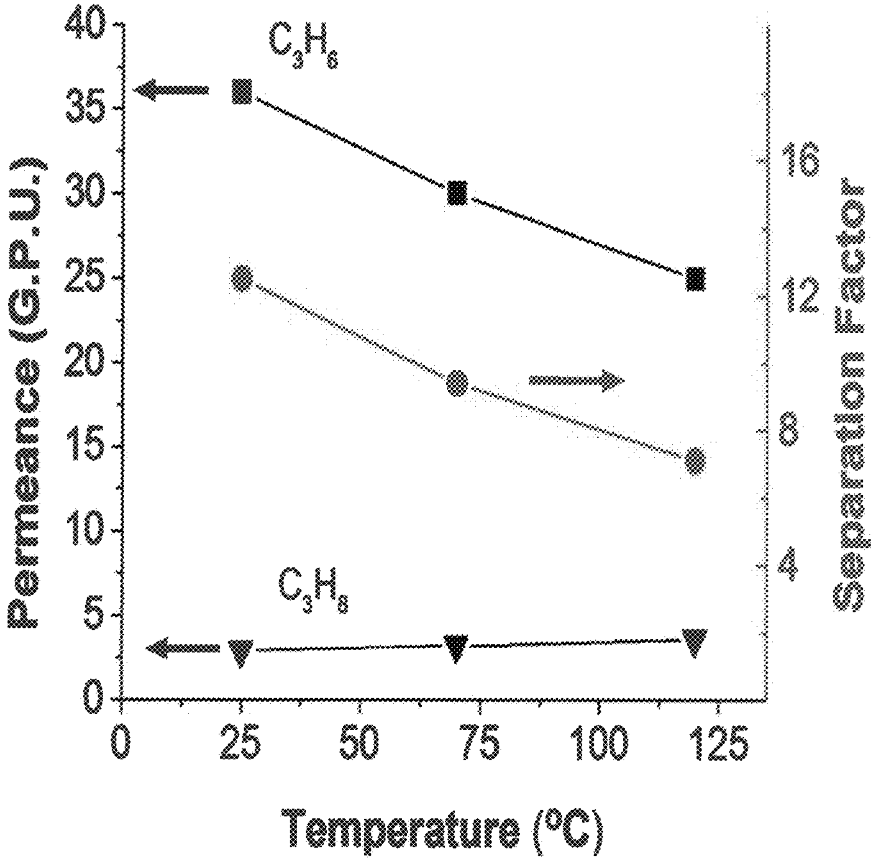
C_3H_6
C_3H_8
Permeance (G.P.U.)
0
5
10
15
20
25
30
35
40
Separation Factor
4
8
12
16
Temperature (°C)
0
25
50
75
100
125

FIG. 23B

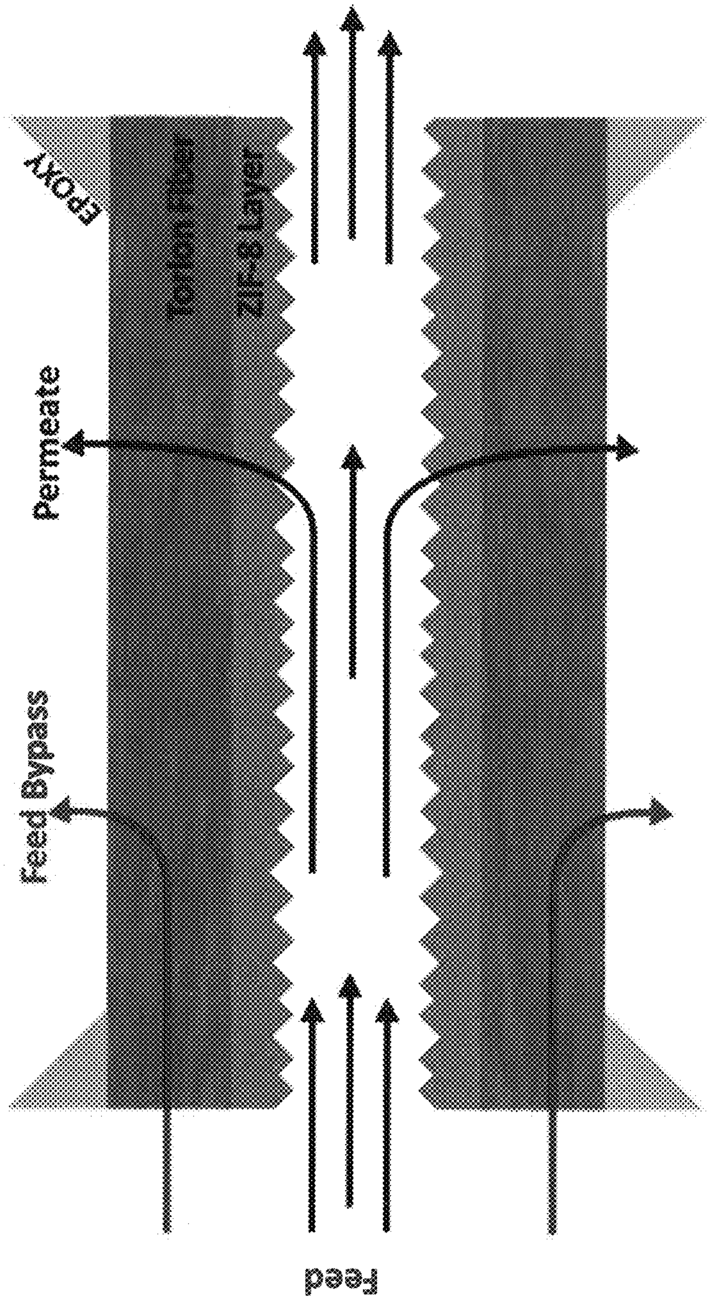

FIG. 24A

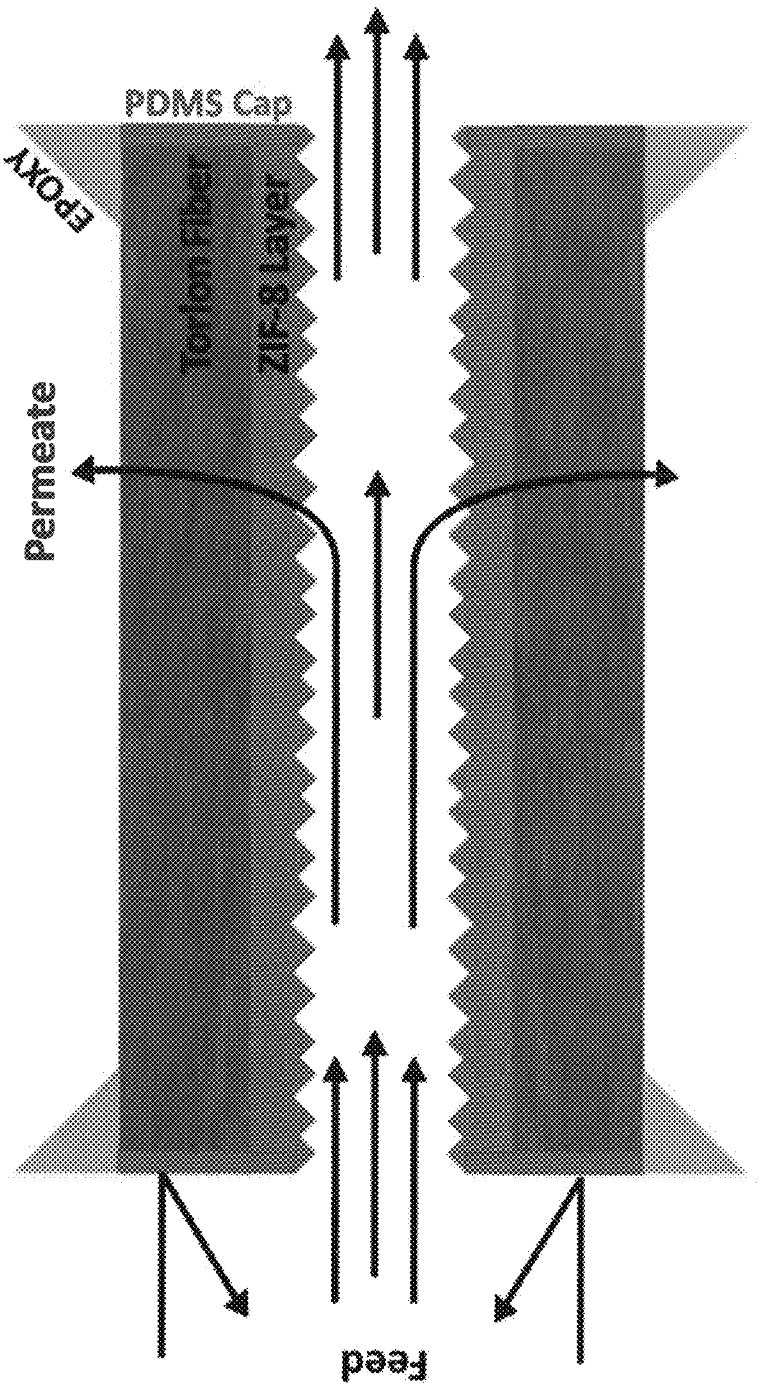

FIG. 24B

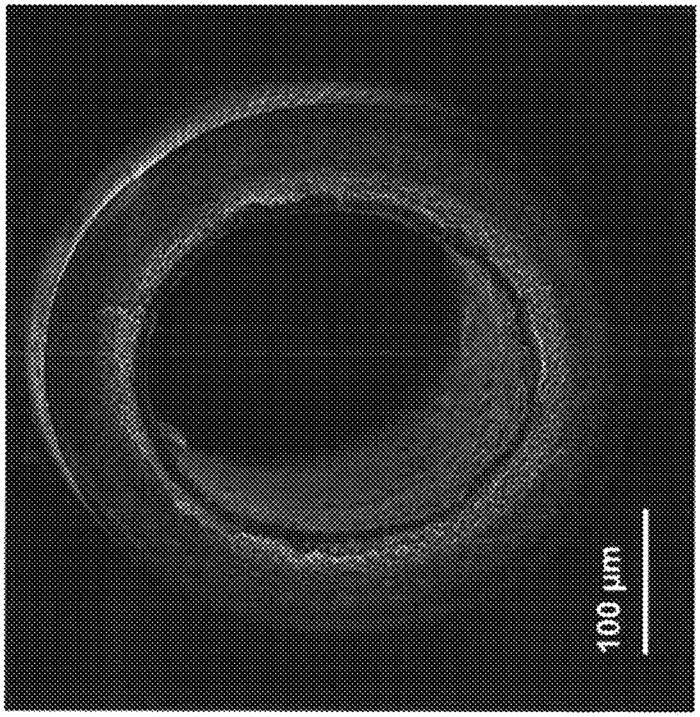

FIG. 25A

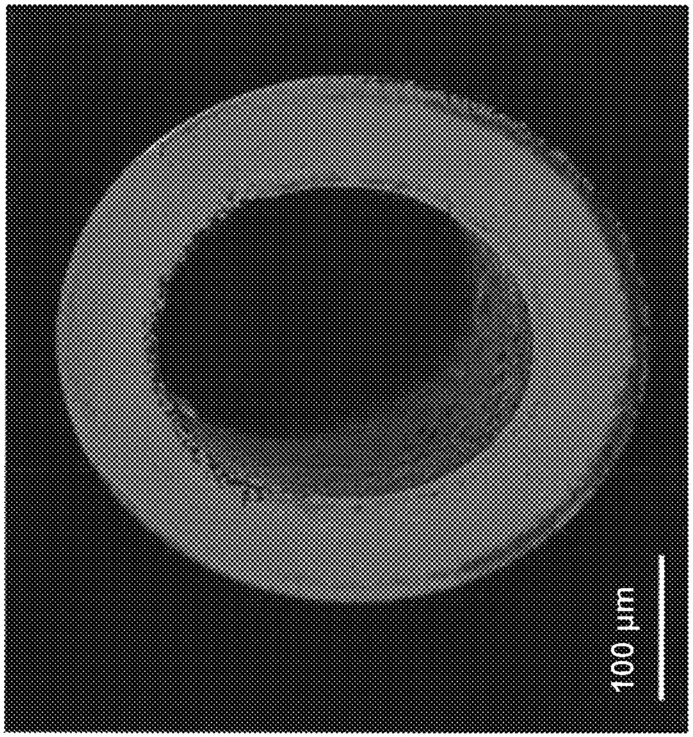

FIG. 25B

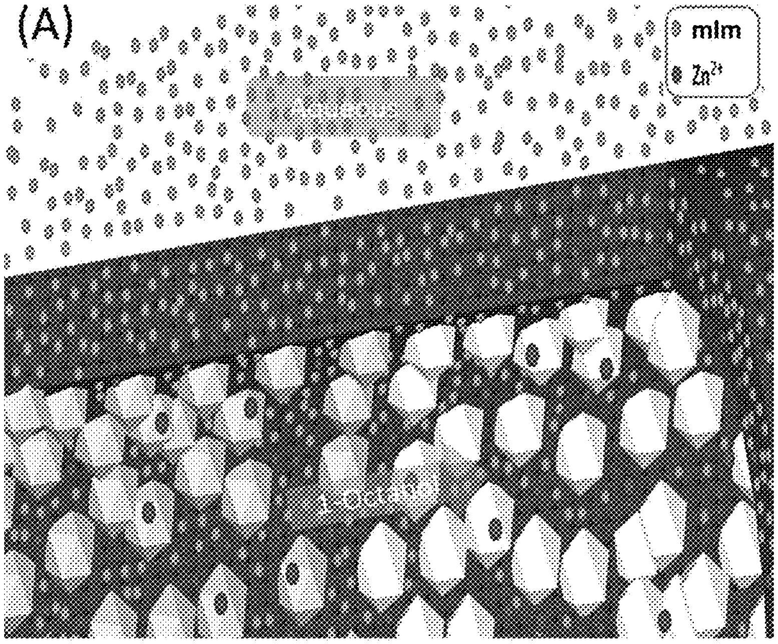

FIG. 26A

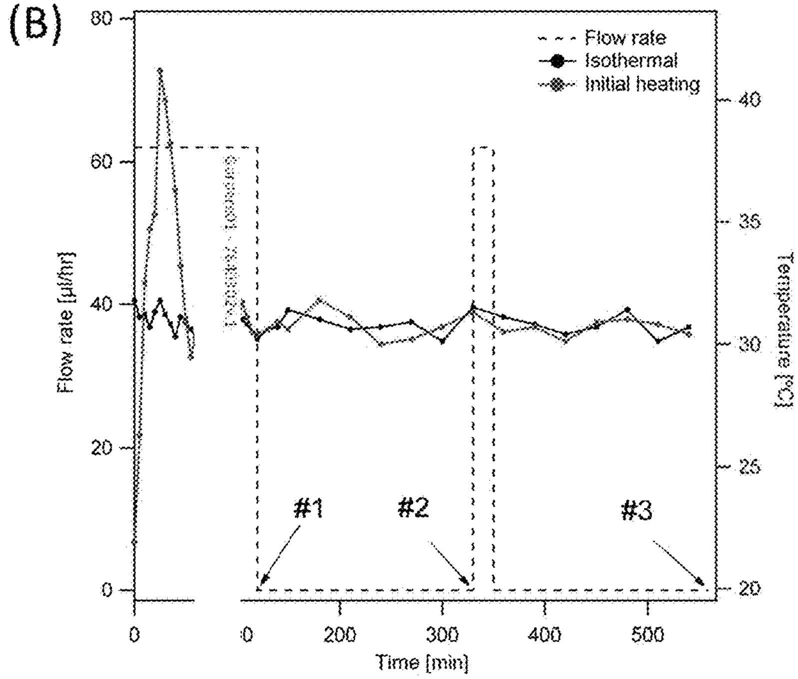

FIG. 26B

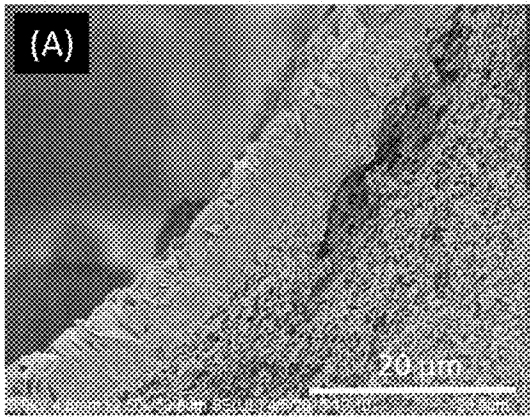

FIG. 27A

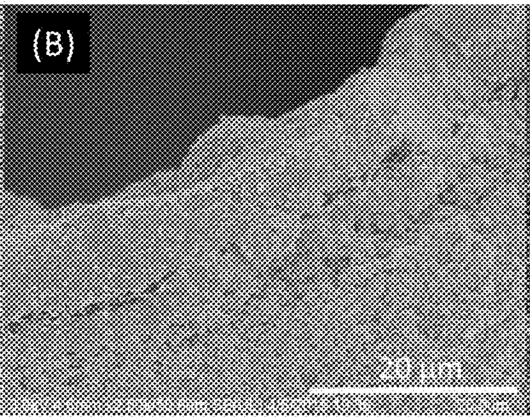

FIG. 27B

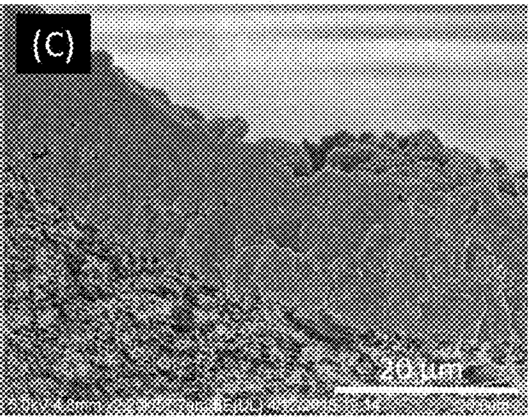

FIG. 27C

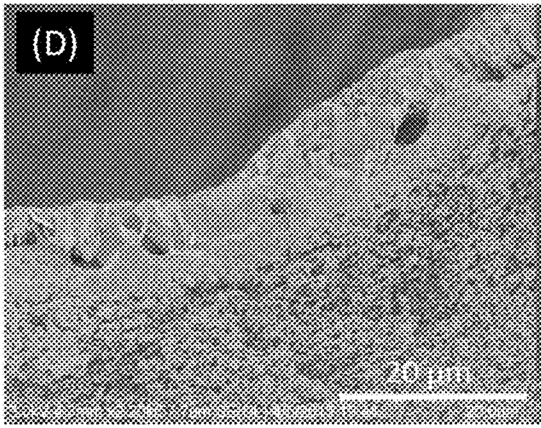

FIG. 27D

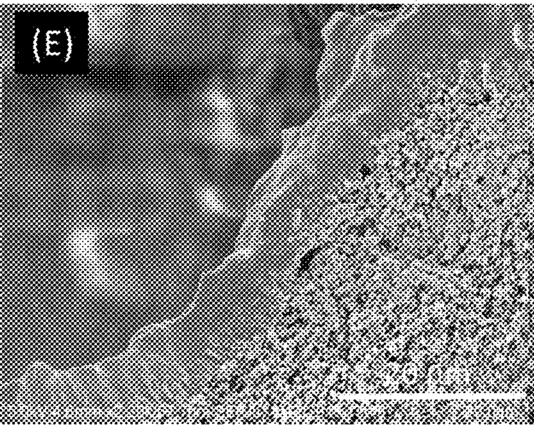

FIG. 27E

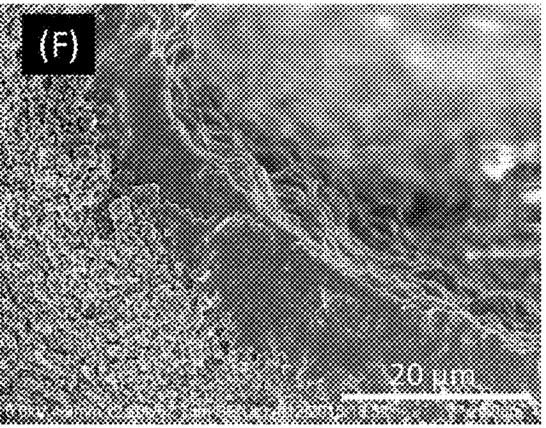

FIG. 27F

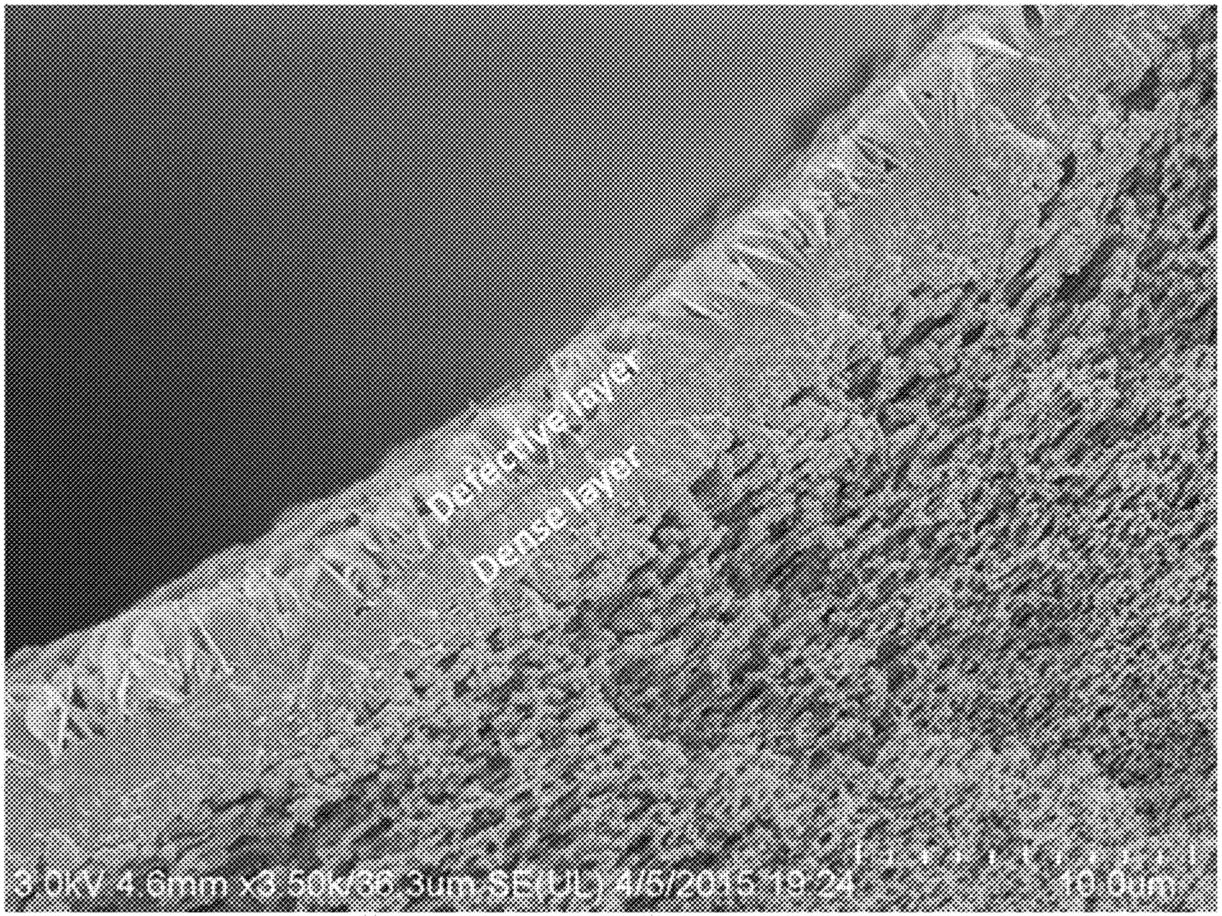
Defective layer
Dense layer
3.0kV 4.6mm x3.50k/36.3um SE(UL) 4/5/2015 19:24
10.0um

FIG. 28

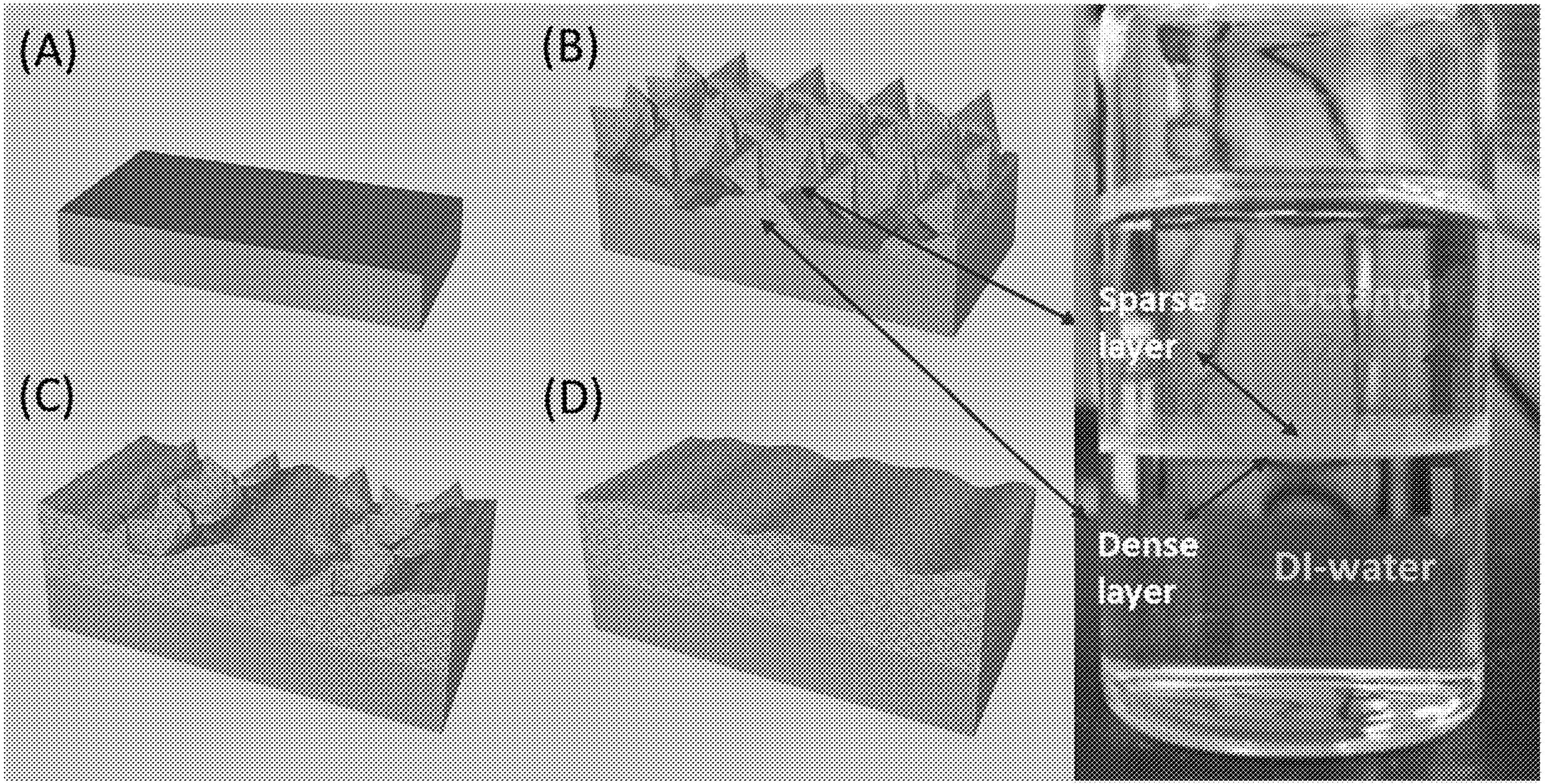

FIG. 29

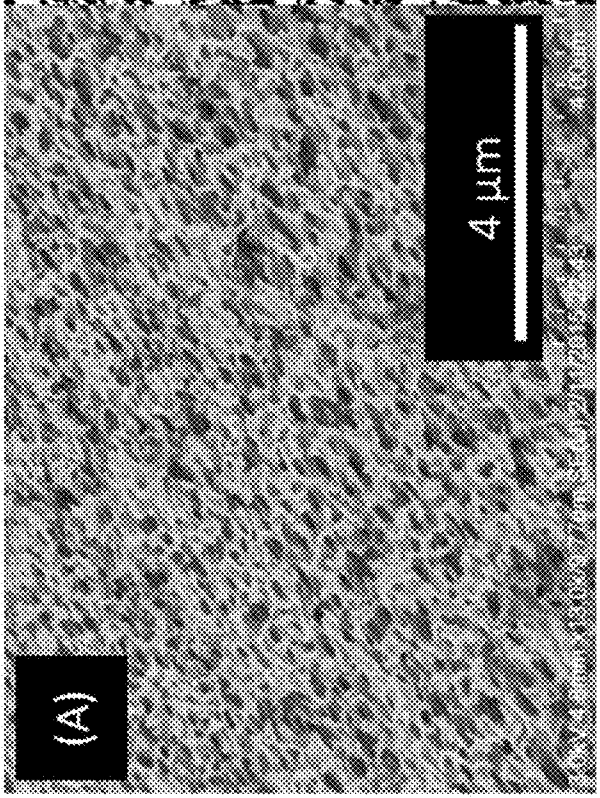

FIG. 30A

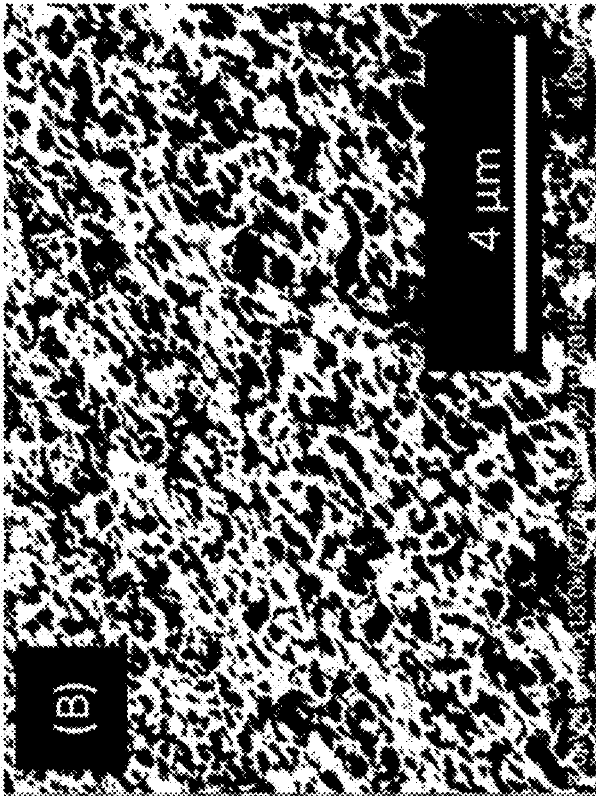

FIG. 30B

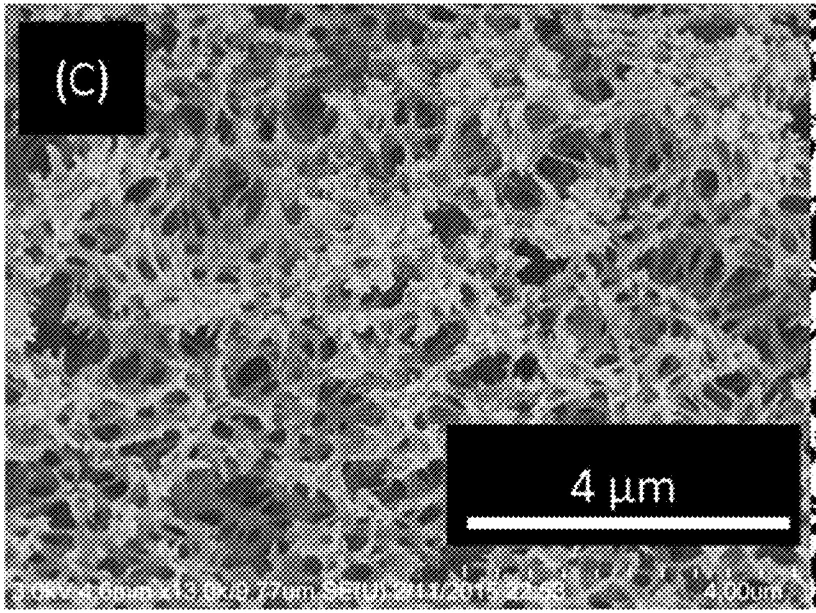

FIG. 30C

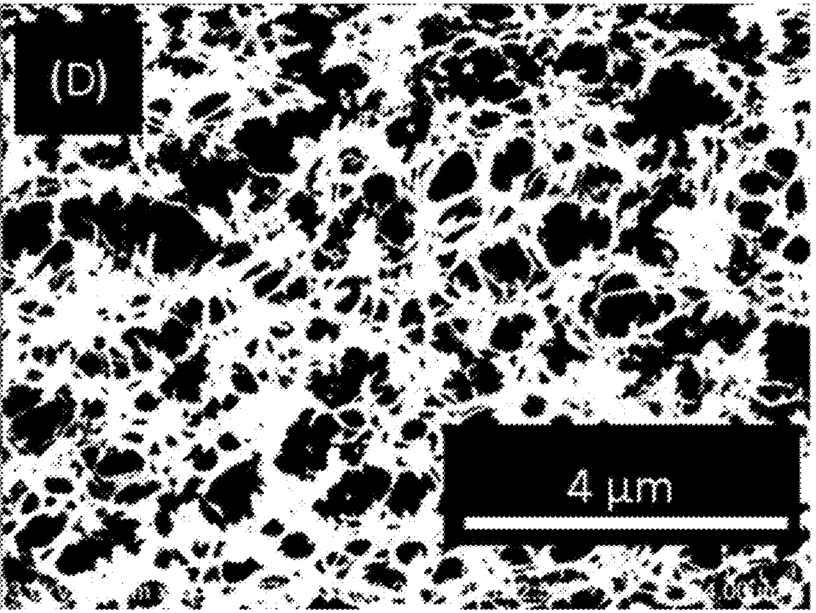

FIG. 30D

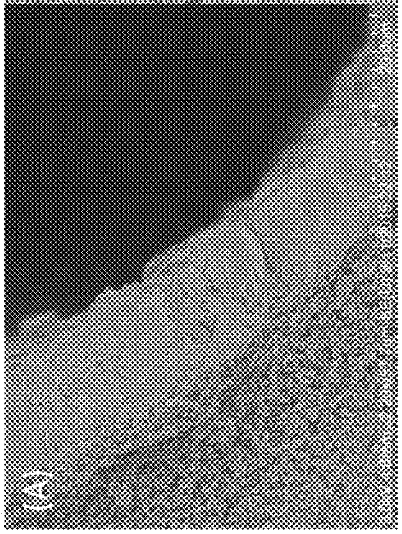

FIG. 31A

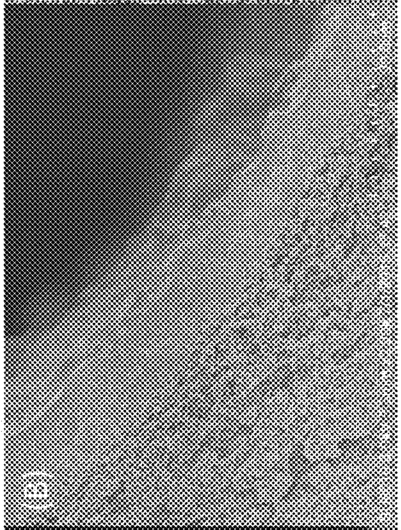

FIG. 31B

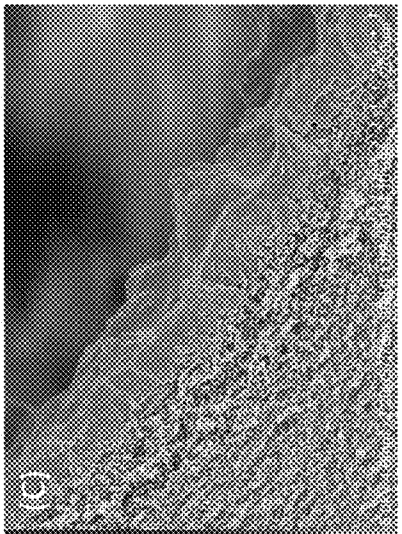

FIG. 31C

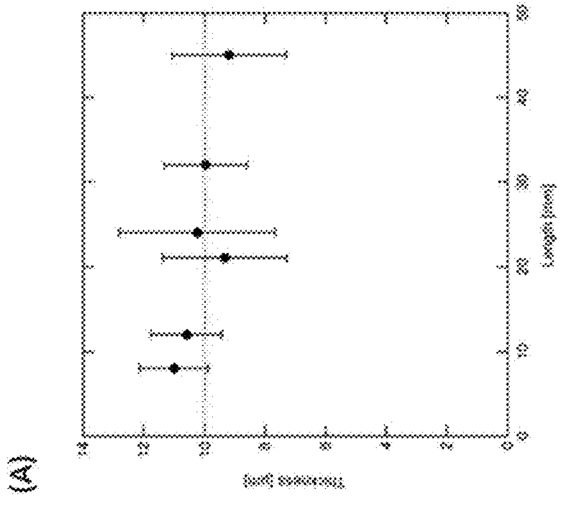

FIG. 32A

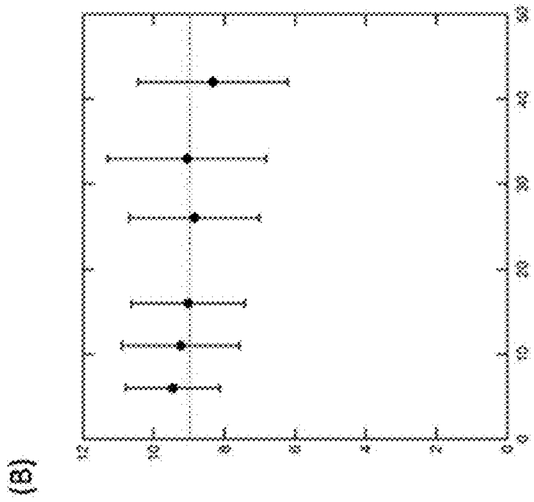

FIG. 32B

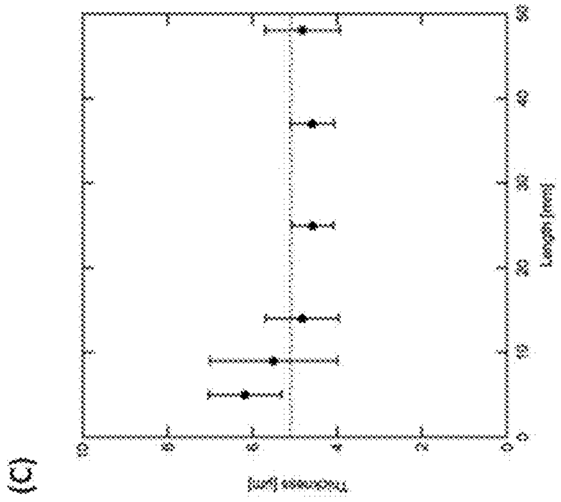

FIG. 32C

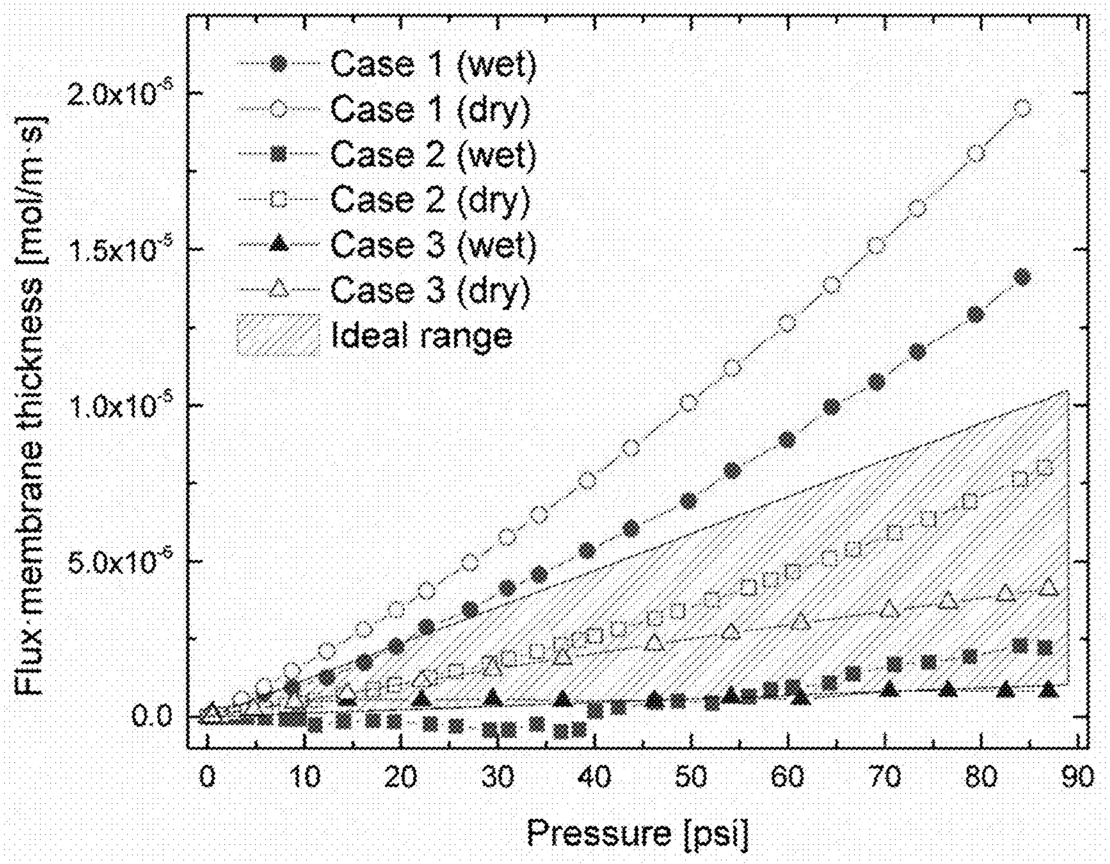
Case 1 (wet)
Case 1 (dry)
Case 2 (wet)
Case 2 (dry)
Case 3 (wet)
Case 3 (dry)
Ideal range
Flux·membrane thickness [mol/m·s]
2.0x10^-5
1.5x10^-5
1.0x10^-5
5.0x10^-6
0.0
0
10
20
30
40
50
60
70
80
90
Pressure [psi]

FIG. 33

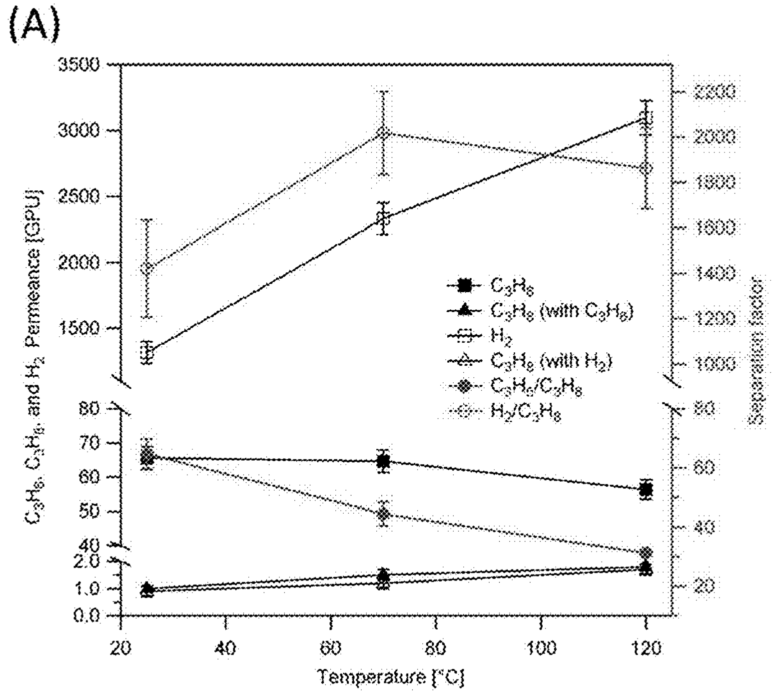

FIG. 34A

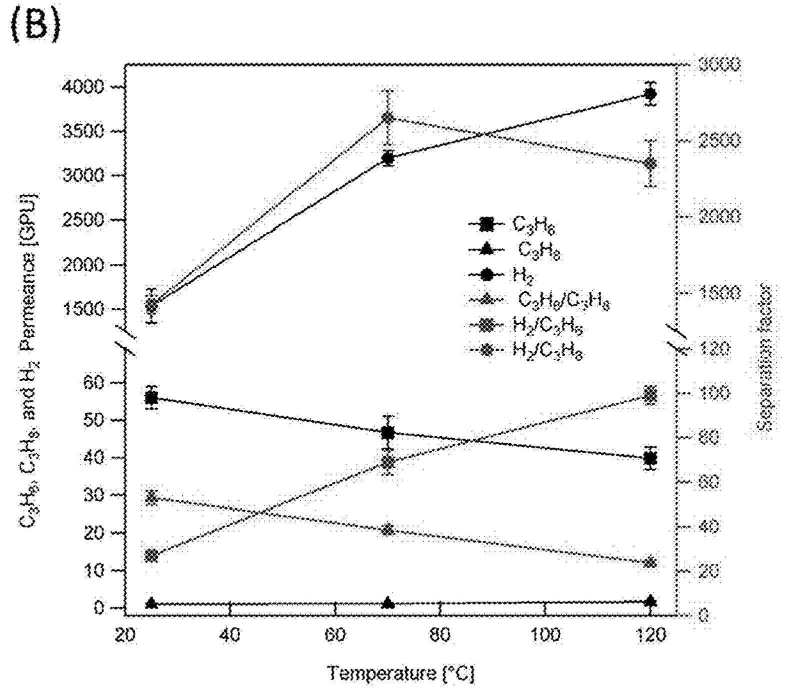

FIG. 34B

HIGH EFFICIENCY, HIGH PERFORMANCE METAL-ORGANIC FRAMEWORK (MOF) MEMBRANES IN HOLLOW FIBERS AND TUBULAR MODULES

PRIOR RELATED APPLICATIONS

The present application is a continuation-in-part of U.S. patent application Ser. No. 14/231,871, which claims priority to U.S. Provisional Patent Application Ser. No. 61/913,592, filed on Dec. 9, 2013 for "Flow Processing and Characterization of Metal-Organic Framework (MOF) Membranes in Hollow Fiber and Tubular Modules" and to U.S. Provisional Patent Application Ser. No. 61/820,489, filed on May 7, 2013 for "Flow Processing and Characterization of Metal-Organic Framework (MOF) Membranes in Tubular and Hollow Fiber Modules."

FEDERALLY SPONSORED RESEARCH STATEMENT

Not Applicable ("N/A")

REFERENCE TO MICROFICHE APPENDIX

N/A

FIELD OF INVENTION

This invention relates to a scalable, in situ flow-processing method to synthesize metal-organic framework (MOF) membranes on or inside hollow fiber and tubular modules and to characterize their molecular transport properties, and, in particular, to a high-efficiency, high-performance zeolitic imidazolate framework (ZIF)-8 mixed material that is free of defects.

BACKGROUND OF THE INVENTION

Molecular sieving membranes have generated great interest as high-performance separation systems for production of clean and renewable fuels, building block chemicals, and specialty chemicals. Compared to thermodynamically-driven separation methods, membrane-based processes can significantly reduce the energy and capital costs of separating molecules on a large scale. For example, energy-intensive methods such as cryogenic distillation are commonly used to separate hydrocarbons because of their quite similar thermodynamic properties. Membranes composed of molecular sieving materials such as zeolites,[1] layered zeolites,[2] or metal-organic frameworks[3] (MOFs) have intrinsic advantages over polymeric membranes such as a simultaneously high permeability and selectivity. Despite their performance limitations, polymeric membranes have continued to dominate industrial membrane separations due to their relative ease of processing into morphologies such as hollow fibers.[4] The greatest scientific challenge facing molecular sieving membranes is the lack of an easily scalable, reliable, and benign fabrication process.[5] This limitation has been particularly severe for zeolite membranes, which are typically fabricated by hydrothermal synthesis on high-cost support materials.

While substantive progress is being made in gradually reducing the barriers to economical zeolitic membranes,[6-7] the advent of metal-organic framework (MOF) molecular sieves has created potential for more scalable membrane fabrication processes under relatively benign conditions.[8] MOFs consist of metal centers connected by coordination bonds to organic linker molecules, and have been used to grow crystalline membranes through techniques similar to those developed for zeolitic membranes. The zeolitic imidazolite framework (ZIF) subclass of MOFs is of particular interest for membrane fabrication, because of its tunable pore size and chemistry,[9] and relatively good thermal and chemical stability.[10-11] In an early demonstration of scalable ZIF membrane processing, we recently demonstrated the growth of ZIF-90 membranes on the outer surfaces of porous polymeric poly(amide-imide) (e.g., TORLON®) hollow fibers (about 250 μm outer diameter) by a seeded growth process[12] at mild conditions (65° C. in methanol solutions). Molecular sieving membranes on the inner surfaces of the hollow fibers are much more challenging to grow but better suited for scalable fabrication and industrial uses, due to the ability to be bundled in close proximity while avoiding membrane-membrane contact points and interfaces that lead to defects during synthesis.

It has been shown that free-standing MOF films and spheroids can be synthesized at the interfaces between two immiscible solvents.[13] However, the growth of defect-controlled membranes on the inner surfaces of microscale hollow fibers (50-300 μm inner (bore) diameter) is a key, and more challenging, advance. As the bore size (and hence volume) is decreased to microscopic dimensions, the likelihood of reactant depletion and local inhomogeneity increase, leading to loss of control over membrane continuity and defect density.[14]

Thus, an Interfacial Microfluidic Membrane Processing (IMMP) approach for preparing defect-controlled and defect-free molecular sieving membranes on the inner surfaces of microscale hollow fibers is needed to improve performance in gas and liquid separations.

SUMMARY OF THE INVENTION

Zeolite and MOF membranes are typically synthesized in a reactor, and then removed for washing and mounting in a separate module. However, in this invention, the inventors demonstrate an in situ flow process to synthesize a membrane on or inside hollow fiber and tubular modules at a controlled location, and to subsequently activate the membrane and measure separation properties in situ without having to remove the membrane. Furthermore, damage to membranes during module construction and handling are eliminated. Lastly, this reactor cell design is capable of providing continuous flow in the bore and shell side of the hollow fiber or tubular module to allow for reagent recycling and to homogenize membrane thickness along the length. By using a single module for synthesis and characterization, membrane growth variables and post-treatments can be controlled accurately. This device also allows in situ characterization of the permeation properties of the module after each treatment step to determine cause and effect.

In other words, this reactor cell design facilitates a scalable and generalizable method of processing molecular sieving membranes (specifically, ZIF-8 membranes) referred to as an Interfacial Microfluidic Membrane Processing (IMMP) approach. The IMMP approach combines three key concepts: first, a two-solvent interfacial approach that can be tuned to achieve positional control over membrane formation (at inner and outer surfaces, as well as inside the bulk, of the porous fiber); second, supply, replenishment, and recycling of reactants at microfluidic conditions in the hollow fiber bore; and third, membrane synthesis in situ directly in the membrane module, which also functions as a membrane synthesis reactor.

In the present invention, the inventors demonstrate an isothermal and initial heating IMMP approach that leads to a mechanism of ZIF-8 membrane growth in hollow fibers that elucidates the roles of reactant transport, film crystallization, and the hollow fiber support microstructure. The inventors also demonstrate how a mechanistic understanding of ZIF-8 hollow fiber membrane formation can be used to engineer a higher-throughput, higher-selectivity ZIF-8 membrane that is free of defects for propane/propylene separations. Further, the inventors present detailed binary and ternary mixed gas permeation measurements to highlight the excellent separation characteristics of these defect-controlled and defect-free ZIF-8 hollow fiber membranes.

In an embodiment, a reactor cell for flow processing molecular sieving membranes comprises a hollow fiber having a first end and a second end, wherein a length of the first end is supported by and sealed into the first hole and a length of the second end is supported by and sealed into the second hole; wherein the first and second ends of the hollow fiber are capped with a capping solution, wherein a molecular sieving membrane that is uniform and at least 95% free of defects is grown on an inner bore surface of the hollow fiber. In an embodiment, the molecular sieving membrane is at least about 97% free of defects and wherein any defects are less than about 20 nm in diameter, length or width. In an embodiment, the molecular sieving membrane is at least about 97% free of defects and wherein any defects are less than about 10 nm in diameter, length or width.

In an embodiment, the lengths of the first and second ends of the hollow fiber are sealed into the first and second holes with an adhesive.

In an embodiment, the capping solution is about 8 wt % to about 10 wt % poly(dimethylsiloxane) (PDMS) in heptane.

In an embodiment, a method of making a reactor cell comprises the steps of: fabricating a reactor chamber extending into the reactor module from the upper surface of the reactor module; fabricating an O-ring groove with an inner dimension slightly larger than and offset from the outer dimension of the reactor chamber; fabricating the first hole extending into the reactor chamber from the first surface and the second hole opposing the first hole and extending into the reactor chamber from the second surface; fabricating a third hole extending into the reactor chamber from a third surface and a fourth hole opposing the third hole and extending into the reactor chamber from a fourth surface; supporting and sealing the length of the first end of the hollow fiber in the first hole and the length of the second end of the hollow fiber into the second hole; capping the first and second ends of the hollow fiber with a capping solution; fabricating the reactor module cover to fit on the upper surface of the reactor module and fastening the reactor module cover to the seal the reactor chamber; fluidly connecting a bore solution to the first inlet; fluidly connecting a shell solution to the second inlet; and growing a molecular sieving membrane that is uniform and at least about 95% free of defects on an inner bore surface of the hollow fiber.

In an embodiment, the bore solution contains a limited Zn^{+2} concentration ranging from about 0.005 to about 0.1 mol/L Zn^{+2} in 1-octanol. In an embodiment, the bore solution contains a limited Zn^{+2} concentration ranging from about 0.01 to about 0.03 mol/L Zn^{+2} in 1-octanol. In an embodiment, the bore solution is about 0.018 mol/L Zn^{+2} in 1-octanol. In an embodiment, the shell solution contains an excess mIm ligand concentration ranging from about 0.5 to about 10 mol/L 2-methyl imidazole (mIm) in deionized water.

In an embodiment, the shell solution contains an excess mIm ligand concentration ranging from about 1.2 to about 1.6 mol/L 2-methyl imidazole (mIm) in deionized water. In an embodiment, the shell solution is about 1.37 mol/L mIm in deionized water. In an embodiment, the method further comprises the step of gently stirring the shell solution to prevent formation of local concentration gradients. In an embodiment, the shell solution is stirred at about 40 rpm to about 80 rpm.

In an embodiment, the method of making the reactor cell further comprises the steps of flowing the bore solution at a first flow rate for a first period, wherein a first temperature is increased to a second temperature during a portion of the first period; stopping the first flow rate of the bore solution for a second period; flowing the bore solution at a second flow rate for a third period; and stopping the second flow rate of the bore solution for a fourth period. In an embodiment, the second temperature is decreased to a third temperature during a portion of the first period.

In an embodiment, the first and second flow rates are about 1 μL/hour to about 1000 μL/hour per individual hollow fiber. In an embodiment, the first and second flow rates are about 10 μL/hour to about 100 μL/hour per individual hollow fiber.

In an embodiment, the first period is about 1 hour to about 3 hours, the second period is about 3 hours to about 4 hours, the third period is about 10 minutes to about 30 minutes, and the fourth period is about 3 hours to about 4 hours.

In an embodiment, the method of making the reactor cell further comprises the step of rinsing the membrane in solvents selected from the group consisting of 1-octanol, heptanes, hexane, methanol and deionized water.

In an embodiment, a method of using the reactor cell comprises the steps of: fluidically connecting a feed mixture to the first inlet; fluidically connecting a sweep gas to the second inlet; collecting a separated mixture from the first outlet; and collecting permeate from the second outlet.

In an embodiment, the feed mixture to the reactor cell is selected from the group consisting of hydrogen/hydrocarbons, hydrogen/propane, propylene/propane and butenes/butanes. In an embodiment, the feed mixture to the reactor cell is selected from the group consisting of hydrogen/propane, propylene/propane and butenes/butanes. In an embodiment, the feed mixture to the reactor cell comprises about 2 mol % to about 95 mol % i-butane, about 2 mol % to about 95 mol % n-butane and mixtures thereof.

In an embodiment, an operating temperature for the reactor cell is from about 30° C. to about 95° C. or any value there between.

In an embodiment, an operating pressure for the reactor is from about 1 bar to about 14 bar or any value there between.

These and other objects, features and advantages will become apparent as reference is made to the following detailed description, preferred embodiments, and examples, given for the purpose of disclosure, and taken in conjunction with the accompanying drawings and appended claims.

BRIEF DESCRIPTION OF THE DRAWINGS

The patent or application file contains at least one drawing executed in color. Copies of this patent or patent application publication with color drawing(s) will be provided by the Office upon request and payment of the necessary fee.

For a further understanding of the nature and objects of the present invention, reference should be made to the following detailed disclosure, taken in conjunction with the accompanying drawings, in which like parts are given like reference numerals, and wherein:

FIG. **1**A illustrates a side perspective view of a hollow fiber or tubular membrane module showing location of a bore and a shell;

FIG. **1**B illustrates a cross-sectional view of a hollow fiber or tubular membrane module showing location of a bore and a shell;

FIG. **2** illustrates an upper, right front perspective view of a reactor according to an embodiment of the present invention;

FIG. **3** illustrates a photograph of a polyamide-imide (e.g., TORLON®) hollow fiber epoxy-sealed inside a reactor according to an embodiment of the present invention;

FIG. **4** illustrates a photograph of a reactor connected to cycling peristaltic pump according to an embodiment of the present invention;

FIG. **5**A illustrates a cross-sectional view of a SEM micrograph of a ZIF-8 membrane grown on an outer (shell) side surface of a seeded polyamide-imide (e.g., TORLON®) hollow fiber;

FIG. **5**B illustrates a top-view of a SEM micrograph of a ZIF-8 membrane grown on outer (shell) side surface of a seeded polyamide-imide (e.g., TORLON®) hollow fiber;

FIG. **6**A illustrates a cross-sectional view of a SEM micrograph of a ZIF-8 membrane grown on a polyamide-imide (e.g., TORLON®) hollow fiber under aqueous flow conditions;

FIG. **6**B illustrates a detailed cross-sectional view of a SEM micrograph of a ZIF-8 membrane grown on a polyamide-imide (e.g., TORLON®) hollow fiber under aqueous flow conditions;

FIG. **7**A illustrates a cross-sectional view of a SEM micrograph of a ZIF-8 membrane grown on a polyamide-imide (e.g., TORLON®) hollow fiber under 1-octanol flow conditions;

FIG. **7**B illustrates a detailed cross-sectional view of a SEM micrograph of ZIF-8 membrane grown on a polyamide-imide (e.g., TORLON®) hollow fiber under 1-octanol flow conditions;

FIG. **8**A illustrates a cross-sectional view of a SEM micrograph of a ZIF-8 membrane grown on a polyamide-imide (e.g., TORLON®) hollow fiber using an Interfacial Microfluidic Membrane Processing (IMMP) approach with 2 mL/min flow rate of a Zn^{+2}/1-octanol bore solution and an aqueous 2-methyl imidazole (mIm) shell solution according to an embodiment of the present invention;

FIG. **8**B illustrates a cross-sectional view of a SEM micrograph of a ZIF-8 membrane grown on a polyamide-imide (e.g., TORLON®) hollow fiber using the IMMP approach with 1 μL/min flow rate of a Zn^{+2}/1-octanol bore solution and an aqueous mIm shell solution according to an embodiment of the present invention;

FIG. **9** illustrates a X-ray Diffraction (XRD) chart of 2Theta (°) vs. Intensity for simulated and experimental ZIF-8 membranes, confirming structure of supported ZIF-8 membranes;

FIG. **10** illustrates an Energy Dispersive X-ray Spectroscopy (EDS) Zinc line profile scan chart of Distance from membrane surface (μm (microns)) vs. Intensity, depicting thickness of membrane to be ~3 μm;

FIG. **11** illustrates a chart of Time vs. Flow Rate for static and continuous flow conditions, showing static growth conditions;

FIG. **12** illustrates a chart of Time vs. Flow Rate for pulsed flow conditions, showing growth and replenishment conditions;

FIG. **13** illustrates a chart of Time (min.) vs. Flow Rate OIL/hour) for pulsed flow conditions, showing growth, static growth and replenishment conditions;

FIG. **14** illustrates a X-ray Diffraction (XRD) chart of 2Theta (°) vs. Intensity for simulated and experimental ZIF-8 membranes on polyamide-imide (e.g., TORLON®) hollow fiber, confirming formation and structure of supported ZIF-8 membranes on inner (bore) side surface of hollow fiber;

FIG. **15** illustrates a schematic of the IMMP approach: (A) depicts a side view of a plurality of hollow fibers (orange) mounted in a reactor cell, (B) depicts an exploded side view of hollow fiber support during synthesis, showing Zn^{2+} ions being supplied by a 1-octanol solution (light red) flowing through the bore of the hollow fiber and methylimidazole linkers being supplied on the outer (shell) side of the hollow fiber in an aqueous solution (light blue), and (C) depicts a further exploded view of hollow fiber support during synthesis, showing the membrane forming on the inner surface of the hollow fiber by reaction of the two precursors to form a polycrystalline ZIF-8 layer (dark blue);

FIG. **16** illustrates a schematic of steady-state gas permeation measurement apparatus, with the reactor cell functioning as the permeation cell;

FIG. **17**A illustrates a cross-sectional view of a SEM micrograph of a ZIF-8 membrane grown in polyamide-imide (e.g., TORLON®) hollow fiber on the inner (bore) side surface by manipulating the location of the two reactants (i.e., zinc nitrate hexahydrate and mIm) and the two solvents (i.e., deionized water (DI) and 1-octanol) as in Example 1;

FIG. **17**B illustrates an EDS elemental maps of carbon (red) and superimposed zinc (green) showing the localization of the ZIF-8 membrane on the inner (bore) side surface of the polyamide-imide (e.g., TORLON®) hollow fiber as in Example 1;

FIG. **18**A illustrates a chart of Time (minutes) vs. Flow Rate OIL/hour), showing static, continuous and intermittent flow conditions used to synthesize ZIF-8 membranes on the inner (bore) side surface of a polyamide-imide (e.g., TORLON®) hollow fibers as in Example 1;

FIG. **18**B illustrates a cross-sectional view of a SEM micrograph of a ZIF-8 membrane grown in a polyamide-imide (e.g., TORLON®) hollow fiber using the IMMP approach with a static flow of a Zn^{+2}/1-octanol bore solution, depicting a discontinuous particle coating on the inner (bore) side surface of the hollow fiber;

FIG. **18**C illustrates a cross-sectional view of a SEM micrograph of a ZIF-8 membrane grown in a polyamide-imide (e.g., TORLON®) hollow fiber using the IMMP approach with a continuous flow of a Zn^{+2}/1-octanol bore solution, depicting a continuous ZIF-8 membrane (about 3 μm thick) on the inner (bore) side surface of the hollow fiber;

FIG. **18**D illustrates a cross-sectional view of a SEM micrograph of a ZIF-8 membrane grown in a polyamide-imide (e.g., TORLON®) hollow fiber using the IMMP approach with an intermittent flow of a Zn^{+2}/1-octanol bore solution, depicting a continuous ZIF-8 membrane (about 8 μm thick) on the inner (bore) side surface of the hollow fiber;

FIG. **19** illustrates an XRD pattern confirming crystal structure of ZIF-8 membrane grown on a polyamide-imide (e.g., TORLON®) hollow fiber using the IMMP approach with intermittent flow of a Zn^{+2}/1-octanol bore solution as in Example 1;

FIG. **20**A illustrates a cross-sectional view of a SEM micrograph of a ZIF-8 membrane grown in a polyamide-imide (e.g., TORLON®) hollow fiber closer to an inner (bore) side surface by manipulating the location of the two reactants (i.e., zinc nitrate hexahydrate and mIm) and the two solvents (i.e., DI and 1-octanol) as in Example 2;

FIG. **20**B illustrates a cross-sectional view of a SEM micrograph of a ZIF-8 membrane grown in a polyamide-imide (e.g., TORLON®) hollow fiber closer to an inner (bore) side surface by manipulating the location of the two reactants (i.e., zinc nitrate hexahydrate and mIm) and the two solvents (i.e., DI and 1-octanol) as in Example 3;

FIG. **20**C illustrates a cross-sectional view of a SEM micrograph of a ZIF-8 membrane grown in a polyamide-imide (e.g., TORLON®) hollow fiber closer to an outer (shell) side surface by manipulating the location of the two reactants (i.e., zinc nitrate hexahydrate and mIm) and the two solvents (i.e., DI and 1-octanol) as in Example 4;

FIG. **20**D illustrates a cross-sectional view of a SEM micrograph of a ZIF-8 membrane grown in a polyamide-imide (e.g., TORLON®) hollow fiber closer to an outer (shell) side surface by manipulating the location of the two reactants (i.e., zinc nitrate hexahydrate and mIm) and the two solvents (i.e., DI and 1-octanol) as in Example 5;

FIG. **21**A illustrates a chart of Temperature (° C.) vs. Permeance (G.P.U.) and Separation Factor, showing binary H_2/C_3H_8 permeation characteristics for an equimolar feed mixture on a ZIF-8 membrane grown in a polyamide-imide (e.g., TORLON®) hollow fiber using the IMMP system and capping ends of the hollow fiber with poly(dimethylsilozane) (PDMS);

FIG. **21**B illustrates a chart of Temperature (° C.) vs. Permeance (G.P.U.) and Separation Factor, showing binary C_3H_6/C_3H_8 permeation characteristics for an equimolar feed mixture on a ZIF-8 membrane grown in a polyamide-imide (e.g., TORLON®) hollow fiber using the IMMP system and capping ends of the hollow fiber with PDMS;

FIG. **22**A illustrates a chart of Temperature (° C.) vs. Permeance (G.P.U.) and Separation Factor, showing binary permeation characteristics for an equimolar H_2/C_3H_8 feed mixture on a ZIF-8 membrane grown in polyamide-imide (e.g., TORLON®) hollow fiber using the IMMP system;

FIG. **22**B illustrates a chart of Temperature (° C.) vs. Permeance (G.P.U.) and Separation Factor, showing binary permeation characteristics for an equimolar C_3H_6/C_3H_8 feed mixture on a ZIF-8 membrane grown in polyamide-imide (e.g., TORLON®) hollow fiber using the IMMP system;

FIG. **23**A illustrates a chart of Temperature (° C.) v. Permeance (G.P.U.) and Separation Factor, showing binary permeation characteristics for an equimolar H_2/C_3H_8 feed mixture on ZIF-8 membranes grown simultaneously in three (3) polyamide-imide (e.g., TORLON®) hollow fiber using the IMMP system and sealing the ends of the fibers with PDMS;

FIG. **23**B illustrates a chart of Temperature (° C.) v. Permeance (G.P.U.) and Separation Factor, showing binary permeation characteristics for an equimolar C_3H_6/C_3H_8 feed mixture on ZIF-8 membranes grown simultaneously in three (3) polyamide-imide (e.g., TORLON®) hollow fiber using the IMMP approach and sealing the ends of the fibers with PDMS;

FIG. **24**A illustrates a schematic showing feed gas molecules bypassing the ZIF-8 membrane through the hollow fiber ends;

FIG. **24**B illustrates a schematic showing suppression of the bypass effect in FIG. **24**A by capping the hollow fiber ends with a PDMS film;

FIG. **25**A illustrates a SEM cross-section image of the inner-surface ZIF-8 membrane after end-capping by penetration of PDMS;

FIG. **25**B illustrates an EDS elemental map of Si (red) showing the penetration of PDMS into the pores of a polyamide-imide (e.g., TORLON®) hollow fiber;

FIG. **26**A illustrates a schematic of the Interfacial Microfluidic Membrane Processing (IMMP) approach, showing two feed streams for a ZIF-8 membrane on a polyamide-imide (e.g., TORLON®) hollow fiber;

FIG. **26**B illustrates a chart of Time vs. Flow rate (μl/hr) and Temperature (° C.), showing bore flow rate and two different temperature profiles (isothermal and initial heating) for the IMMP approach to synthesize ZIF-8 membranes on an inner surface of polyamide imide (e.g., TORLON®) hollow fibers with the numbered temporal locations (#1, #2, and #3) indicating the times where the ZIF-8 membrane growth were arrested;

FIG. **27**A illustrates an exemplary cross-sectional SEM image of a ZIF-8 membrane grown on a polyamide-imide (e.g., TORLON®) hollow fiber after 2 hours of continuous membrane growth (Step 1) using isothermal IMMP approach;

FIG. **27**B illustrates an exemplary cross-sectional SEM image of a ZIF-8 membrane grown on a polyamide-imide (e.g., TORLON®) hollow fiber after 2 hours of continuous membrane growth (Step 1) and 3.5 hours of static membrane growth (Step 2) using isothermal IMMP approach;

FIG. **27**C illustrates an exemplary cross-sectional SEM image of a ZIF-8 membrane grown on a polyamide-imide (e.g., TORLON®) hollow fiber after 2 hours of continuous membrane growth (Step 1), 3.5 hr of static membrane growth (Step 2) and 20 minutes of second continuous membrane growth followed by 3.5 hours of second static membrane growth (Step 3) using isothermal IMMP approach;

FIG. **27**D illustrates an exemplary cross-sectional SEM image of a ZIF-8 membrane grown on a polyamide-imide (e.g., TORLON®) hollow fiber after 2 hours of continuous membrane growth (Step 1 using initial heating IMMP approach;

FIG. **27**E illustrates an exemplary cross-sectional SEM image of a ZIF-8 membrane grown on a polyamide-imide (e.g., TORLON®) hollow fiber after 2 hours of continuous membrane growth (Step 1) and 3.5 hours of static membrane growth (Step 2) using initial heating IMMP approach;

FIG. **27**F illustrates an exemplary cross-sectional SEM image of a ZIF-8 membrane grown on a polyamide-imide (e.g., TORLON®) hollow fiber after 2 hours of continuous membrane growth (Step 1), 3.5 hours of static membrane growth (Step 2) and 20 minutes of second continuous membrane growth followed by 3.5 hours of second static membrane growth (Step 3) using initial heating IMMP approach;

FIG. **28** illustrates a magnified SEM image of dense and defective ZIF-8 membrane layers grown on a polyamide-imide (e.g., TORLON®) hollow fiber after 120 minutes of continuous membrane growth using isothermal IMMP approach;

FIG. **29** illustrates a schematic of the ZIF-8 membrane growth mechanism on polyamide-imide (e.g., TORLON®) hollow fibers: (A) depicts a side perspective view of a hollow fiber (tan) at 0 hours and (B) depicts a side perspective view of a ZIF-8 membrane (gray) grown on the hollow fiber (tan) during synthesis after 2 hours of continuous membrane growth (Step 1), (C) depicts a side perspective view of the ZIF-8 membrane (gray) grown on the hollow fiber (tan) during synthesis after 2 hours of continuous membrane growth (Step 1) and 3.5 hours of static membrane growth (Step 2), (D) depicts a side perspective view of the ZIF-8 membrane (gray) grown on the hollow fiber (tan) during synthesis after 2 hours of continuous membrane growth (Step 1), 3.5 hours of static membrane growth (Step 2) and 20 minutes of second continuous membrane growth followed by a final 3.5 hours of second static membrane growth (Step 3); and a (E) depicts a photograph of the two reactants (i.e., zinc nitrite hexahydride and mIm) in the two solvents (i.e., DI and 1-octanol) after 15 minutes of interfacial contact in a glass vial;

FIG. **30**A illustrates a cross-sectional SEM image of a polyamide imide (e.g., TORLON®) hollow fiber;

FIG. **30**B illustrates an associated binary image for estimation of porosity of the image in FIG. **30**A;

FIG. **30**C illustrates a cross-sectional SEM image of a modified polyamide imide (e.g., TORLON®) hollow fiber;

FIG. **30**D illustrates an associated binary images for estimation of the porosity of the image in FIG. **30**C;

FIG. **31**A illustrates exemplary cross-sectional SEM images of a ZIF-8 membrane grown on a polyamide-imide (e.g., TORLON®) hollow fiber using isothermal IMMP approach as in Case 1;

FIG. **31**B illustrates exemplary cross-sectional SEM images of a ZIF-8 membrane grown on a polyamide-imide (e.g., TORLON®) hollow fiber using isothermal IMMP approach as in Case 2;

FIG. **31**C illustrates exemplary cross-sectional SEM images of a ZIF-8 membrane grown on a polyamide-imide (e.g., TORLON®) hollow fiber using initial heating IMMP approach as in Case 3;

FIG. **32**A illustrates a chart of Length (mm) vs Thickness (μm) for a ZIF-8 membrane grown on a polyamide-imide (e.g., TORLON®) hollow fiber using isothermal IMMP approach with the red dotted lines indicating the average thickness of about 10.0 μm for the ZIF-8 membrane;

FIG. **32**B illustrates a chart of Length (mm) v.s Thickness (μm) for a ZIF-8 membrane grown on a modified polyamide-imide (e.g., TORLON®) hollow fiber with the red dotted lines indicating the average thickness of about 9.1 μm for the ZIF-8 membrane;

FIG. **32**C illustrates a chart of Length (mm) v.s Thickness (μm) for a ZIF-8 membrane grown on a modified polyamide-imide (e.g., TORLON®) hollow fiber using initial heating IMMP approach with the red dotted lines indicating the average thickness of about 5 μm for the ZIF-8 membrane;

FIG. **33** illustrates a chart of Pressure (psi) vs. Flux membrane thickness (mol/m·s), showing helium permeabilities (expressed as flux×membrane thickness) measured at room temperature under dry and wetted conditions for ZIF-8 membranes grown on polyamide-imide (e.g., TORLON®) hollow fibers as in Cases 1-3;

FIG. **34**A illustrates a chart of Temperature (C) vs. Permeance (G.P.U.) and Separation Factor, showing binary H_2/C_3H_8 and C_3H_6/C_3H_8 permeation characteristics for an equimolar feed mixture on a ZIF-8 membrane grown on polyamide-imide (e.g., TORLON®) hollow fiber as in Case 3;

FIG. **34**B illustrates a chart of Temperature (C) vs. Permeance (G.P.U.) and Separation Factor, showing ternary $H_2/C_3H_6/C_3H_8$ permeation characteristics for equimolar feed mixtures on a ZIF-8 membrane grown on polyamide-imide (e.g., TORLON®) hollow fiber as in Case 3.

DETAILED DESCRIPTION OF EMBODIMENTS OF THE INVENTION

The following detailed description of various embodiments of the present invention references the accompanying drawings, which illustrate specific embodiments in which the invention can be practiced. While the illustrative embodiments of the invention have been described with particularity, it will be understood that various other modifications will be apparent to and can be readily made by those skilled in the art without departing from the spirit and scope of the invention. Accordingly, it is not intended that the scope of the claims appended hereto be limited to the examples and descriptions set forth herein but rather that the claims be construed as encompassing all the features of patentable novelty which reside in the present invention, including all features which would be treated as equivalents thereof by those skilled in the art to which the invention pertains. Therefore, the scope of the present invention is defined only by the appended claims, along with the full scope of equivalents to which such claims are entitled.

In this invention, the inventors demonstrate an in situ flow process to synthesize a membrane on or inside a hollow fiber or tubular membrane module at a controlled location, and to subsequently activate the membrane and measure separation properties in situ without having to remove the membrane. By using a single module for synthesis and characterization, membrane growth variables and post-treatments can be controlled accurately. This device also allows in situ characterization of the permeation properties of the module after each treatment step to determine cause and effect.

Hollow Fiber or Tubular Membrane Module Detail

In an embodiment of the present invention, a membrane was synthesized on or inside a hollow fiber or tubular membrane module. A side perspective view of a hollow fiber or tubular membrane module **100** is depicted in FIG. **1**A. As shown in FIG. **1**A, the hollow fiber or tubular membrane module **100** comprises a shell **105** and a bore **110**.

A cross-sectional view of a hollow fiber or tubular membrane module **100** is depicted in FIG. **1**B. As shown in FIG. **1**B, the hollow fiber or tubular membrane module **100** comprises a shell **105** and a bore **110**. In an embodiment, the hollow fiber or tubular module may have an inner (bore) diameter of about 50 μm to about 5000 μm. In an embodiment, the hollow fiber or tubular module may have an inner (bore) diameter of about 50 μm to about 300 μm.

Design Considerations/Machining Detail for Reactor Cell

A reactor cell of the present invention may be cubic-, rectangular-, cylindrical- or cylindrical-like shaped (e.g., elliptical base), and the like. In an embodiment, a reactor module **200** was fabricated to have a base shape and a first height, and a reactor module cover **420** was fabricated to have the same base shape as the reactor module **200** and a second height. In an embodiment, the base shape may be selected from the group consisting of square, rectangular, circular and ellipse.

Suitable materials for the reactor module and/or cover include any metal, or any plastic compatible with an adhesive (e.g., epoxy), alcohol solvents and water. In an embodiment, the metal may be selected from the group consisting of stainless steel, stainless steel alloys such as MONEL® (Special Metals Corp.) and HASTALLOY® (Haynes International, Inc.), and the like. In an embodiment, the plastic may be selected from the group consisting of polyether ketone (PEEK), polymethylene (e.g., DELRIN® (DuPont Co.)), polytetrafluorethylene (PTFE) (e.g., TEFLON® (Du-

Pont Co.)), and the like. In an embodiment, stainless steel 304 was used to fabricate the reactor module **200** and cover **420**.

Although a rectangular reactor module **200** and cover **420** are depicted in FIGS. **2-4**, a person of ordinary skill in the art could easily adapt these teachings to cubic, cylindrical and cylindrical-like reactor modules and covers. Accordingly, although the rectangular reactor module **200** and cover **420** are discussed in detail below, this discussion should not be interpreted to exclude cubic, cylindrical and cylindrical-like reactor modules and covers.

Although the reactor module and cover were machined from metal blocks, a person of ordinary skill in the art (POSITA) could easily adapt these teaching to other suitable methods of fabricating parts. In an embodiment, the fabrication method may be selected from machining, molding, printing and combinations thereof. For example, if a plastic material is used, the reactor module and cover may be molded by compression or injection molding or printed on a 3-D printer as customary in the art. Accordingly, although machining is discussed in detail below, this discussion should not be interpreted to exclude molding and printing techniques.

An upper, right front perspective view of a reactor module **200** is depicted in FIG. **2**. As shown in FIG. **2**, the reactor module **200** has a first length **205**, a second length **210** and a third length **215**. Further, the reactor module **200** has an upper surface **220**, a first side surface **225**, a second side surface **230** (not shown), a third side surface **235** and a fourth side surface **240** (not shown). The reactor module **200** may be constructed from a metal or a plastic as discussed above. In an embodiment, the reactor module **200** was constructed from stainless steel 304.

The reactor module **200** has a reactor chamber **245** with a reactor chamber diameter **250** and reactor chamber depth **255** (not shown) extending into the reactor module **200** from the upper surface **220**. Further, the reactor module **200** has an O-ring groove **260** extending into the reactor module **200** from the upper surface **220** and surrounding the reactor chamber **245**.

In an embodiment, the reactor chamber may be cylindrical. In such cylindrical embodiment, the inner diameter of the O-ring groove **260** is slightly larger than and offset from the reactor chamber diameter **250**.

In an embodiment, the reactor chamber may not be cylindrical. For such non-cylindrical embodiments, an O-ring groove with an inner dimension slightly larger than and offset from an outer dimension of the reactor chamber may be machined in the upper surface of the reactor module.

In an embodiment, the reactor module **200** has a temperature probe chamber **290** (not shown) with a temperature probe diameter **295** (not shown) and a temperature probe depth (not shown) extending into the reactor module **200** from the upper **220** or first side **225**, second side **230**, third side **240**, fourth side **245** surface. Suitable temperature probes **490** include resistance temperature detectors (RTDs), thermocouples, thermometers, and the like.

The reactor module **200** has a plurality of holes **285** extending into the reactor module **300** material from the upper surface **225** to attach a reactor module cover (not shown). In an embodiment, if the temperature probe chamber **290** extends into the reactor module **200** from the upper surface **220**, the reactor module cover **420** will have a temperature probe hole with a temperature probe diameter **295** extending through the reactor module cover **420** and aligning with the temperature probe diameter **295** of the temperature probe chamber **290** in the reactor module **200**. The reactor module cover **420** may be constructed from a metal or a plastic as discussed above. In an embodiment, the reactor module **200** was constructed from stainless steel 304.

The reactor module **200** has a first hole **265** extending into the reaction chamber **245** from a first side surface **225**, a second hole **270** extending into the reaction chamber **245** from a second side surface **230** (not shown), a third hole **275** extending into the reaction chamber **245** from a third side surface **235**, and a fourth hole **280** extending into the reaction chamber **245** from a fourth side surface **240** (not shown).

In an embodiment, the first **265** and second **270** holes may extend only partially into the first **225** and second **230** side surfaces, respectively, of the reactor chamber **245** such that a first and second smaller hole may extend into the reaction chamber **245** to accept a hollow fiber or tubular membrane module **100** as shown in FIG. **3**. In an embodiment, the hollow fiber or tubular membrane module **100** may be held (and sealed) in place in the first and second smaller holes with an adhesive such as an epoxy. In an embodiment, the first **265**, second **270**, third **275** and fourth **280** holes are threaded to accept various fittings as are customarily used in the art.

In an embodiment, the third **275** and fourth **280** holes extending into the third **235** and fourth **240** side surfaces of the reactor module **200** (i.e., surfaces perpendicular to the mounted hollow fiber or tubular membrane module **100**) may be slightly offset either vertically or horizontally from each other to facilitate mixing during flow conditions.

For example, a laboratory-scale reactor module **300** was constructed from a rectangular stainless steel block with a first length **305** of about 3-inches, a second length **310** of about 3-inches and a third length **315** of about 1.5-inches as depicted in FIGS. **3-4**. A reactor chamber **345** with reactor chamber diameter **350** of about 2-inches and a depth of about 1.38-inches was machined into the center of the stainless steel block.

Next, first **365**, second **370**, third **375** and fourth **380** holes were drilled for ⅛-inch NPT fittings through the first **325** (not shown), second **330** (not shown), third **335** (not shown) and fourth **340** (not shown) side surfaces of the stainless steel block. Although ⅛-inch NPT fittings were used, a POSITA could easily adapt this teaching to other fittings. Accordingly, although the ⅛-inch NPT fittings are disclosed, this disclosure should not be interpreted to exclude other fittings.

The first **365** and second **370** holes extended only partially into the first **325** and second **330** side surfaces, respectively, of the reactor chamber **345** such that a first and second smaller holes with a diameter of about 0.5 mm extended into the reaction chamber **345** to accept a hollow fiber or tubular membrane module **100** as shown in FIG. **3**. In an embodiment, the first **365** and second **370** holes extended into the first **325** and second **330** side surfaces, respectively, at a height of about 1-inch such that about 0.1-inch wall remained and second smaller holes with a diameter of about 0.02-inch were drilled through the 0.1-inch wall to create an aperture for mounting the hollow fiber or tubular membrane module **100**. These smaller holes may be used to support the hollow fiber or tubular membrane module **100**. The hollow fiber or tubular membrane module **100** may be mounted (and sealed) in place in the first and second smaller holes with an adhesive such as an epoxy.

Although the smaller holes were used to support the hollow fiber or tubular membrane, a person of ordinary skill in the art (POSITA) could easily adapt these teachings to use an insert to support the hollow fiber or tubular membranes(s) or to bundle the hollow fiber or tubular membranes such that the smaller holes are unnecessary. Accordingly, although smaller holes are discussed in detail above, this discussion should not be interpreted to exclude other techniques of supporting the hollow fiber or tubular membrane.

The third **375** and fourth **380** holes extending into the third **335** and fourth **340** side surfaces, respectively, of the reactor module **300** (i.e., surfaces perpendicular to the mounted hollow fiber or tubular membrane module **100**) were offset vertically from each other by about ⅛ to ¼-inch to facilitate mixing during flow conditions. In an embodiment, the third **375** and fourth **380** holes extended into the third **335** and fourth **340** sides, respectively, at a height of about 1⅛-inch such that the third **375** and fourth **380** holes extended into the reactor chamber **345**.

In an embodiment (not shown), the first hole **365** may extend into the reactor chamber **345** from the first side surface **325**, the second hole **370** opposing the first hole **365** may extend into the reactor chamber **345** from the second surface **330**, the third hole **375** may extend into the reactor chamber **345** from the first surface **325** and the fourth hole **380** opposing the third hole **375** may extend into the reactor chamber **345** from the second surface **330**.

In an embodiment (not shown), the first hole **365** may extend into the reactor chamber **345** from the first side surface **325**, the second hole **370** opposing the first hole **365** may extend into the reactor chamber **345** from the second surface **330**, the third hole **375** may extend into the reactor chamber **345** from an upper surface of a reactor module cover **420** and the fourth hole **380** opposing the third hole **375** extends into the reactor chamber **345** from a bottom surface of the reactor chamber **345**.

Although a few possible alternative configurations for an inlet (i.e., third hole **375**) and an outlet (i.e., fourth hole **380**) for an outer (shell) side solution have been discussed above, a POSITA could easily adapt this teaching to other designs. For example, the inlet and the outlet of the outer (shell) side solution may be positioned to create turbulent flow.

As depicted in FIG. **4**, the reactor module **400** must be airtight to be used to measure gas and liquid permeation. To provide an airtight seal, an O-ring groove **360** with a diameter of about 2¼-inches and cross-section of about 0.06-inches (AS568-035) was machined in the upper surface **320** of the reactor module **300** to receive an O-ring (see FIG. **3**).

In an embodiment, the reactor chamber may not be cylindrical. For such non-cylindrical embodiments, an O-ring groove with an inner dimension slightly larger than and offset from an outer dimension of the reactor chamber may be machined in the upper surface of the reactor module.

A plurality of threaded holes **385** were machined into each corner of the upper surface **320** of the reactor module **300**, **400** about 0.35-inches away from the O-ring groove **360** to receive a plurality of 10-32 hexagonal screws **485** as shown in FIGS. **3-4**. Although 10-32 hexagonal screws were used to secure a reactor module cover **420** (see FIG. **4**) to the reactor module **300**, a POSITA could easily adapt this teaching to other fasteners. Accordingly, although the 10-32 hexagonal screws are discussed in detail, this discussion should not be interpreted to exclude other fasteners.

A temperature probe chamber **290** with temperature probe diameter **295** was machined in the reactor module **300**, **400** outside of the O-ring groove **360** to receive a temperature probe **490** as shown in FIGS. **2-4**. As shown in FIG. **4**, the temperature probe **490** (e.g., heat probe, thermometer) is inserted in the temperature probe chamber **290**. Suitable temperature probes **490** include heat probe, resistance temperature detectors (RTDs), thermocouples, thermometers, and the like.

A rectangular block was used to fabricate a reactor module cover **420**. A photograph of a reactor module **400** and cover **420** is depicted in FIG. **4**. As shown in FIG. **4**, the reactor module cover **420** has a first length **425** of about 3-inches, a second length **430** (not shown) of about 3-inches and a third length **435** (not shown) of about ¼-inch. A plurality of holes (not shown) was machined in the reactor module cover **420** extending through the cover **420** and aligning with the diameters of the threaded holes **385** in the reactor module **400**. In an embodiment, the reactor module cover **420** was constructed from stainless steel 304.

A temperature probe hole (not shown) was machined in the reactor module cover **420** extending through the cover **420** and aligning with the temperature probe diameter **295** of the temperature probe chamber **290** in the reactor module **400**. As illustrated in FIG. **4**, the temperature probe **490** (e.g., heat probe, thermometer) is inserted in the temperature probe hole (not shown) of the cover **420** and into the temperature probe chamber **290** (not shown) of the reactor module **400**. Suitable temperature probes **490** include heat probes, resistance temperature detectors (RTDs), thermocouples, thermometers, and the like.

The reactor module cover **420** provides a flange-seal by tightening the cover **420** onto the reactor module **400** via the plurality of 10-32 hexagonal screws **485**.

Temperature Control of Reactor Cell/Module

The reactor module **400** may be heated and/or cooled to a temperature between about 0° C. and about 200° C. As shown in FIG. **4**, the laboratory-scale reactor module **400** was placed on a stir plate, and heated to about 30° C. with a temperature probe **490**. In an embodiment, the temperature probe **490** was set at about 30° C. and inserted into the temperature probe chamber **290** of the reactor module **400**.

Although a temperature probe **490** was used to heat the reactor module **400**, a POSITA could easily adapt this teaching to other heating and/or cooling methods. Accordingly, although the temperature probe heating method is discussed in detail, this discussion should not be interpreted to exclude other heating and/or cooling methods. For example, suitable heaters include temperature probes, hot plates, heating coils, enclosure heaters, silicone rubber heaters, polyester heaters, polyimide heaters, strip heaters, band heaters, tubular heaters, cartridge heaters, and the like. For example, suitable coolers include liquid baths, cooling coils, enclosure coolers, thermoelectric coolers, thermoelectric chillers, heat sinks, fans, and the like.

The temperature of the reactor module **400** may be set with a temperature probe **490** or measured with a thermometer. Although a temperature probe **490** was used, a POSITA could easily adapt this teaching to other combinations of heaters (discussed above) and temperature probes. Suitable temperature probes **490** include resistance temperature detectors (RTDs), thermocouples, thermometers, and the like.

Mounting/Sealing Hollow Fiber in Reactor Cell/Module

A length of a hollow fiber or tubular membrane module **100** may be threaded through the first and second smaller holes in the reactor module **200**, **300**. In an embodiment, a porous polyamide-imide (e.g., TORLON® (Solvay Advanced Polymers)) hollow fiber **100** with a length of about 4-inches was threaded through the first and second smaller holes of the reactor module **200**, **300**.

The hollow fiber or tubular membrane module **100** may be mounted (and sealed) in place in the first and second smaller holes with an adhesive such as an epoxy (e.g., transluscent epoxy (3M)). In an embodiment, the hollow fiber **100** was held (and sealed) in place in the first and second smaller holes with a small drop of epoxy on the shell of each fiber where the fiber passes through the aperture. After the epoxy was allowed to cure for about 90 minutes, the excess fiber ends were removed with tweezers, taking care not to crush or block the fiber ends. In an embodiment, a plurality of hollow fibers **100** may be mounted (and sealed) using this same method.

To ensure that the mounted hollow fiber(s) **100** was/were properly sealed and that the ends were not crushed or blocked, the reactor module **400** should be tested for use as a permeation cell by measuring the leak rate and the N_2 permeances of the mounted fiber(s), as discussed below.

Performance as Permeation Cell

The reactor module **400** was tested for use as a permeation cell by measuring the leak-rate and the permeance of a known standard. Using a porous polyamide-imide (e.g., TORLON®) hollow fiber as a standard, a N_2 permeance of 53,000 G.P.U., which is consistent with the reported values in the literature, was measured with the reactor cell **400**.[12,16] Based on flow-based leak tests, the leak-rate was determined to be less than 0.1 psi/hour.

Constant Flow Synthesis of ZIF-8 Membranes

Using a macroporous polyamide-imide (e.g., TORLON®) hollow fiber and the material ZIF-8 as an archetype for a hollow fiber or tubular membrane synthesis, a series of constant flow membrane synthesis experiments were performed. Several examples of ZIF-8 membrane fabrication using this reactor module **400** are described below, and their results are shown in the SEM micrographs of FIGS. **5**-**8**.

Performance in Membrane Synthesis: Static Conditions

Starting with a seeded polyamide-imide (e.g., TORLON®) hollow fiber **100** mounted in the reactor module **400**,[12] an aqueous synthesis gel consisting of about 0.22 g Zinc nitrate hexahydrate (Zn^{+2}) in about 40 mL of deionized water (DI) (about 0.018 mol/L) and about 9 g 2-methyl imidazole (mIm) in about 80 mL deionized water (DI) (about 1.37 mol/L) was poured on the outer (shell) side surface **105** of the hollow fiber **100**. After 6 hours at 30° C., the shell solution was removed and the hollow fiber **100** was thoroughly rinsed with deionized water (DI) and methanol.

A cross-sectional view of a SEM micrograph of a ZIF-8 membrane grown on an outer (shell) side surface of a seeded polyamide-imide (e.g., TORLON®) hollow fiber is shown in FIG. **5**A; and a top view of a SEM micrograph of the ZIF-8 membrane grown on the outer (shell) side surface **105** of the seeded polyamide-imide (e.g., TORLON®) hollow fiber is shown in FIG. **5**B. Based upon FIGS. **5**A-**5**B, the ZIF-8 membrane is formed on the outer (shell) side surface **105** of the hollow fiber **100**. Cross-sectional images of ZIF-8 inner surface membrane were examined using Hitachi SU 8010 scanning electron microscope after a thin layer of gold was sputtered onto the cross-sectional surface. To obtain a clean cut, the hollow fibers were soaked with a hexane solution for about 30 minutes followed by dipping into liquid nitrogen.

Performance in Membrane Synthesis: Flow Conditions

Reactions that are performed under flowing conditions are easier to control and allow recycling; therefore, ZIF-8 membranes were grown by flowing reagents through the bore **110** of the hollow fiber **100** (see FIGS. **6**-**7**).

First, an aqueous Zn^{+2} solution containing about 0.22 g Zinc nitrate hexahydrate (Zn^{+2}) in about 40 mL deionized water (DI) (about 0.018 mol/L) was flowed through the bore **110** at 2 mL/min while an aqueous mIm solution containing 9 g mIm in about 80 mL deionized water (DI) (about 1.37 mol/L) was poured on the outer (shell) side surface **105**. The reaction was stopped after 6 hours and the hollow fiber **100** was rinsed with deionized water (DI) and methanol.

A cross-sectional view of a SEM micrograph of a ZIF-8 membrane grown under aqueous flow conditions is shown in FIG. **6**A; and a detailed (10×) cross-sectional view of the SEM micrograph of the ZIF-8 membrane grown under aqueous flow conditions is shown in FIG. **6**B. Based upon FIGS. **6**A-**6**B, the ZIF-8 membrane is formed on the inner (bore) side surface **110** of the hollow fiber **100**.

To determine the effect of solvent, the aforementioned experiment was repeated using a different solvent (i.e., 1-octanol).

Second, a Zn^{+2}/1-octanol solution containing about 0.22 g Zinc nitrate hexahydrate (Zn^{+2}) in about 40 mL 1-octanol (about 0.018 mol/L) was flowed through the bore **110** at 2 mL/min while a mIm/1-octanol solution containing about 9 g mIm in about 80 mL 1-octanol (about 1.37 mol/L) was poured on the outer (shell) side surface **105**. The reaction was stopped after 6 hours and the hollow fiber **100** was rinsed with deionized water (DI) and methanol.

A cross-sectional view of a SEM micrograph of a ZIF-8 membrane grown under 1-octanol flow conditions is shown in FIG. **7**A; and a detailed (10×) cross-sectional view of the SEM image of the ZIF-8 membrane grown under 1-octanol flow conditions is shown in FIG. **7**B. Based upon FIGS. **7**A-**7**B, the ZIF-8 membrane is formed on the inner (bore) side surface **110** of the hollow fiber **100**.

Accordingly, for both the aqueous (see FIG. **6**) and 1-octanol (see FIG. **7**) flow systems, the ZIF-8 membrane growth was observed in the inner (bore) side surface **110** of the hollow fiber **100** instead of on the outer (shell) side surface **105**.

Performance in Membrane Synthesis: Interfacial Synthesis

The next experiment involved using interfacial synthesis technique whereby immiscible solvents are used as a means to physically separate the organic and inorganic precursors. Specifically, a Zn^{+2}/1-octanol solution containing about 0.22 g Zinc nitrate hexahydrate (Zn^{+2}) in about 40 mL 1-octanol (about 0.018 mol/L) was flowed at 2 mL/min through the bore **110** while an aqueous mIm solution containing about 9 g mIm in about 80 mL deionized water (DI) (about 1.37 mol/L) was poured into the reactor chamber **345** immersing the outer (shell) side surface **105** of the hollow fiber **100**. The reaction was stopped after 6 hours and the hollow fiber **100** was flushed with neat 1-octanol, heptane, and deionized water (DI).

To determine the effect of flow rate, the aforementioned experiment was repeated using a slower flow rate (1 μL/min).

A cross-sectional view of a SEM micrograph of a ZIF-8 membrane grown under 1-octanol flow conditions of 2 mL/min bore flow rate, using an interfacial system is shown in FIG. **8**A; and a cross-sectional view of the SEM micrograph of the ZIF-8 membrane grown under 1-octanol flow conditions of 1 μL/min bore flow rate, using the interfacial system is shown in FIG. **8**B.

Accordingly, for the interfacial system, both the 2 mL/min (see FIG. **8**A) and 1 μL/min (see FIG. **8**B) bore flow rates, the ZIF-8 membrane growth was observed in the interior (bore) side surface **110** of the hollow fiber **100** instead of on the outer (shell) side surface **105**.

Table 1 shows the measurement of single-component gas permeation properties of three of the ZIF-8 membranes using the reactor module **400**. The entire process of membrane formation and permeation measurement can be done in situ within the same pre-fabricated reactor module **400**, thereby avoiding the difficulties associated with previous membrane fabrication processes.

TABLE 1

Measurement of Single-Component Gas Permeation Properties for In-Situ grown ZIF-8 Membrane

Example	Support	Flow Rate	Thickness (μm)	Permeance (G.P.U.) N_2	SF_6	Selectivity N_2/SF_6
ZIF-8_Outer (see FIGS. 5A-5B)	Torlon Tube	Static	3	800	430	1.9
ZIF-8_Inner_1 (see FIG. 8A)	Torlon Tube	2 mL/min	5-15	240	100	2.4
ZIF-8_Inner_2 (see FIG. 8B)	Torlon Tube	1 μL/min	2-3	320	60	5.3

An X-ray Diffraction (XRD) chart of 2Theta (°) vs. intensity for simulated and experimental ZIF-8 membranes, confirming the structure of supported ZIF-8 membranes is shown in FIG. **9**. XRD patterns were measured on a PANalytical X'Pert Pro diffractometer at room temperature using Cu Kα radiation of λ=0.154 nm and a scanning range of 5-40° 2θ.

An EDS Zinc line profile scan of distance from membrane surface (μm (microns)) vs. intensity, depicting the thickness of the ZIF-8 membrane to be about 3 μm is shown in FIG. **10**.

Performance in Membrane Synthesis: Static, Continuous and Pulsed Flow Conditions

In an embodiment, ZIF-8 membranes were grown by flowing reagents through the bore **110** of the hollow fiber **100** (see FIGS. **6**-**7**, **18**B-**18**C) under static, continuous and pulsed flow conditions. See FIGS. **11**-**12** & **18**A.

First, a Zn^{+2}/1-octanol solution containing about 0.22 g Zinc nitrate hexahydrate (Zn^{+2}) in about 40 mL 1-octanol (about 0.018 mol/L) was continuously flowed through the bore **110** at about 60 μL/hour while an aqueous mIm solution containing about 9 g mIm in about 80 mL deionized water (DI) (about 1.37 mol/L) was poured on the outer (shell) side surface **105**. The reaction was stopped after about 9 hours and the hollow fiber **100** was rinsed with 1-octanol, heptanes, deionized water (DI) and methanol.

Second, a Zn^{+2}/1-octanol solution containing about 0.22 g Zinc nitrate hexahydrate (Zn^{+2}) in about 40 mL 1-octanol (about 0.018 mol/L) was held static in the bore **110** while an aqueous mIm solution containing about 9 g mIm in about 80 mL deionized water (DI) (about 1.37 mol/L) was poured on the outer (shell) side surface **105**. The reaction was stopped after about 9 hours and the hollow fiber **100** was rinsed with 1-octanol, deionized water (DI), heptanes and methanol.

A chart of Time vs. Flow Rate static and continuous flow through the bore **110** of the hollow fiber **100** is illustrated in FIG. **11**. No continuous ZIF-8 membrane was formed on the inside of the bore **110** of the hollow fiber **100** under static conditions. In contrast, a continuous ZIF-8 membrane was formed on the inside of the bore **110** of the hollow fiber **100** by continuously flowing bore solution at about 60 μL/hour, however, the membrane had a low H_2/C_3H_8 selectivity.

A chart of Time vs. Flow Rate for pulsed flow conditions through the bore **110** of the hollow fiber **100** is illustrated in FIG. **12**. Under pulsed flow conditions, a ZIF-8 membrane was formed on the inside of the bore **110** of the hollow membrane 100, and, further, the pulsed-flow membrane had a higher H_2/C_3H_8 selectivity than the continuous-flow membrane discussed above.

To further test the effect of flow conditions, the aforementioned experiment was repeated using a one phase aqueous solvent system, a single phase organic solvent system (1-octanol), and a biphasic interfacial solvent system (aqueous/1-octanol), respectively.

First, an aqueous Zn^{+2} solution containing about 0.22 g Zinc nitrate hexahydrate (Zn^{+2}) in about 40 mL deionized water (DI) (about 0.018 mol/L) was flowed through the bore **110** at about 10 μL/hour while an aqueous mIm solution containing about 9 g mIm in about 80 mL deionized water (DI) (about 1.37 mol/L) was poured on the outer (shell) side surface **105**. After about 2 hours of bore solution flow, the pump was stopped for about 3.5 hours to provide a static growth step. After about 3.5 hours, the pump was continued for about 20 minutes. After about 20 minutes, the pump was stopped for another 3.5 hours to provide another static growth step. The reaction was stopped after about 9 hours and the hollow fiber **100** was rinsed with deionized water (DI) and methanol.

Second, a Zn^{+2}/1-octanol solution containing about 0.022 g Zinc nitrate hexahydrate (Zn^{+2}) in about 40 mL 1-octanol (about 0.018 mol/L) was flowed through the bore **110** at about 10 μL/hour while a mIm/1-octanol solution containing about 9 g mIm in about 80 mL 1-octanol (about 1.37 mol/L) was poured on the outer (shell) side surface **105**. After about 2 hours of bore solution flow, the pump was stopped for about 3.5 hours to provide a static growth step. After about 3.5 hours, the pump was continued for about 20 minutes. After about 20 minutes, the pump was stopped for another 3.5 hours to provide another static growth step. The reaction was stopped after about 9 hours and the hollow fiber **100** was rinsed with 1-octanol, deionized water (DI), heptanes and methanol.

Third, a Zn^{+2}/1-octanol solution containing about 0.11 g Zinc nitrate hexahydrate (Zn^{+2}) in about 40 mL 1-octanol (about 0.018 mol/L) was flowed through the bore **110** at about 10 μL/hour while an aqueous mIm solution containing about 9 g mIm in about 80 mL deionized water (DI) (about 1.37 mol/L) was poured on the outer (shell) side surface **105**. After about 2 hours of bore solution flow, the pump was stopped for about 3.5 hours to provide a static growth step. After about 3.5 hours, the pump was continued for about 20 minutes. After about 20 minutes, the pump was stopped for another 3.5 hours to provide another static growth step. The reaction was stopped after about 9 hours and the hollow fiber **100** was rinsed with 1-octanol, deionized water (DI), heptanes and methanol.

A chart of Time vs. Flow Rate summarizing the examined static, continuous and pulsed flow conditions through the bore **110** of the hollow fiber **100** is illustrated in FIG. **18**A.

A cross-sectional view of a SEM micrograph of a ZIF-8 membrane grown in a polyamide-imide (e.g., TORLON®) hollow fiber with a static flow of a Zn^{+2}/1-octanol bore solution is illustrated in FIG. **18**B. As shown in FIG. **18**B, static growth conditions produce dense, non-continuous coatings of ZIF-8 particles in the inner (bore) side surface **110** of the hollow fiber **100**. This is due to the lack of sufficient Zn^{2+} ions available in the microscale bore of the hollow fiber **100** to sustain the film growth after the initial nucleation and growth of ZIF-8 crystals at the inner (bore) side surface **110** of the hollow fiber **100**.

A cross-sectional view of a SEM micrograph of a ZIF-8 membrane grown on a polyamide-imide (e.g., TORLON®) hollow fiber with continuous flow of a Zn^{+2}/1-octanol bore solution is illustrated in FIG. **18**B. As shown in FIG. **18**C, continuous flow growth conditions produced a thin, continuous membrane (about 3 μm thickness) that was formed in the inner (bore) side surface **110** of the hollow fiber **100**. This is due to the relatively rapid transport of reactants to the interface under continuous flow, leading to rapid formation and closure of the ZIF-8 layer. The growing membrane itself becomes a barrier between the two immiscible solvents, and confines the liquid-liquid interface into the gaps and interstices between the ZIF-8 crystals. See FIG. **15**.

A cross-sectional view of a SEM micrograph of a ZIF-8 membrane grown on a polyamide-imide (e.g., TORLON®) hollow fiber with intermittent flow of a Zn^{+2}/1-octanol bore solution is illustrated in FIG. **18**D. As shown in FIG. **18**D, intermittent flow growth conditions produced a thicker, continuous membrane (about 8 μm thickness) that was formed in the inner (bore) side surface **110** of the hollow fiber **100**. The flow profile included an initial continuous growth step, followed by a static growth step interrupted by a brief reactant replenishment step. In an embodiment, the flow profile included an initial continuous growth step of about 10 μL/hour of a Zn^{+2}/1-octanol bore solution for about 2 hours, followed by a static growth step of about 0 μL/hour of the bore solution for about 3.5 hours, followed by a replenishment step of about 10 μL/hour of bore solution for about 20 minutes and followed by another static growth step of about 0 μL/hour of bore solution for about 3.5 hours. See FIG. **18**A: flow profile 2.

Additionally, FIG. **17**A shows lower-magnification images of ZIF-8 membranes formed on two hollow fibers **100**; and FIG. **17**B shows the zinc elemental mapping, confirming the localization of the membrane to the inner (bore) side surface **110** of the hollow fiber **100**. X-ray diffraction confirmed the ZIF-8 crystal structure of the film. See FIG. **19**.

Performance in Membrane Synthesis: Pulsed Flow Synthesis

Table 2 shows measurement of gas and liquid permeation properties for various supported ZIF-8 membranes.

TABLE 2

Measurement of Gas and Liquid Permeation Properties

Reference	Support	Thickness (μm)	Permeance (G.P.U.) H_2	CO_2	CH_4	C_3H_8	C_6H_{14}	C_6H_{12}	C_6H_6
Y. Pan	YSZ Tube	2.5	4400	1200	360	4			
Y. Pan	Al_2O_3 Disk	2.5	1100	390	240	2			
AJB	Torlon ®	8	2900	500	270	60	2600	600	290

A X-ray Diffraction (XRD) chart of 2Theta (°) vs. intensity for simulated and experimental ZIF-8 membranes and polyamide-imide (e.g., TORLON®) hollow fiber, confirming formation and structure of supported ZIF-8 membranes on the bore **110** of the hollow fiber **100** is shown in FIG. **14**. XRD patterns were measured on a PANalytical X'Pert Pro diffractometer at room temperature using Cu Kα radiation of λ=0.154 nm and a scanning range of 5-40° 2θ.

Performance in Membrane Synthesis: Pulsed Flow and Stirred Synthesis

Table 3 shows the single-component gas permeation properties of a ZIF-8 membrane measured in situ using the reactor module **400** and gently stirring the outer (shell) side **105** solution.

TABLE 3

Measurement of Single-Component Gas Permeation Properties for grown ZIF-8 Membrane

Sample	Support	Flow Rate	Thickness (μm)	Permeance (G.P.U.) H_2	CH_4	C_3H_8	Selectivity H_2/C_3H_8
ZIF-8_10 μL/hour Pulsed	Torlon ®	10 μL/hour	8	4200	400	35	120

Table 4 shows measurement of gas permeation properties of a ZIF-8 membrane when the mixture feed consisted of a 1:1 H_2/C_3H_8 mixture.

TABLE 4

Measurement of Mixed Gas Permeation Properties

Sample	Support	Thickness (μm)	Permeance (G.P.U.) H_2	Permeance (G.P.U.) C_3H_8	Selectivity H_2/C_3H_8
Y. Pan	YSZ Tube	2.5	2000	4	470
ZIF-8_1010 μL/hour	Torlon ®	8	2250	26.4	85

Y. Pan, et al., J. MEMBR. SCI. 421 (2012) 292.

Pulsed-Flow Synthesis of ZIF-8 Membranes

Using a macroporous polyamide-imide (e.g., TORLON®) hollow fiber and the material ZIF-8 as an archetype for a hollow fiber or tubular membrane synthesis, a series of pulsed flow membrane synthesis experiments were performed. Table 5 shows combinations of precursor solutions and locations (bore/shell) tested to synthesize ZIF-8 membranes using a reactor module **400**. Several examples of ZIF-8 membrane fabrication using the reactor module **400** are described below, and their results are shown in the SEM micrographs of FIGS. **17**A-**17**B, **18**A-**18**D and **20**A-**20**D. For the experiments, a temperature probe **490** set at 30° C. was inserted into the reactor module **400** during membrane growth.

TABLE 5

Combinations of Precursor Solutions Tested to Synthesize ZIF-8 Membranes Using IMMP Approach

Example	Bore Solution	Shell Solution	Molar Ratio Zn^{+2}/mIm	Membrane Location
1 (see FIGS. 17A-17B and 18A-18D)	0.018 mol/L Zn^{+2} in 1-octanol	1.37 mol/L mIm in DI	75	Bore (inner surface)
2 (see FIG. 20A)	0.018 mol/L Zn^{+2} in 1-octanol	1.37 mol/L mIm in DI	75	In fiber, closer to bore surface
3 (see FIG. 20B)	0.018 mol/L Zn^{+2} in 1-octanol	1.37 mol/L mIm in DI	75	In fiber, closer to bore surface
4 (see FIG. 20C)	1.37 mol/L mIm in DI	0.018 mol/L Zn^{+2} in 1-octanol	75	Shell (outer surface)
5 (see FIG. 20D)	1.37 mol/L mIm in DI	0.018 mol/L Zn^{+2} in 1-octanol	75	Shell (outer surface)

Example 1

First, about 10 mL of neat 1-octanol solvent was flowed through a bore **110** using a syringe pump.

Second, about 3 mL of a Zn^{+2}/1-octanol solution containing 0.11 g Zinc nitrate hexahydrate (Zn^{+2}) in about 40 mL 1-octanol (about 0.018 mol/L) was flowed through the bore **110** of a horizontal hollow fiber **100** at a flow rate of about 10 μL/hour. In an embodiment, a limited Zn^{+2}/1-octanol solution containing about 0.005 mol/L to about 0.1 mol/L Zn^{+2} in 1-octanol may be used. In an embodiment, a limited Zn^{+2}/1-octanol solution containing about 0.01 mol/L to about 0.03 mol/L Zn^{+2} in 1-octanol may be used. Increasing the Zn^{+2} concentration to about 0.03 mol/L leads to reduction of the membrane thickness and increase in crystal nucleation.

About 70 mL of an aqueous mIm solution containing about 9 g mIm in about 80 mL dionized water (DI) (about 1.37 mol/L) was slowly poured into the reactor module **400**, immersing the outer (shell) side surface **105** of the hollow fiber **100**. In an embodiment, an excess aqueous mIm solution containing about 0.5 mol/L to about 10 mol/L mIm in deionized water (DI) may be used, provided that the mIm concentration is in excess. In an embodiment, an excess aqueous mIm solution containing about 1.2 mol/L to about 1.6 mol/L mIm in deionized water (DI) may be used.

The aqueous mIm (shell) solution was gently stirred at about 60 rpm to prevent the formation of local concentration gradients. In an embodiment, the aqueous mIm solution may be stirred at about 40 rpm to about 80 rpm.

After about 2 hours of bore solution flow, the pump was stopped for about 3.5 hours to provide a static growth step. After about 3.5 hours, the pump was continued for about 20 minutes. After about 20 minutes, the pump was stopped for another 3.5 hours to provide another static growth step. In an embodiment, the bore solution flows at a first flow rate for a first period, the bore solution is stopped for a second period, the bore solution flows at a second flow rate for a third period and the bore solution is stopped for a fourth period. In an embodiment, the first and second flow rate is about 10 μL/hour to about 100 μL/hour. In an embodiment, the first period is about 1 hour to about 3 hours, the second period is about 3 hours to about 4 hours, the third period is about 10 minutes to about 30 minutes and the fourth period is about 3 hours to about 4 hours.

To stop the reaction, about 10 mL of neat 1-octanol solvent was pushed through the bore **110** while the outer (shell) side surface **105** was soaked in about 70 mL of neat DI (and replaced three times) to remove the excess Zn^{+2}. Next, about 10 mL heptanes were pushed through the bore **110** while the outer (shell) side surface **105** was soaked in about 70 mL heptanes to remove the 1-octanol. Next, about 10 mL of hexane was pushed through the bore **110** while the outer (shell) side surface **105** was soaked in hexane to remove the heptanes. Then, about 20 mL methanol was flowed through the bore **110** while the outer (shell) side surface **105** was soaked in about 70 mL methanol to remove the DI. The reactor module **400** was allowed to air dry at least 4 days before permeation testing.

Example 2

First, about 10 mL DI was first flowed through the bore **110** followed by about 3 mL of an aqueous Zn^{+2} (bore) solution (about 0.018 mol/L). About 70 mL of an aqueous mIm solution (about 1.37 mol/L) was added to the outer (shell) side surface **105** (i.e., slowly poured into the reactor module **400** and was gently stirred at about 60 rpm to prevent the formation of local concentration gradients) while the aqueous Zn^{+2} (bore) solution was flowed at about 10 μL/hour for about 2 hours. After about 2 hours of bore solution flow, the pump was stopped for about 3.5 hours to provide a static growth step. After about 3.5 hours, the pump was continued for about 20 minutes. After about 20 minutes, the pump was stopped for another 3.5 hours to provide another static growth step.

To stop the reaction, about 20 mL DI was flowed through the bore **110** while the outer (shell) side surface **105** was soaked in about 70 mL of neat DI (and replaced three times) to remove the excess Zn^{+2}. Then, about 20 mL methanol was flowed through the bore **110** while the outer (shell) side surface **105** was soaked in about 70 mL methanol to remove the DI. The reactor cell **400** was allowed to air dry at least 4 days before permeation testing.

Example 3

First, about 10 mL 1-octanol was first flowed through the bore **110** followed by about 3 mL of a Zn^{+2}/1-octanol (bore) solution (about 0.018 mol/L). About 70 mL of an mIm/1-octanol solution (about 1.37 mol/L) was added to the outer (shell) side surface **105** while the Zn^{+2}/1-octanol (bore) solution was flowed at about 10 μL/hour for about 2 hours. After about 2 hours of bore solution flow, the pump was stopped for about 3.5 hours to provide a static growth step. After about 3.5 hours, the pump was continued for about 20 minutes. After about 20 minutes, the pump was stopped for another 3.5 hours to provide another static growth step.

To stop the reaction, about 10 mL neat 1-octanol solvent was pushed through the bore **110** while the outer (shell) side surface **105** was soaked in about 70 mL of neat 1-octanol solvent. Then, about 10 mL of heptanes were pushed through the bore **110** while the outer (shell) side surface **105** was soaked in about 70 mL of heptanes to remove the 1-octanol. Then, about 10 mL of hexane was pushed through the bore **110** while the outer (shell) side surface **105** was soaked in about 70 mL of hexane to remove the heptanes. Then, about 10 mL of methanol was pushed through the bore **110** while the outer (shell) side surface **105** was soaked in about 70 mL of methanol. The reactor module **400** was allowed to air dry at least 4 days before permeation testing.

Example 4

First, about 10 mL neat 1-octanol solvent was flowed through the bore **110** followed by about 3 mL of mIm/1-octanol (bore) solution (about 1.37 mol/L).

Second, about 70 mL of an aqueous Zn^{+2} solution (about 0.018 mol/L) was added to the outer (shell) side surface **105** while the mIm/octanol (bore) solution was flowed at about 10 μL/hour for about 2 hours. After about 2 hours of bore solution flow, the pump was stopped for about 3.5 hours to provide a static growth step. After about 3.5 hours, the pump was continued for about 20 minutes. After about 20 minutes, the pump was stopped for another 3.5 hours to provide another static growth step.

To stop the reaction, about 10 mL of neat 1-octanol solvent was pushed through the bore **110** while the outer (shell) side surface **105** was soaked in about 70 mL of neat DI (and replaced three times) to remove the excess Zn^{+2}. Next, about 10 mL heptanes were pushed through the bore **110** while the outer (shell) side surface **105** was soaked in about 70 mL heptanes to remove the 1-octanol. Next, about 10 mL of hexane was pushed through the bore **110** while the outer (shell) side surface **105** was soaked in hexane to remove the heptanes. Then, about 20 mL methanol was flowed through the bore **110** while the outer (shell) side surface **105** was soaked in about 70 mL methanol to remove the DI. The reactor module **400** was allowed to air dry at least 4 days before permeation testing.

Example 5

First, about 10 mL DI was flowed through the bore **110** followed by about 3 mL of an aqueous mIm solution (about 1.37 mol/L).

Second, about 70 mL of a Zn^{+2}/1-octanol solution (about 0.018 mol/L) was added to the outer (shell) side surface **105** while the aqueous mIm (bore) solution was flowed at about 10 μL/hour for about 2 hours. After about 2 hours of bore solution flow, the pump was stopped for about 3.5 hours to provide a static growth step. After about 3.5 hours, the pump was continued for about 20 minutes. After about 20 minutes, the pump was stopped for another 3.5 hours to provide another static growth step.

The reaction was stopped by flowing about 20 mL DI through the bore **110** and exchanging the outer (shell) side surface **105** solution with neat 1-octanol solvent. Then, about 10 mL heptanes were flowed through the bore **110** while the outer (shell) side surface **105** was soaked in about 70 mL of heptanes. Then, about 10 mL hexane was flowed through the bore **110** while the outer (shell) side surface **105** was soaked in about 70 mL of hexane. Then, about 20 mL methanol was flowed through the bore **110** while the outer (shell) side surface **105** was soaked in about 70 mL of methanol.

Capping of Hollow Fiber Ends

A capping solution containing poly(dimethylsiloxane) (PDMS) (e.g., SYLGARD® 184 (Corning)) in a solvent may be used as a filler material to cap both ends of the hollow fiber **100**. In an embodiment, a capping solution containing about 9 wt % PDMS in heptane was heated at about 90° C. with vigorous stirring for about 4 hours to thermally crosslink the PDMS. In an embodiment, a capping solution of about 8 wt % to 10 wt % PDMS in heptane may be used.

After cooling to about 25° C., about 2 μL droplet was applied from a pipette to each hollow fiber **100** end, using capillary action. Immediately upon applying the sealing solution, Argon gas was immediately flowed through the inner (bore) side **110** and followed by curing at about 120° C. for about 2 hours.

Performance of ZIF-8 Membranes Made Using IMMP Reactor Cell/Module

The separation properties of the ZIF-8 membrane grown on the inner bore of the polyamide-imide (e.g., TORLON®) hollow fiber **100** were characterized by hydrogen (H_2)/propane (C_3H_8) and propylene (C_3H_6)/propane (C_3H_8) binary equimolar mixture permeation as a function of temperature, with the reactor module **400** directly acting as a permeation cell. See FIG. **16**. In an embodiment, the feed mixture may be selected from the group consisting of hydrogen/hydrocarbons, hydrogen/propane, propylene/propane and butenes/butanes.

A steady-state Wicke Kallenbach technique was used to test binary H_2/C_3H_8 and C_3H_6/C_3H_8 mixtures. Specifically, 1:1 feed mixtures were flowed through a bore **110** of the ZIF-8 membrane grown on the polyamide-imide (e.g., TORLON®) hollow fiber **100** at about 20 mL/min while an argon sweep gas was flowed across an outer (shell) side surface **105** of the hollow fiber **100** at about 20 mL/minute. See e.g., FIGS. **21**A-**21**B, **22**A-**22**B and **23**A-**23**B. In FIGS. **21**A-**21**B, **22**A-**22**B and **23**A-**23**B, the error bars were estimated from characterization of three independent ZIF-8 membrane samples.

A gas chromatograph with TCD and FID detectors was used to determine the composition of permeate. At least 3

GC injections were collected (median permeance values were reported) at each temperature after waiting 30 minutes for steady-state conditions.

The ZIF-8 membranes in polyamide-imide (e.g., TORLON®) hollow fibers **100** were formed using the reaction conditions of Example 1 under intermittent flow conditions (see FIG. **18**A: flow profile 2). The as-made ZIF-8 membranes on polyamide-imide (e.g., TORLON®) hollow fibers **100** exhibited clear molecular sieving properties: high H_2 permeances, sharp H_2/C_3H_8 separation factors as high as 125 at 120° C. (see FIG. **22**A), and strong temperature dependence of H_2 permeance with temperature, indicating activated molecular transport through the ZIF-8 pores. Further, the example ZIF-8 membrane on polyamide-imide (e.g., TORLON®) hollow fiber **100** proved to be robust showing no decline in permeation properties after six weeks of testing and multiple heating/cooling cycles.

While the permeation properties were dominated by molecular sieving, the C_3 isomer (especially C_3H_8) permeances were much larger than those expected from previous studies[8, 17-20] and prevented a high C_3H_6/C_3H_8 separation factor. See FIG. **23**B. It was hypothesized that the high C_3 isomer permeances were due to both molecular transport through the ZIF-8 membrane as well as due to bypassing of the ZIF-8 membrane by the feed molecules through the ends of the fiber. See FIG. **24**A.

To suppress this membrane bypass, the inventors include a capping step to the IMMP approach, accomplished by applying a controlled amount of a solution containing poly (dimethylsiloxane) (PDMS) to the ends of the mounted hollow fibers **100**. See FIG. **24**B. The PDMS solution is readily absorbed by capillary action into the hollow fiber **100**, and blocks the pores of the hollow fiber **100** support. See FIGS. **25**A and **25**B. SEM cross-sectional imaging (see FIG. **25**A) and EDX mapping (see FIG. **25**B) indicated that the fiber matrix is completely covered by PDMS while the bore remains unblocked. Since the permeances of the feed gases through PDMS are 3 orders of magnitude lower than through the macroporous hollow fiber **100** support, the C_3H_8 flux should decrease substantially after capping. After curing the PDMS-sealed hollow fibers **100**, the H_2/C_3H_8 separation factor is now much higher (370 at 120° C.) (see FIG. **21**A) and the C_3H_6/C_3H_8 separation factor is also higher (12 at 25° C.) (see FIG. **21**B), consistent with previously reported ZIF-8 membranes with low defect densities.[8, 17-20] Notably, the C_3H_8 permeance decreased by a factor of 10 after capping. This indicates that most of the propane was previously bypassing the ZIF-8 layer and that the addition of the capping step to the IMMP largely shuts down this non-selective permeation path. The permeate stream contains 92% C_3H_6/8% C_3H_8, which is a significant upgrade from the equimolar feed stream.

Performance of Bundle of ZIF-8 Membranes Made Using IMMP Reactor Cell/Module

In large-scale gas separations with hollow fiber membranes, high membrane areas per unit module volume are achieved by bundling large numbers of fibers in the permeation module. The present invention has the advantage of being inherently a modular approach that should allow independent processing of membranes in each fiber constituting a bundle.

To demonstrate this concept, the inventors applied reactor module **400** to the simultaneous processing of three polyamide-imide (e.g., TORLON®) hollow fiber **100** supports. The processing conditions were identical to the case of the single-fiber membranes, except that the total feed solution initially introduced to the bore and the flow rate on the bore side was increased by a factor of 3 so that the flow rate through individual hollow fibers **100** was maintained constant in relation to the single-fiber membrane fabrication described earlier. The ends of the hollow fibers **100** were capped in a similar manner as described earlier.

FIGS. **23**A and **23**B show that the H_2/C_3H_8 and C_3H_6/C_3H_8 separation behavior is near-identical to the single-fiber membranes (see FIGS. **21**A and **21**B), thereby clearly demonstrating the potential for scalability of the IMMP approach. The inventors also note that the separation factor values of the ZIF-8 membranes are very sensitive to the small permeance of C_3H_8 (~2.5 G.P.U. in the present invention). With further improvements in the capping methods (e.g., using less permeable polymers than PDMS) and optimization of the ZIF-8 membrane growth conditions, the small C_3H_8 permeance can be further reduced and the separation factor further increased, leading to a highly attractive membrane platform for hydrocarbon separations. Given the overall importance of tunable ZIF materials for a range of hydrocarbon separations, the membrane processing approach reported here overcomes many of the limitations of current processes and moves significantly towards realizing scalable molecular sieving MOF membranes.

Improved Membrane Synthesis Using IMMP Reactor Cell/Module

Using a macroporous polyamide (e.g., TORLON®) hollow fiber and the material ZIF-8 as an archetype for hollow fiber and tubular membrane synthesis, a series of isothermal and initial heating membrane synthesis experiments were performed. Several examples of ZIF-8 membrane fabrication using this reactor module **400** are described below, and their results are shown in SEM micrographs of FIGS. **27**A-**27**F, **30**C and **31**A-**31**C.

FIG. **26**A shows a schematic of the IMMP reactor module **400** for ZIF-8 membrane fabrication on the inner bore side surface **110** of the polyamide imide (e.g., TORLON®) hollow fibers. The formation of a ZIF-8 membrane is achieved by contacting the two reactant streams (i.e., Zn^{2+} ions dissolved in 1-octanol on the inner bore side surface **110**, and 2-methylimidazole (mIm) dissolved in deionized water (DI) on the outer (shell) side surface **105**) across the polyamide-imide (e.g., TORLON®) hollow fiber support. In these experiments, the two solvents are chosen to be immiscible, thereby allowing a sharp interface between the two phases. The use of a large excess of mIm (e.g., mIm/Zn^{+2} concentration ratio=75) allows the Zn^{2+} to act as a limiting reactant, thereby leading to ZIF-8 film formation on the inner surface.

The temporal flow profile in the bore side is shown in FIG. **26**B. It comprises four steps: about 120 minutes of membrane formation under a continuous flow of about 62 μL/hour of a $Zn^{2\pm}$/octanol solution (Step 1), about 210 minutes of membrane growth under static conditions (Step 2), about 20 minutes of $Zn^{2\pm}$/octanol solution replenishment at a continuous flow of about 62 μL/hour (Step 3), and a final 210 minutes of static membrane growth (Step 4).

Two different temperature profiles are also shown in FIG. **26**B, as discussed further below. They comprise an isothermal profile (e.g., about 30° C.) and an initial heating profile (e.g., increased linearly from about 22° C. to about 42° C. in about 25 minutes and decreased from 42° C. to 30° C. in about 60 minutes), as discussed further below.

Membrane Formation Process Using IMMP Reactor Module/Cell

To investigate the membrane formation process, the inventors repeated the IMMP approach multiple times and arrested the ZIF-8 membrane growth at three different points as indicated by the numbered temporal locations (i.e., arrest points #1, #2 and #3) in FIG. **26**B.

Starting with a polyamide-imide (e.g., TORLON®) hollow fiber mounted in the IMMP reactor module **400**,[12] a Zn^{+2}/1-octanol solution containing about 0.22 g Zinc nitrate hexahydrate (Zn^{+2}) in about 40 mL 1-octanol (about 0.018 mol/L) was flowed through the bore **110** of the hollow fiber **100** while an aqueous mIm solution containing about 9 g of mIm in about 80 mL deionized water (DI) (about 1.37 mol/L) was poured into the reactor chamber **345** immersing the outer (shell) side surface **105** of the hollow fiber **100** while stirring the solution at about 60 rpm for about 120 minutes to provide a continuous membrane growth step.

The temperature of the reactor module **400** was maintained at about 31.0±0.5° C. throughout the IMMP process. See FIG. **26**B.

For each arrest point #1, #2 and #3, about 10 mL of neat 1-octanol was pushed through the bore side **110** of the hollow fiber **100** while exchanging the shell side **105** solution with about 70 mL neat methanol (MeOH) and replaced three times.

After the 120 minutes of continuous membrane growth step (arrest point #1), the flow rate of the Zn^{+2}/1-octanol solution through the bore **110** of the hollow fiber **100** was stopped for about 210 minutes to provide a static membrane growth step.

After the 210 minutes of static membrane growth step (arrest point #2), the flow rate of the Zn^{+2}/1-octanol solution through the bore **110** of the hollow fiber **100** was continued for about 20 minutes to provide a second continuous membrane growth step.

After the 20 minutes of second continuous membrane growth step, the flow rate of about 0.6 mL/hour through the bore **110** of the hollow fiber **100** was stopped for about 210 minutes to provide a second static membrane growth step.

After the 210 minutes of second static membrane growth step (arrest point #3), the reaction was stopped.

To stop the reaction, about 10 mL of neat 1-octanol solvent was pushed through the bore **110** while the outer (shell) side surface **105** was soaked in about 70 mL of neat DI (and replaced three times) to remove the excess Zn^{+2}. Next, about 10 mL heptanes were pushed through the bore **110** while the outer (shell) side surface **105** was soaked in about 70 mL heptanes to remove the 1-octanol. Next, similar procedure was performed with a more volatile hexane solution. Then, about 10 mL hexane was pushed through the bore **110** while outer (shell) side surface **105** was soaked in about 70 mL hexane to remove the heptanes. Finally, about 20 mL of MeOH was pushed through the bore **110** while the outer (shell) side surface **105** was soaked in about 70 mL methanol to remove the DI. The membrane was dried at about room temperature (e.g., about 25° C.) for about 2 days.

Binary propylene (C_3H_6)/propane (C_3H_8) permeation measurements were conducted in situ for each arrest point #1, #2 and #3, and, finally, after completion of the IMMP process, the ZIF-8 membrane on the polyamide-imide (e.g., TORLON®) hollow fiber **100** was removed from the IMMP reactor module **400** and cross-sectioned for SEM imaging and thickness measurements, as discussed below.

FIGS. **27**A-**27**C show the development of the ZIF-8 membrane morphology at the three different arrest points #1, #2 and #3 shown in FIG. **26**B. Tables 6 & 7 show information about average thickness and C_3H_6/C_3H_8 permeation characteristics for each of these arrest points.

After the 120 minutes of the continuous membrane growth step (arrest point #1), a dual-layer ZIF-8 membrane may be observed on the inner bore surface **110** of the hollow fiber **100** (see FIGS. **27**A & **28**) with an overall thickness of about 7 μm (see Table 6), of which about 4.5 μm is a dense ZIF-8 membrane layer and the remainder is a discontinuous membrane layer composed of plate-like structures.

Without wishing to be bound to any theory, the inventors believe this morphology arises from the rapid penetration of mIm (which is soluble in both water and octanol) into the octanol phase. At the inner surface of the fiber, mIm may be rapidly consumed by reaction with Zn^{2+} to form a dense ZIF-8 membrane layer. However, the formation of this initial dense layer may act as a barrier that restricts the availabilty of mIm species further into the octanol phase, leading to the diffusion-limited formation of a second discontinuous film morphology on top of the dense layer (see FIGS. **29**A-**29**B).

Since this effect is difficult to observe directly inside the hollow fiber **100**, the inventors performed a similar experiment by contacting the two phases in a transparent glass vial (see FIG. **29**E). As shown in FIG. **29**E, a dense membrane layer forms at the DI/1-octanol interface and a cloudy layer with sparse crystallization forms further into the 1-octanol phase. Further, the dense membrane layer has nanoscopic defects which lead to high permeances of both propylene (C_3H_6) and propane (C_3H_8) (about 31 G.P.U. and 11 G.P.U., respectively) and a low propylene selectivity (about 2.8). The initial continuous growth step of the IMMP approach does not yield a viable ZIF-8 membrane, and, therefore, further IMMP processing is required.

After 210 minutes of the static membrane growth step (arrest point #2) during which there was no continuous replenishment of the limiting reactant Zn^{2+}, a single layer ZIF-8 membrane on the inner bore surface **110** of the hollow fiber **100** was observed with an overall thickness of about 10 μm (see Table 6). The overall ZIF-8 membrane growth rate during the static membrane growth step is much lower than during the initial continuous membrane growth step due to limited availability of Zn^{2+} as well as slow diffusion of mIm through defects in the dense layer. FIG. **27**B reveals that the dual-layer morphology is replaced with a single dense membrane layer during the static membrane growth step. The discontinuous membrane layer is gradually densified by slow addition of crystallized material as depicted in FIG. **29**C. The information in Table 7 shows a decrease in permeance for both C_3H_6 and C_3H_8 (about 26 G.P.U. and about 1.8 G.P.U., respectively) and an increase in propylene (C_3H_6) selectivity (about 14.3), indicating that nanoscopic defects are being filled in with ZIF-8 material and that the static membrane growth step is important for defect control.

After the 20 minutes of the second continuous membrane growth step followed by 210 minutes of the second static membrane growth step (arrest point #3), a single, continuous layer ZIF-8 membrane on the inner bore surface **110** of the hollow fiber **100** was observed with an overall thickness of about 12 μm (see Table 6). FIGS. **27**C & **29**D reveal that the single membrane layer is further densified to a continuous membrane layer during the second static membrane growth and second static membrane growth steps. The information in Table 7 shows a further decrease in permeance for both C_3H_6 and C_3H_8 (about 23 G.P.U. and about 1.3 G.P.U., respectively) (i.e., 1 G.P.U.=3.348×10^{-10} $molm^{-2}$ s^{-1} Pa^{-1}) and a further increase in C_3H_6 selectivity (about 17).

TABLE 6

Measurement of an average thickness for In-Situ grown ZIF-8 Membrane after each Interfacial Microfluidic Membrane Processing (IMMP) process step.

Processing	Average Thickness (μm) After Step 1 (Arrest Point #1)		Average Thickness (μm) After Step 2 (Arrest Point #2)		Average Thickness (μm) After Step 3 (Arrest Point #3)	
Method	Dense	Discontinuous	Dense	Discontinuous	Dense	Discontinuous
Isothermal	4.5 ± 0.5	2.7 ± 0.4	10.2 ± 2.1	N/A	12.3 ± 1.6	N/A
Initial Heating	2.5 ± 0.6	3.2 ± 0.9	7.0 ± 1.2	N/A	8.0 ± 2.3	N/A

TABLE 7

Measurement of Gas Permeation Properties of In-Situ grown ZIF-8 membrane after each IMMP process step in binary C_3H_6/C_3H_8 with an equimolar feed mixture.

	After Step 1 (Arrest Point #1)			After Step 2 (Arrest Point #2)			After Step 3 (After Arrest Point #3)		
Processing	Permeance (G.P.U.)		Selectivity	Permeance (G.P.U.)		Selectivity	Permeance (G.P.U.)		Selectivity
Method	C_3H_6	C_3H_8	C_3H_6/C_3H_8	C_3H_6	C_3H_8	C_3H_6/C_3H_8	C_3H_6	C_3H_8	C_3H_6/C_3H_8
Isothermal	31	11	2.8	26	1.8	14.3	23	1.3	17.7
Initial Heating	45	14	3.2	30	2.5	12	33	1.9	17.5

Role of Polyamide-Imide (e.g., TORLON®) Hollow Fiber

Further, the inventors confirmed that all permeation measurements are reliably measuring the intrinsic properties of the ZIF-8 membranes with negligible effects of polyamide-imide (e.g., TORLON®) hollow fiber support in determining the defect density and selectivity of the membrane. The fabricated polyamide-imide (e.g., TORLON®) hollow fibers have an outer diameter (OD) of about 300 μm and an inner diameter (ID) of about 200 μm, as discussed below.

For scanning probe microscopy (SPM) of the hollow fiber support surfaces, the hollow fibers were immersed in hexane followed by immersion of the saturated fibers in liquid nitrogen. Then, the hollow fibers were gently broken into several pieces, which were then transferred to a silicon wafer for the SPM surface roughness measurements. The RMS surface roughness was obtained by averaging data from several 2 μm×2 μm area images. The RMS roughness was measured as 63±5 nm, which is much smaller than the ZIF-8 membrane thickness and is not expected to lead to large heterogeneities in the film thickness (see Table 6).

The inventors also characterized the porosity of the hollow fibers from SEM images using the Khare and Burris method.[21] For this purpose (see FIGS. **30**A-**30**B), binary images were obtained from cross-sectional SEM images of the support via the image analysis program ImageJ.[22] The porosity (c) and average pore size of the fibers were estimated at 44% and 290 nm, respectively.

The hollow fibers are also highly permeable, as characterized by their N_2 permeance of 54000 G.P.U. and permeability of 2.7×10^6 Barrer (i.e., 1 Barrer=1 G.P.U. μm) at 25° C.

Without wishing to be bound to any theory, the inventors believe that hollow fibers with larger porosity and somewhat larger pore size may allow faster formation of a thin ZIF-8 membrane layer and better anchoring of this membrane layer to the fiber surface.

Negligible Effects of External Mass Transfer Resistances

Further, the inventors confirmed that all permeation measurements are reliably measuring the intrinsic properties of the ZIF-8 membranes with negligible effects of external mass transfer resistances. The total permeation resistance (R_{Total}) through the membrane was modeled as a result of three series resistances: membrane layer ($R_{membrane}$), support (R_{Torlon}), and external ($R_{external}$). To quantify the contributions of the support+external mass transport resistances to the total resistance through the membrane, the inventors obtained single-component gas permeation data through a bare polyamide-imide (e.g., TORLON®) hollow fiber at 25° C.

For an accurate estimate from a bare polyamide-imide (e.g., TORLON®) hollow fiber that has been exposed to actual IMMP process conditions, the inventors performed IMMP approach on the bare hollow fiber **100** with only the aquesous mIm solution and no Zn^{+2} metal source in the 1-octanol solution (to prevent ZIF-8 formation).

Using the measured bare hollow fiber permeances along with the permeances from the ZIF-8 membrane (Case 1), Equations 1 & 2 were used to back-calculate the value of $R_{Torlon}+R_{external}$ and, therefore, determine the corrected values of $R_{membrane}$ and $P_{membrane}$ (G.P.U.) as shown in Table 8. External and support resistances lead to only a correction of 0.01-5% in the permeance measurements for the three gases, which is negligible.

$$R_{membrnae} = \frac{1}{P_{membrane}} \tag{1}$$

$$R_{Total} = R_{membrane} + R_{Torlon+external} \tag{2}$$

TABLE 8

Single gas permeance results before and after considering the effect of polyamide-imide (e.g., TORLON ®) hollow fiber and external mass transfer resistances at 25° C.

Gas	Measured Permeance (G.P.U.)	Corrected Permeance (G.P.U.)	Error
Propane (C_3H_8)	1.0	1.0	0.01%
Propylene (C_3H_6)	66.5	66.8	0.5%
Hydrogen (H_2)	1537	1596	3.7%

Fabrication of Polyamide-Imide (e.g., TORLON®) Hollow Fiber Supports

Polyamide imide (e.g., TORLON®) hollow fibers of outer diameter (OD) of about 300 μm and inner diameter (ID) of about 200 μm were produced by a spinning method. The polymer dope compositions and spinning conditions are shown in Table 9.

TABLE 9

Spinning conditions of polyamide imide (e.g., TORLON ®) hollow fiber porous support.

Dope composition (PAI/$LiNO_3$/NMP/ethanol) (wt %)	15/15/66/4
Dope flow rate (ml/hr)	360
Bore fluid (NMP/H_2O) (wt %)	80/20
Bore fluid flow rate (ml/hr)	120
Air gap (cm)	16
Take up rate (m/min)	45
Operating temperature (° C.)	25
Quench bath temperature (° C.)	25

A polyamide-imide (e.g., TORLON®) core dope was fed to the spinneret compartment. The extruded polymer dope passed through an air-gap and into a water quench bath (primary coagulant) where the fiber phases separate. A standard bore fluid used in this experiment comprised a non-volatile solvent (NMP) and deionized water (DI) with the weight ratio of 80:20.

Then, the fiber was passed over a TEFLON® guide and collected on a rotating take-up drum partially submerged in a second water bath, which was continuously replenished with fresh water.

Next, fibers spun under identical conditions were removed from the take-up drum, tied loosely and soaked in DI for about 4 days at room temperature (i.e., about 25° C.) with fresh DI added daily to remove any residual NMP and promote complete removal of the water-soluble $LiNO_3$.

Then, the water in the hollow fiber was exchanged with a solvent by immersion for about 1 hour each in three batches of fresh methanol (to remove excess water) and then about 1 hour each in three batches of fresh hexane (to remove excess methanol).

After about 2 hours air drying step, the hollow fibers were dried at about 130° C. for about 24 hours to completely remove any residual NMP.

The hollow fibers had an RMS roughness of 63±5 nm, which is much smaller than the ZIF-8 membrane thickness and is not expected to lead to large heterogeneities in the film thickness (see Table 6). Further, the porosity and average pore size of the hollow fibers were estimated at 44% and 290 nm, respectively (see FIGS. **30**A-**30**B).

Fabrication of Improved Polyamide Imide (e.g., TORLON®) Hollow Fiber Supports

The improved polyamide imide (e.g., TORLON®) hollow fibers of outer diamer (OD) of about 360 μm and inner diameter (ID) of about 270 μm and enhanced porosity were fabricated by a modified spinning approach. The modified polymer dope compositions and spinning conditions are shown in Table 10.

TABLE 10

Modified spinning conditions of polyamide imide (e.g., TORLON ®) hollow fiber porous support.

Dope composition (PAI/$LiNO_3$/NMP/ethanol) (wt %)	15/15/66/4
Dope flow rate (ml/hr)	300
Bore fluid (NMP/H_2O) (wt %)	85/15
Bore fluid flow rate (ml/hr)	100
Air gap (cm)	15
Take up rate (m/min)	40
Operating temperature (° C.)	27
Quench bath temperature (° C.)	25

Non-volatile solvent (NMP), non-solvent (water) and pore formers ($LiNO_3$) in the dope composition, quench bath temperatures (i.e., about 25° C.), take-up rate (i.e., about 40 m/minute) and air gap height (i.e., about 15 cm) were applied in order to identify a robust process to produce improved hollow fibers with engineered surface porosity. The key parameters control the morphology of the improved hollow fibers include composition of the polymer dope, composition of the bore liquid, height of the air gap and spinning speed.

A polyamide-imide (e.g., TORLON®) core dope was fed to the spinneret compartment. The extruded polymer dope passed through an air-gap and into a water quench bath (primary coagulant) where the fiber phases separate. To increase the porosity of the hollow fibers, a bore fluid used in this experiment comprised NMP and deionized water (DI) with the weight ratio of 85:15 (instead of 80:20).

Then, the fiber was passed over a TEFLON® guide and collected on a rotating take-up drum partially submerged in a second water bath, which was continuously replenished with fresh water.

Next, fibers spun under identical conditions were removed from the take-up drum, tied loosely and soaked in DI for about 5 days at room temperature (i.e., about 25° C.) with fresh DI added daily to remove any residual NMP and promote complete removal of the water-soluble $LiNO_3$.

Then, the water in the hollow fiber was exchanged with a solvent by immersion for about 1 hour each in three batches of fresh methanol (to remove excess water) and then about 1 hour each in three batches of fresh hexane (to remove excess methanol).

After about 2 hours air drying step, the hollow fibers were dried at about 130° C. for about 24 hours to completely remove any residual NMP.

The resulting hollow fibers had an RMS roughness of 62±6 nm which is similar to the previous hollow fibers (discussed above) and, thus, provides a flat surface for ZIF-8 membrane layer formation. However, the porosity and average pore size of the improved hollow fibers were much larger at 55% and 480 nm, respectively (see FIGS. **30**C-**30**D).

Improved Membrane Synthesis

To investigate the effect of modified hollow fibers in conjunction with a modified IMMP approach, the inventors prepared ZIF-8 membranes in three different ways: Case 1 uses a fabricated polyamide-imide (e.g., TORLON®) hollow fiber and an isothermal IMMP approach; Case 2 uses an improved polyamide-imide (e.g., TORLON®) hollow fiber prepared using a modified spinning technique and a modified initial heating IMMP approach; and Case 3 uses the improved polyamide-imide (e.g., TORLON®) hollow fiber and the modified initial heating IMMP approach.

Performance in Membrane Synthesis Using IMMP Reactor Cell/Module: Isothermal Temperatures

Starting with a fabricated polyamide-imide (e.g., TORLON®) hollow fiber mounted in the IMMP reactor module **400**,[12] about 10 mL of neat 1-octanol was flowed at about 2 mL/min through a bore **110** of a hollow fiber **100** using a syringe pump. Then, about 3 mL of a Zn+2/1-octanol solution containing about 0.22 g Zinc nitrate hexahydrate (Zn^{+2}) in about 40 mL 1-octanol (about 0.018 mol/L) was flowed at about 0.6 mL/hour through the bore **110** of the hollow fiber **100** while an aqueous mum solution containing about 9 g of mum in about 80 mL deionized water (DI) (about 1.37 mol/L) was poured into the reactor chamber **345** immersing the outer (shell) side surface **105** of the hollow fiber **100** while stirring the solution at about 60 rpm for about 120 minutes to provide a continuous membrane growth step. The fabrication of the hollow fiber **100** is discussed below.

The temperature of reactor module **400** was set and maintained at about 30° C.

After the 120 minute continuous membrane growth step, the flow rate of about 0.6 mL/hour through the bore **110** of the hollow fiber **100** was stopped for about 210 minutes to provide a static membrane growth step.

After the 210 minute static membrane growth step, the flow rate of about 0.6 mL/hour through the bore **110** of the hollow fiber **100** was continued for about 20 minutes to provide a second continuous membrane growth step.

After the 20 minute second continuous membrane growth step, the flow rate of about 0.6 mL/hour through the bore **110** of the hollow fiber **100** was stopped for about 210 minutes to provide a second static membrane growth step.

After the 210 minute second static membrane growth step, the reaction was stopped.

To stop the reaction, about 10 mL of neat 1-octanol solvent was flowed at about 2 mL/min through the bore **110** while the outer (shell) side surface **105** was soaked in about 70 mL of neat DI (and replaced three times) to remove the excess Zn^{+2}. Next, about 10 mL heptanes were flowed at about 2 mL/min through the bore **110** while the outer (shell) side surface **105** was soaked in about 70 mL heptanes to remove the 1-octanol. Next, similar procedure was performed with a more volatile hexane solution. Then, about 10 mL hexane was flowed at about 2 mL/min through the bore **110** while outer (shell) side surface **105** was soaked in about 70 mL hexane to remove the heptanes. Finally, about 20 mL of MeOH was flowed at about 2 mL/min through the bore **110** while the outer (shell) side surface **105** was soaked in about 70 mL methanol to remove the DI. The membrane was dried at about room temperature (e.g., about 25° C.) for about 2 days.

Cross-sectional views of SEM micrographs of ZIF-8 membranes grown under various IMMP process conditions are shown in FIGS. **31**A-**32**C. FIGS. **31**A-**31**C shows cross-sectional SEM images of the ZIF-8 membranes obtained in Cases 1, 2 and 3, depicting uniform membrane layers for each case. FIG. **32**A-**32**C show detailed measurements of membrane thickness at different axial locations along the 5 cm length of the hollow fiber for Cases 1, 2 and 3. Notably, the membrane thickness in Case 3 (about 5 μm) is much lower than for Case 1 and Case 2 (about 10 μm, and about 9 μm, respectively) indicating that the initial heating IMMP approach remains effective in reducing the membrane thickness on the improved hollow fiber support.

The separation properties of the ZIF-8 membranes grown on the inner bore of the polyamide-imide (e.g., TORLON®) hollow fiber **100** were characterized by hydrogen(H_2)/propane (C_3H_8) and propylene (C_3H_6)/propane (C_3H_8) binary equimolar mixture permeation as a function of temperature, with the reactor module **400** directly acting as a permeation cell. See FIG. **16**. The separation properties of the ZIF-8 membranes were also characterized by $H_2/C_3H_6/C_3H_8$ tertiary equimolar mixture permeation as a function of temperature. In an embodiment, the feed mixture may be selected from the group consisting of hydrogen/hydrocarbons, hydrogen/propane, propylene/propane and butenes/butanes.

A steady-state Wicke Kallenbach technique was used to test binary H_2/C_3H_8 and C_3H_6/C_3H_8 and tertiary $H_2/C_3H_6/C_3H_8$ mixtures.[24] Specifically, 1:1 or 1:1:1 feed mixtures were flowed at 1 atmosphere through a bore **110** of the ZIF-8 membrane grown on the polyamide-imide (e.g., TORLON®) hollow fiber **100** at a precisely controlled flow rate (e.g., about 10 mL/minutes) via a mass flow controller (MFC) while an argon sweep gas was flowed across an outer (shell) side surface **105** of the hollow fiber **100** at about 30 mL/minute. The injected gases were contacted in a mixer before entering the feed side of the reactor/permeation module. A similar apparatus was used for measurements at higher feed pressures (up to 6 bar), except that MFCs rated for high-pressure operation were used.

An online gas chromatograph (Shimadzu GC-2014) with TCD and FID detectors was used to determine the composition of permeate.

Membrane defect characterization was performed with permporosimetry equipment with the IMMP reactor module **400** directly acting as a permeation cell. First, helium was introduced into one end of the bore **110** of the ZIF-8 membrane while plugging the other end with a Swagelok fitting. The pressure differential between the bore side **110** and the shell side **105** was, thus, controlled from 0 psi to 90 psi helium while the shell side **105** helium flow rate was measured using a digital flow meter. Then, the bore **110** of the ZIF-8 membrane was saturated with Fluorinert (FC-40) solution that has a low surface tension. Then, the shell side **105** helium flow rate was measured again.

Atomic force microscopy (AFM) images of inner surfaces of the hollow fibers were obtained with an ICON Dimension® scanning probe microscope (Bruker). The AFM was operated under tapping mode with Mikromasch NSC14 silicon cantilevers (8 nm tip radius, 5 N/m force constant, and 160 kHz typical resonance frequency).

Table 11 shows information about C_3H_6/C_3H_8 permeation characteristics for various IMMP processes in Cases 1, 2 and 3.

TABLE 11

Measurement of Gas Permeation Properties of In-Situ grown ZIF-8 membranes C_3H_6/C_3H_8 equimolar mixed gas permeance results at 25° C.

	Permeance (G.P.U.)		Selectivity
Example	C_3H_6	C_3H_8	C_3H_6/C_3H_8
Case 1	27 ± 4	3 ± 1	9 ± 1
Case 2	34 ± 4	1.4 ± 0.3	24 ± 3
Case 3	66 ± 3	1.0 ± 0.1	65 ± 5

Without wishing to be bound by any theory, the inventors believe that increasing the rate of formation of the initial dense barrier layer may significantly reduce its thickness during the initial continuous membrane growth step, since a more rapidly formed barrier layer would effectively inhibit further reaction-limited dense film growth. This would result in a reduced overall membrane thickness and, hence, a higher permeance.

Performance in Membrane Synthesis Using IMMP Reactor Cell/Module: Initial Heating

Starting with a fabricated polyamide-imide (e.g., TORLON®) hollow fiber mounted in the IMMP reactor module **400**,[12] about 10 mL of neat 1-octanol was flowed at about 2 mL/min through a bore **110** of a hollow fiber **100** using a syringe pump. Then, about 3 mL of a Zn+2/1-octanol solution containing about 0.22 g Zinc nitrate hexahydrate (Zn^{+2}) in about 40 mL 1-octanol (about 0.018 mol/L) was flowed at about 0.6 mL/hour through the bore **110** of the hollow fiber **100** while an aqueous mum solution containing about 9 g of mum in about 80 mL deionized water (DI) (about 1.37 mol/L) was poured into the reactor chamber **345** immersing the outer (shell) side surface **105** of the hollow fiber **100** while stirring the solution at about 60 rpm for about 120 minutes to provide a continuous membrane growth step. The fabrication of the hollow fiber **100** is discussed above.

The temperature of the reactor module **400** was initially set at about 22° C. During the continuous membrane growth step, the temperature of the reactor module **400** was increased linearly from about 22° C. to about 42° C. in about 25 minutes (about 0.8° C./min) to increase the formation of the initial dense membrane layer. Then, the temperature of the reactor module **400** was decreased from about 42° C. to about 30° C. in about 60 minutes (about 0.2° C./min) For the remainder of the synthesis, the temperature of the reactor module was set and maintained at about 30° C.

After the 120 minute continuous membrane growth step, the flow rate of about 0.6 mL/hour through the bore **110** of the hollow fiber **100** was stopped for about 210 minutes to provide a static membrane growth step.

After the 210 minute static membrane growth step, the flow rate of about 0.6 mL/hour through the bore **110** of the hollow fiber **100** was continued for about 20 minutes to provide a second continuous membrane growth step.

After the 20 minute second continuous membrane growth step, the flow rate of about 0.6 mL/hour through the bore **110** of the hollow fiber **100** was stopped for about 210 minutes to provide a second static membrane growth step.

After the 210 minute second static membrane growth step, the reaction was stopped.

To stop the reaction, about 10 mL of neat 1-octanol solvent was flowed at about 2 mL/min through the bore **110** while the outer (shell) side surface **105** was soaked in about 70 mL of neat DI (and replaced three times) to remove the excess Zn^{+2}. Next, about 10 mL heptanes were flowed at about 2 mL/min through the bore **110** while the outer (shell) side surface **105** was soaked in about 70 mL heptanes to remove the 1-octanol. Next, a similar procedure was performed with a more volatile hexane solution. Then, about 10 mL hexane was flowed at about 2 mL/min through the bore **110** while outer (shell) side surface **105** was soaked in about 70 mL hexane to remove the heptanes. Finally, about 20 mL of MeOH was flowed at about 2 mL/min through the bore **110** while the outer (shell) side surface **105** was soaked in about 70 mL methanol to remove the DI. The membrane was dried at about room temperature (e.g., about 25° C.) for about 2 days.

The initial heating IMMP approach increased the rate of formation of the initial dense layer. See FIGS. **27**D-**27**F. A considerably thinner (about 2.5 μm) dense membrane layer is formed initially, leading to thinner final membrane thickness (about 8 μm) with a correspondingly higher propylene permeance (about 33 G.P.U.) and no loss of selectivity over the isothermal case. See Tables 6 & 7.

Performance in Membrane Synthesis Using IMMP Reactor Cell/Module: Improved Hollow Fiber Support and Initial Heating

Starting with a fabricated, improved polyamide-imide (e.g., TORLON®) hollow fiber mounted in the IMMP reactor module **400**,[12] about 10 mL of neat 1-octanol was flowed at about 2 mL/min through a bore **110** of a hollow fiber **100** using a syringe pump. Then, about 3 mL of a Zn+2/1-octanol solution containing about 0.22 g Zinc nitrate hexahydrate (Zn^{+2}) in about 40 mL 1-octanol (about 0.018 mol/L) was flowed at about 0.6 mL/hour through the bore **110** of the hollow fiber **100** while an aqueous mum solution containing about 9 g of mum in about 80 mL deionized water (DI) (about 1.37 mol/L) was poured into the reactor chamber **345** immersing the outer (shell) side surface **105** of the hollow fiber **100** while stirring the solution at about 60 rpm for about 120 minutes to provide a continuous membrane growth step. The fabrication of the improved hollow fiber **100** is discussed above.

The temperature of the reactor module **400** was initially set at about 22° C. During the continuous membrane growth step, the temperature of the reactor module **400** was increased linearly from about 22° C. to about 42° C. in about 25 minutes (i.e., at about 0.8° C./min) Then, the temperature of the reactor module **400** was decreased from about 42° C. to about 30° C. in about 60 minutes (i.e., about 0.2° C./min) For the remainder of the synthesis, the temperature of the reactor module was set and maintained at about 30° C.

After the 120 minute continuous membrane growth step, the flow rate of about 0.6 mL/hour through the bore **110** of the hollow fiber **100** was stopped for about 210 minutes to provide a static membrane growth step.

After the 210 minute static membrane growth step, the flow rate of about 0.6 mL/hour through the bore **110** of the hollow fiber **100** was continued for about 20 minutes to provide a second continuous membrane growth step.

After the 20 minute second continuous membrane growth step, the flow rate of about 0.6 mL/hour through the bore **110** of the hollow fiber **100** was stopped for about 210 minutes to provide a second static membrane growth step.

After the 210 minute second static membrane growth step, the reaction was stopped.

To stop the reaction, about 10 mL of neat 1-octanol solvent was flowed at about 2 mL/min through the bore **110** while the outer (shell) side surface **105** was soaked in about 70 mL of neat DI (and replaced three times) to remove the excess Zn^{+2}. Next, about 10 mL heptanes were flowed at about 2 mL/min through the bore **110** while the outer (shell) side surface **105** was soaked in about 70 mL heptanes to remove the 1-octanol. Next, a similar procedure was performed with a more volatile hexane solution. Then, about 10 mL hexane was flowed at about 2 mL/min through the bore **110** while outer (shell) side surface **105** was soaked in about 70 mL hexane to remove the heptanes. Finally, about 20 mL of MeOH was flowed at about 2 mL/min through the bore **110** while the outer (shell) side surface **105** was soaked in about 70 mL methanol to remove the DI. The membrane was dried at about room temperature (e.g., about 25° C.) for about 2 days.

To compare the performance of these ZIF-8 membranes, equimolar C_3H_6/C_3H_8 mixed-gas permeation data were collected using a steady-state Wicke-Kallenbach technique at 25° C. with the IMMP reactor directly acting as a permeation module (see Table 11). The Case 3 ZIF-8 membrane shows much higher C_3H_6 permeance than the Cases 1 and 2 membranes due to a much lower thickness. Also, the Case 3 membrane also shows much higher C_3H_6/C_3H_8 selectivity due to a significant drop in the C_3H_8 permeance.

Without wishing to be bound by any theory, the inventors believe that the ZIF-8 membrane defects are decreased due to better anchoring of the membrane layer on the more porous hollow fiber support. The microstructural changes were investigated in more detail with helium permporosimetry.[22] The helium flux was measured under dry conditions and, then, after wetting with Fluorinert (FC-40) liquid that has a low surface tension, helium permeance is measured as a function of pressure in the feed gas. Under wetted conditions, ZIF-8 membranes that have mesopore defects such as pinholes or cracks would show a sudden increment in helium permeance at a pressure that is sufficient to displace the wetting liquid from the mesopore defects. The defect size can then be estimated by the Cantor equation.[23] However, such phenomena are not observed in the pressure range 0-90 psi for any of the Case 1-3 ZIF-8 membranes (see FIG. **33**), showing that continuous membrane layers are formed over the entire fiber with no large defects (i.e., defects less than 20 nm in diameter, length or width at 90 psi helium).

However, the dry helium permeabilities (see FIG. **33**) also allow the qualitative characterization of nanoscopic defects (i.e., less than 20 nm). The ideal range of helium permeability from a ZIF-8 membrane free of defects is represented by the shaded area in FIG. **33**, which is obtained using the range of corrected diffusivity and adsorption isotherm parameters for helium in ZIF-8 as given by Zhang et al.[24] The Case 1 ZIF-8 membranes display significantly higher dry helium permeability outside the ideal region, clearly indicating the presence of nanoscopic defects. However, the dry helium permeability progressively declines and reaches the ideal region in Case 2 and Case 3 ZIF-8 membranes, indicating that both membrane thickness and defect density have been reduced. The Case 3 ZIF-8 membrane has the lowest dry helium permeability, corresponding to the most defect-free membranes which also has the best separation performance as shown in Table 11.

Finally, the inventors characterized the binary and ternary mixture separation properties of the Case 3 ZIF-8 membranes in more detail as a function of temperature from about 25° C. to about 120° C. FIG. **34**A shows equimolar binary (H_2/C_3H_8 and C_3H_6/C_3H_8) mixture permeation properties. Clear molecular sieving effects are observed for the improved ZIF-8 membranes on polyamide-imide (e.g., TORLON®) hollow fibers with H_2/C_3H_8 and C_3H_6/C_3H_8 separation factors of about 2000 at 70° C. and about 65 at 25° C., respectively. This performance is much improved from previously reported ZIF-8 membranes on polyamide-imide (e.g., TORLON®) hollow fibers with separation factors of about 370 at 120° C. and about 12 at 25° C., respectively).[25] This data shows a strong temperature dependence of the C_3H_6 permeance, resulting in a moderate decrease in separation factor as temperature increases. However, the ZIF-8 membranes still achieve a C_3H_6/C_3H_8 separation factor of about 31 G.P.U. at 120° C.

FIG. **34**B shows the equimolar ternary ($H_2/C_3H_6/C_3H_8$) mixture separation properties. This feed mixture simulates the composition of an exit stream from near-equilibrium propane dehydrogenation (PDH) reactors that are used for propylene production. The Case ZIF-8 membrane continues to effectively separate C_3H_6 from C_3H_8 in the presence of H_2 with separation factor of about 53 at 25° C. It is also noted that these Case 3 membranes can be utilized to separate H_2 from C_3H_6 (i.e., H_2/C_3H_6 separation factor of 99±3 at 120° C., which industrially attractive).[19]

Further, the Case 3 ZIF-8 membrane was tested for binary C_3H_6/C_3H_8 separation performance at feed pressures up to 6 bar at 25° C. The selectivity remains high and shows only minor (about 13-15%) reduction at 6 bar. The C_3H_6 permeance shows a reduction of about 25%, which is expected in molecular sieve materials due to pore saturation effects. However, it is important to note that the actual C_3H_6 flux (throughput) at 6 bar is about 3.75 to 4 times higher due to the much greater driving force.

In conclusion, the mechanistic findings and resulting significant improvements in membrane performance supports a two-stage separation of ternary $H_2/C_3H_6/C_3H_8$ mixtures (e.g., a first ZIF-8 membrane stage of small total area that takes advantage of the very high H_2 permeance to separate it from C_3H_6 and C_3H_8, followed by a second ZIF-8 membrane stage of larger area that separates C_3H_6 from C_3H_8). Such two-stage separation is possible due to the significant advancements of the present invention, first, the modification of the IMMP approach to include an initial heating growth step and, secondly, the engineering of a modified hollow fiber support with enhanced surface properties.

In a hydrocarbon separation embodiment, the feed mixture to the reactor cell **400** comprises about 2 mol % to about 95 mol % hydrogen, about 2 mol % to about 95 mol % i-butane, about 2 mol % to about 95 mol % n-butane and mixtures thereof. For example, the feed mixture may comprise about 0 mol % to about 2 mol % ethane, about 0 mol % to about 5 mol % n-propane, about 0 mol % to about 5 mol % i-propane, about 0 mol % to about 5 mol % butenes, about 2 mol % to about 95 mol % i-butane, about 2 mol % to about 95 mol % n-butane, about 0 mol % to about 2 mol % pentenes and about 0 mol % to about 15 mol % pentanes and mixtures thereof.

In a hydrocarbon separation embodiment, an operating temperature for the reactor cell **400** is from about 30° C. to about 120° C. or any value there between. In an embodiment, the operating temperature is about 30° C. In an embodiment, the operating temperature is about 70° C. In an embodiment, the operating temperature is about 120° C.

In a hydrocarbon separation embodiment, an operating pressure for the reactor cell **400** is from about 1 bar to about 14 bar or any value there between. In an embodiment, the operating pressure is about 1 bar. In an embodiment, the operating pressure is about 4 bar. In an embodiment, the operating pressure is about 7 bar. In an embodiment, the operating pressure is about 10 bar. In an embodiment, the operating pressure is about 14 bar.

The embodiments and examples set forth herein are presented to best explain the present invention and its practical application and to thereby enable those skilled in the art to make and utilize the invention. However, those skilled in the art will recognize that the foregoing description and examples have been presented for the purpose of illustration and example only. The description as set forth is not intended to be exhaustive or to limit the invention to the precise form disclosed. Many modifications and variations are possible in light of the above teaching without departing from the spirit and scope of the following claims. The invention is specifically intended to be as broad as the claims below and their equivalents.

Definitions

As used herein, the terms "a," "an," "the," and "said" means one or more, unless the context dictates otherwise.

As used herein, the term "about" means the stated value plus or minus a margin of error or plus or minus 10% if no method of measurement is indicated.

As used herein, the term "or" means "and/or" unless explicitly indicated to refer to alternatives only or if the alternatives are mutually exclusive.

As used herein, the terms "comprising," "comprises," and "comprise" are open-ended transition terms used to transition from a subject recited before the term to one or more elements recited after the term, where the element or elements listed after the transition term are not necessarily the only elements that make up the subject.

As used herein, the terms "containing," "contains," and "contain" have the same open-ended meaning as "comprising," "comprises," and "comprise," provided above.

As used herein, the terms "having," "has," and "have" have the same open-ended meaning as "comprising," "comprises," and "comprise," provided above.

As used herein, the terms "including," "includes," and "include" have the same open-ended meaning as "comprising," "comprises," and "comprise," provided above.

As used herein, the phrase "consisting of" is a closed transition term used to transition from a subject recited before the term to one or more material elements recited after the term, where the material element or elements listed after the transition term are the only material elements that make up the subject.

As used herein, the term "free of defects" means that the metal-organic framework (MOF) membrane coating is from about 95% to about 100% free of defects (and any range or value there between), and, preferably, from about 97% to about 100% free of defects or about 100% free of defects, and that any existing defect sizes is less than about 20 nanometer (and any range or value there between) in diameter, length or width, and, preferably, the defect sizes are less than 10 nanometers in diameter, length or width such that the membrane coating is essentially continuous to prevent gas or liquid being treated from leaking through a defect (e.g., pore, crack, void, etc.).

As used herein, the phrase "growth solvent" means a liquid in which the MOF seed crystals can be increased in size, either by crystal deposition or synthesis, but without harming the polymer.

As used herein, the term "mesoporous" means having a 3D structure of interconnected pores, wherein the pore sizes range in diameter from about 0.1 nanometer to about 10 nanometers (and any range or value there between), and, preferably, the pore sizes range in diameter from about 1 nanometer to about 5 nanometers or from about 2 nanometers to about 4 nanometers. However, the pores sizes may be varied depending on the gases to be separated.

As used herein, the phrase "nanocrystals" means the seed crystals have an average size of less than one micron, preferably about 400-600 nm, and a size distribution of about ±10%. For polymers with very small pores, a smaller seed crystal may be needed, and therefore the seed crystal size can be reduced as needed.

As used herein, the phrase "non-solvent" means a liquid in which the MOF precursors have a low solubility, such that on introducing the non-solvent to the mixture, the precursors are unable to stay in solution and condense quickly to form a large number of nuclei, which are the seeds for growing a large number of very small crystals.

As used herein, the term "polymer" means polymers made from one or more monomeric unit, and, thus, the term is intended to include polymers, copolymers, block copolymers, terpolymers and the like unless explicitly limited to specific types of polymers.

As used herein, the phrase "seed solvent" means a liquid in which the MOF nanocrystals can be carried into the pores of the polymer. Thus, the seed crystals should have low solubility in the solvent and the solvent should penetrate or wet the pores of the polymer, but without harming the polymer.

As used herein, the term "simultaneously" means occurring at the same time or about the same time, including concurrently.

As used herein, "starting material" means that the recited chemical is made or purchased for use as an early reactant in the synthetic pathway. However, if made, rather than purchased, there may be other ingredients that pre-date same.

ABBREVIATIONS

Abbreviations are used in this disclosure, as follows:

AFM	Atomic force microscopy
DI	Deionized water
DLS	Dynamic light scattering
EDS	Energy dispersive X-ray spectroscopy
H_2	Hydrogen
IMMP	Interfacial Microfluidic Membrane Processing
mIm	2-methyl imidazole
MOF	Metal organic framework
PDMS	Poly(dimethylsiloxane)
C_3H_8	Propane
C3H6	Propylene
SEM	Scanning electron microscope
SPM	Scanning probe microscopy
XRD	X-ray diffraction
ZIF	Zeolitic imidazolate framework
ZIF-8	Zeolitic imidazolate framework 8
ZIF-90	Zeolitic imidazolate framework 90

INCORPORATION BY REFERENCE

All patents and patent applications, articles, reports, and other documents cited herein are fully incorporated by reference to the extent they are not inconsistent with this invention, as follows:

1) J. Gascon, et al., CHEM. MATER. 24 (2012) 2829-2844.
2) K. Varoon, et al., SCIENCE 334(6052) (2011) 72-75.
3) M. Shah, et al., IND. ENG. CHEM. RES. 51 (2012) 2179-2199.
4) M. G. Buonomenna, RSC ADVANCES 3 (2013) 5694-5740.

5) M. Tsapatsis, Science 334(6057) (2011) 767-768.
6) T. Cao, et al., Science 334(6062) (2011) 1533-1538.
7) J. Choi, et al., Science 325(5940) (2009) 590-593.
8) Y. Pan, et al., J. Membr. Sci. 421-422 (2012) 292-298.
9) J. A. Thompson, et al., Chem. Mater. 24 (2012) 1930-1936.
10) K. S. Park, et al., Proc. Natl. Acad. Sci. U.S.A. 103(27) (2006) 10186-10191.
11) A. Huang, et al., *J. Am. Chem. Soc.* 132(44) (2010) 15562-15564.
12) A. J. Brown, et al., Angela. Chem. 124 (2012) 10767-10770.
13) R. Ameloot, et al., Nat. Chem. 3 (2011) 382-387.
14) M. Pera-Titus, et al., J. Membr. Sci. 278 (2006) 401-409.
15) K. Li, et al., J. Am. Chem. Soc. 131(30) (2009) 10368-10369.
16) K. S. Jang, et al., Chem. Mater. 23 (2011) 3025-3028.
17) Y. Pan, et al., J. Membr. Sci. 390-391 (2012) 93-98.
18) H. Bux, et al., Chem. Mater. 23 (2011) 2262-2269.
19) Y. Pan, Z. Lai, Chem. Commun. 47(37) (2011) 10275-10277.
20) H. T. Kwon, et al., Chem. Commun. 49 (2013) 3854-3856.
21) H. S. Khare, et al., Polymer 51 (2010) 719-729.
22) W. S. Rasband, "*ImageJ*", U.S. National Institutes of Health, Bethesda Md., USA.
23) D. Korelskiy, et al., J. Membr. Sci. 417-418 (2012) 183-192.
24) J. Kärger, et al., Diffusion in Zeolites and Other Microporous Solids (Wiley, 1992).
25) J. I. Calvo, et al., J. Colloid & Interface Sci. 176(2) (1995) 467-478.
26) C. Zhang, et al., J. Phys. Chem. Lett. 3(16) (2012) 2130-2134.
27) A. J. Brown, et al., S. Nair, Science 345(6192) (2014) 72-75.

What is claimed is:

1. A reactor cell for flow processing molecular sieving membranes, comprising:

a reactor module having a base shape and a first height, wherein the base shape is selected from the group consisting of square, rectangular, circular and ellipse; wherein a reactor chamber extends into the reactor module from an upper surface; wherein a first hole extends into the reactor chamber from a first surface, a second hole opposing the first hole extends into the reactor chamber from a second surface, a third hole extends into the reactor chamber from a third surface and a fourth hole opposing the third hole extends into the reactor chamber from a fourth surface; wherein the first hole is fluidically connected to a first inlet, the second hole is fluidically connected to a first outlet, the third hole is fluidically connected to a second inlet and the fourth hole is fluidically connected to a second outlet;

a reactor module cover having the same base shape as the reactor module and a second height, wherein the reactor module cover is fastened to the reactor module to seal the reactor chamber; and

a hollow fiber having a first end and a second end, wherein a length of the first end is supported by and sealed into the first hole and a length of the second end is supported by and sealed into the second hole; wherein the first and second ends of the hollow fiber are capped with a capping solution, wherein a molecular sieving membrane that is uniform and at least 95% free of defects is grown on an inner bore surface of the hollow fiber.

2. The device of claim **1**, wherein the molecular sieving membrane is at least about 97% free of defects and wherein any defects are less than about 20 nm in diameter, length or width.

3. The device of claim **1**, wherein the molecular sieving membrane is at least about 97% free of defects and wherein any defects are less than about 10 nm in diameter, length or width.

4. The device of claim **1**, wherein the first hole extends into the reactor chamber from the first surface, the second hole opposing the first hole extends into the reactor chamber from the second surface, the third hole extends into the reactor chamber from the first surface and the fourth hole opposing the third hole extends into the reactor chamber from the second surface.

5. The device of claim **1**, wherein the first hole extends into the reactor chamber from the first surface, the second hole opposing the first hole extends into the reactor chamber from the second surface, the third hole extends into the reactor chamber from an upper surface of a reactor module cover and the fourth hole opposing the third hole extends into the reactor chamber from a bottom surface of the reactor chamber.

6. The device of claim **1**, wherein the lengths of the first and second ends of the hollow fiber are sealed into the first and second holes with an adhesive.

7. The device of claim **1**, wherein the capping solution is about 8 wt % to about 10 wt % poly(dimethylsiloxane) (PDMS) in heptane.

8. A method of making a reactor cell device, the reactor cell device comprising

a reactor module having a base shape and a first height, wherein the base shape is selected from the group consisting of square, rectangular, circular and ellipse; wherein a reactor chamber extends into the reactor module from an upper surface; wherein a first hole extends into the reactor chamber from a first surface, a second hole opposing the first hole extends into the reactor chamber from a second surface, a third hole extends into the reactor chamber from a third surface and a fourth hole opposing the third hole extends into the reactor chamber from a fourth surface; wherein the first hole is fluidically connected to a first inlet, the second hole is fluidically connected to a first outlet, the third hole is fluidically connected to a second inlet and the fourth hole is fluidically connected to a second outlet;

a reactor module cover having the same base shape as the reactor module and a second height, wherein the reactor module cover is fastened to the reactor module to seal the reactor chamber; and

a hollow fiber having a first end and a second end, wherein a length of the first end is supported by and sealed into the first hole and a length of the second end is supported by and sealed into the second hole; wherein the first and second ends of the hollow fiber are capped with a capping solution, wherein a molecular sieving membrane that is uniform and at least 95% free of defects is grown on an inner bore surface of the hollow fiber,

making the reactor cell device comprising the steps of:

fabricating the reactor chamber extending into the reactor module from the upper surface of the reactor module;

fabricating an O-ring groove with an inner dimension slightly larger than and offset from the outer dimension of the reactor chamber;

fabricating the first hole extending into the reactor chamber from the first surface and the second hole opposing the first hole and extending into the reactor chamber from the second surface;

fabricating a third hole extending into the reactor chamber from a third surface and a fourth hole opposing the third hole and extending into the reactor chamber from a fourth surface;

supporting and sealing the length of the first end of the hollow fiber in the first hole and the length of the second end of the hollow fiber into the second hole;

capping the first and second ends of the hollow fiber with a capping solution;

fabricating the reactor module cover to fit on the upper surface of the reactor module and fastening the reactor module cover to the seal the reactor chamber;

fluidly connecting a bore solution to the first inlet;

fluidly connecting a shell solution to the second inlet; and

growing the molecular sieving membrane that is uniform and at least about 95% free of defects on an inner bore surface of the hollow fiber.

9. The method of claim **8**, wherein the molecular sieving membrane is at least about 97% free of defects and wherein any defects are less than about 20 nanometers in diameter, length or width.

10. The method of claim **8**, wherein the molecular sieving membrane is at least about 97% free of defects and wherein any defects are less than about 10 nanometers in diameter, length or width.

11. The method of claim **8**, wherein the bore solution contains a limited Zn+2 concentration ranging from about 0.005 to about 0.1 mol/L Zn+2 in 1-octanol.

12. The method of claim **8**, wherein the bore solution contains a limited Zn+2 concentration ranging from about 0.01 to about 0.03 mol/L Zn+2 in 1-octanol.

13. The method of claim **8**, wherein the bore solution is about 0.018 mol/L Zn+2 in 1-octanol.

14. The method of claim **8**, wherein the shell solution contains an excess mum ligand concentration ranging from about 0.5 to about 10 mol/L 2-methyl imidazole (mum) in deionized water.

15. The method of claim **8**, wherein the shell solution contains an excess mum ligand concentration ranging from about 1.2 to about 1.6 mol/L 2-methyl imidazole (mum) in deionized water.

16. The method of claim **8**, wherein the shell solution is about 1.37 mol/L mum in deionized water.

17. The method of claim **8**, further comprising the step of gently stirring the shell solution to prevent formation of local concentration gradients.

18. The method of claim **14**, wherein the shell solution is stirred at about 40 rpm to about 80 rpm.

19. The method of claim **8**, further comprising the steps of

a. flowing the bore solution at a first flow rate for a first period, wherein a first temperature is increased to a second temperature during a portion of the first period;
b. stopping the first flow rate of the bore solution for a second period;
c. flowing the bore solution at a second flow rate for a third period; and
d. stopping the second flow rate of the bore solution for a fourth period.

20. The method of claim **19**, wherein the second temperature is decreased to a third temperature during a portion of the first period.

21. The method of claim **19**, wherein the first and second flow rates are about 1 μL/hour to about 1000 μL/hour per individual hollow fiber.

22. The method of claim **19**, wherein the first and second flow rates are about 10 μL/hour to about 100 μL/hour per individual hollow fiber.

23. The method of claim **19**, wherein the first period is about 1 hour to about 3 hours, the second period is about 3 hours to about 4 hours, the third period is about 10 minutes to about 30 minutes, and the fourth period is about 3 hours to about 4 hours.

24. The method of claim **19**, further comprising the step of rinsing the membrane in solvents selected from the group consisting of 1-octanol, heptanes, hexane, methanol and deionized water.

25. A method of using a reactor cell device, comprising:

providing a reactor cell device of claim **8**,

fluidically connecting a feed mixture to the first inlet;

fluidically connecting a sweep gas to the second inlet;

collecting a separated mixture from the first outlet; and

collecting permeate from the second outlet.

26. The method of claim **25**, wherein the feed mixture to the device is selected from the group consisting of hydrogen/hydrocarbons, hydrogen/propane, propylene/propane and butenes/butanes.

27. The method of claim **25**, wherein the feed mixture to the device is selected from the group consisting of hydrogen/propane, propylene/propane and butenes/butanes.

28. The method of claim **26**, wherein the feed mixture to the device comprises about 2 mol % to about 95 mol % i-butane, about 2 mol % to about 95 mol % n-butane and mixtures thereof.

29. The method of claim **25**, wherein an operating temperature for the device is from about 30° C. to about 95° C. or any value there between.

30. The method of claim **25**, wherein an operating pressure for the device is from about 1 bar to about 14 bar or any value there between.

* * * * *